

This file is part of the following work:

**Hemingson, Christopher Rae (2021) *The colours of coral reef fishes*. PhD Thesis,
James Cook University.**

Access to this file is available from:

<https://doi.org/10.25903/tgze%2Dwf34>

Copyright © 2021 Christopher Rae Hemingson.

The author has certified to JCU that they have made a reasonable effort to gain permission and acknowledge the owners of any third party copyright material included in this document. If you believe that this is not the case, please email

researchonline@jcu.edu.au

The Colours of Coral Reef Fishes

Christopher Rae Hemingson

BSc in Wildlife and Fisheries Science, Texas A&M University

MSc in Marine Biology and Ecology, James Cook University

February 2021

for the degree of Doctor of Philosophy

College of Science and Engineering,
Centre of Excellence for Coral Reef Studies and
The Hub for Coral Reef Ecosystem Function,
James Cook University,
Townsville, Queensland, Australia

Acknowledgements

First, I thank my primary supervisor, David Bellwood. Your continual guidance, unwavering support, and invaluable anecdotal life experience gave me so much as a developing researcher. The dynamic you created within your lab group is something special, and my time spent at JCU will be forever cherished. I am also grateful for my secondary supervisor, Peter Cowman. Your invaluable expertise in evolutionary studies gave me a solid foundation upon which most of my PhD was built. And special thanks must be given to Orpha Bellwood for providing an environment that felt more like a family rather than a workplace. Whether it be scheduling a lab dinner or inviting us over on holidays when we could not be with our own families, the caring and inclusive environment you created did not go unnoticed.

Thank you to everyone who either helped me in the field or let me volunteer on their own field trips: Renato Morais, Alexandre Siqueira, Pauline Narvaez, Victor Huertas, Michalis Mihalitsis, Sterling Tebbett, Tory Chase, Robert Streit, Eric Fakan and Maria Palacios. It was a treat to participate on your field trips and even, in some instances, to conduct my own research. I learned so much from partaking in the various projects and experiments unique to each trip and gained an appreciation for so many other research areas outside of my own.

To everyone in the Bellwood lab: Victor Huertas, Michalis Mihalitsis, Sterling Tebbett, Robert Streit, Renato Morais, Alexandre Siqueira, Jodie Schlaefer, William Collins, Casey Bowden, Arun Oakley-Cogan, Juliano Morais, Sam Swan, and Jessica Valenzuela. This lab group was key to my success and I would not have achieved what I did without their incredible support. The countless insightful conversations over coffees in both the Tin Box and in ATSIP were invaluable. We had many amazing journeys; be it sharing beers at Trois Brasseurs in French Polynesia or reclaiming the Throne at King “O’Ales” in Canberra. You were a family that was always there when I needed it whether my troubles were academia related or life related. Thank you for making the Australian chapter of my life a memorable one. It has been an incredible ride.

I am grateful for the support staff that made the research, conferences, travel, and training throughout my PhD possible. In particular, I appreciate the dedicated work by the staff at Lizard and Orpheus Island Research Station's for supporting my six research trips. Praise must also be given to the JCU IT, Admin, and Centre of Excellence staff who provided the infrastructure and managed numerous aspects that go on behind the scenes to ensure effective research. I am thankful for the incredible photos of reef fishes that Francois Libert gave me permission to use and for the small, but valuable, piece of photography equipment donated by Don Williams at Image Science Associates. I also owe recognition to the amazing staff and participants of the various conferences and workshops I have attended: the Australian Coral Reef Society Conference, the Indo-Pacific Fish Conference, the Australian Society for Fish Biology Conference, and Transmitting Science. The environment created at these amazing venues made it easy for knowledge to be shared, new techniques to be learned, and friendships to be made.

Thank you to each unique iteration of housemates in the PhD House; from version 1.0 to 6.0. I have always placed great value in my home being a place of comfort and peace. Each iteration of the PhD House had its own unique identity and was special in its own way. In particular, I am grateful for Victor Huertas, Michalis Mihalitsis, Eric Fakan, and Taryn Laubenstein. I have many wonderful memories of our time spent conversing, drinking, playing Settlers of Catan, and watching the Wire. Much Obligated.

To the original 'Mancave' crew: Daniel Menchaca, Brandon and Jeremy Johnson, Eric Wright, Jeff Callen, Josh Rowden and Chuck Hardesty whose friendship now spans over two decades. Having a place and friend group to escape the stresses of a PhD was invaluable. I owe you all for sacrificing your own sleep schedule for the many late nights/early mornings that were spent virtually. Additionally, thank you Erin Prejean, whose friendship has now survived three continents. Your unwavering support and letting me discuss both my highs and my lows is deeply appreciated. Our reminiscing has ensured I never forget my roots.

And last, to my family. To my mother Jill, my father Greg, and my brother Michael: I could not wish for a more supportive family that has not once questioned my decision to pursue knowledge and the difficult realities that come with it. Moving to the other side of the world is not a simple choice to

make, and yet I was met with a resounding ‘yes’ when I presented this question. Dad, your curiosity for understanding how things work is inspiring, and your logical and rational approach to this understanding has been key to my success in science. Mom, your compassionate and playful nature has ensured that I never take myself too seriously in science and that I always treat people with kindness and respect, even if I may disagree ideologically. And Michael, your steadfast support has taught me to ‘stick with it’, even when things do not go according to plan – which is quite often. Thank you all for supporting me and encouraging me to achieve great things.

Statement of the Contribution of Others

This thesis was supported by funding provided to me by the College of Science and Engineering at James Cook University (two Competitive Research Training Grants). Additionally, this thesis benefitted from funding provided to David Bellwood through both the Australian Research Council's Centre of Excellence for Coral Reef Studies (CE140100020) and an Australian Research Council's Laureate Fellowship (FL190100062). My doctoral degree was supported by a Post Graduate Research Scholarship from James Cook University.

This thesis was conducted under the supervision of both David Bellwood and Peter Cowman. David Bellwood contributed substantially to the conceptual guidance, interpretation, and drafting of all thesis chapters. Peter Cowman contributed likewise, with the exception of **Chapter 5**. In **Chapter 2**, Alexandre Siqueira conducted some of the data analyses and aided in their conceptual interpretation. Similarly, Michalis Mihalitsis aided in the conceptual design and interpretation of data in **Chapter 5**. Tory Chase and Sterling Tebbett helped conduct the fieldwork and data collection for **Chapter 5**. The long term cryptobenthic fish sampling dataset and specimens used in **Chapter 5** were provided by David Bellwood.

All work reported in this thesis was conducted in accordance with the Great Barrier Marine Park Authority permit number G17/38142.1 to David Bellwood and JCU Animal Ethics Committee Approval A2529 to David Bellwood and myself.

Abstract

Coral reefs are complex systems shaped by numerous evolutionary and ecological processes. Each process introduces its own unique ‘push’ and ‘pull’ on the evolution of a given species; shaping how it ultimately behaves, interacts, and functions within its environment. Colouration is a prime example of a trait that is shaped by numerous evolutionary forces. Coral reefs are often regarded as one of the most colourful ecosystems on Earth, with reef organisms displaying a remarkable diversity of colours and patterns. However, the processes that have shaped the evolution of colouration across reef fishes, and other organisms, remain to be resolved.

This thesis investigated the complex evolutionary history and ecological relationships that shape colouration (i.e. colours and their patterns) across one of the most colourful groups of vertebrates on the planet; reef fishes. Combined, the chapters cover a broad range of questions and used multiple, complementary approaches. The specific aims of this thesis were: 1) to unravel the evolutionary history of specific colour patterns on coral reef fishes, 2) to determine in-detail how the morphology and ecology of a species shapes its appearance, and 3) to investigate the relationship between coral reef habitat features and fish colouration.

The first data chapter (**Chapter 2**) investigated the processes that shaped the evolution of reef fish eyespots at a global scale. The eyespot is a widespread and conspicuous colour pattern that has been experimentally demonstrated to reduce predation by resembling an eye. Its ease of identification makes it a perfect candidate to study colouration at a global, evolutionary scale. After surveying almost half of all coral reef fish species (42%, 2664 spp.) eyespots were demonstrated to have an extremely strong phylogenetic signal, meaning they are either very common or notably rare within specific clades. Furthermore, the presence of an eyespot and its location on the fish’s body are strongly determined by the ecology of the species, suggesting that this marking only provides a functional benefit (i.e. deterring predation) in specific, ecological contexts. But, while functional, it is not a universal solution to reducing predation.

The second data chapter (**Chapter 3**) built upon these findings and investigated in detail which morphological features shape the size and presence of eyespots in coral reef fishes. The eyespot's 'pupil' in most fish species was consistently larger than their real pupil (presumably to draw attention to it), and rarely occurs on fishes that are greater than 10 cm in length, indicating that the functionality of this colour pattern is both fish size and context dependent.

In **Chapter 4**, the focus shifted to investigate if the factors that shape the evolution of colouration in terrestrial systems are similar to those in the marine environment. Terrestrial research has demonstrated that traits important for identity (like colouration) tend to be more pronounced and different in species that evolved in sympatry (shared areas of occurrence) than in those that evolved in allopatry (different areas of occurrence) – the concept of character displacement. This was examined in reef fishes using a novel image analysis technique to compare both the colour and pattern (i.e. their colouration) of closely related butterflyfish species (family: Chaetodontidae). The quantitative evidence revealed that species in sympatry had markedly different colourations, but those in allopatry were more similar in appearance. This supports the findings from terrestrial ecosystems and identified what may be a 'universal' rule shaping colour pattern evolution across species.

The final data chapter (**Chapter 5**) explored how aspects of the local environment shape the colouration of fish communities. Multiple reef patches were surveyed that varied in their cover of different substratum types; ranging from a high cover of structurally complex coral species to habitats dominated by turf algae and coral rubble. As the cover of structurally complex corals increases, so did the diversity of colours found present in their resident fish assemblages (quantified as an 'assemblage colouration'). Conversely, as the cover of turf algae and coral rubble increased, the resident fish assemblages became more similar in appearance. Integrating our results with a long-term dataset on reef fish assemblages, collected in the same location, demonstrated that the 1998 mass coral bleaching event was responsible for a profound and significant change in the relative occurrence of different colours in resident fish assemblages. These results indicate that reef degradation may lead to less colourful coral reefs.

Chapter 6 aggregates recent methodological advances in the field of colour science. This chapter serves as a starting point for researchers entering the field of biological colour patterns. It first covers some of the key considerations that need to be made when photographing specimens for colour analyses. It then covers many of the current resources available to assess biological colouration, including both the older techniques and newer tools. Finally, it shows how these resources can be integrated to ask exciting new questions in biological colour science.

Overall, this thesis demonstrated that an organism's colouration is not simply determined by one, single process. On coral reefs, there are numerous, interacting processes that ultimately dictate a fish's colouration. Herein, phylogenetic history, morphology, behaviour, and environment have all been shown to influence the colouration of fishes; as both individual species and local assemblages. Although colouration in reef fishes is often attractive and bold, it may also provide valuable clues to the functions of colour and the role of ecology and history in shaping the beautiful fishes that characterise modern coral reefs.

Table of Contents

Acknowledgements	i
Statement of the Contribution of Others	iv
Abstract	v
Table of Contents	viii
List of Tables	x
List of Figures	xi
Chapter 1: General Introduction	1
Chapter 2: Drivers of eyespot evolution in coral reef fishes	8
2.1 Introduction.....	8
2.2 Methods	9
2.3 Results.....	15
2.4 Discussion.....	19
Chapter 3: Body size determines eyespot size and presence in coral reef fishes	26
3.1 Introduction.....	26
3.2 Methods	28
3.3 Results.....	32
3.4 Discussion.....	35
Chapter 4: The influence of range overlap and symmetry in shaping the evolution of reef fish colouration	39
4.1 Introduction.....	39
4.2 Methods	42
4.3 Results.....	48
4.4 Discussion.....	50
Chapter 5: Fish communities on coral reefs are becoming less colourful	57
5.1 Introduction.....	57
5.2 Methods	59
5.3 Results.....	64

5.4 Discussion.....	68
Chapter 6: A practical guide to analysing colours and patterns in biology: integrating theory, principles, and practice.....	74
6.1 Introduction.....	74
6.2 Methodological Approaches	77
6.3 Conclusions and Moving Forward.....	92
Chapter 7: General Discussion.....	93
References	97
Appendix A	125
Appendix B.....	134
Appendix C	144
Appendix D	159
Appendix E.....	179

List of Tables

- Table 2.1** The conflicting evidence of eyespot function. Some highlighted eyespot studies and their summarised findings. In the column ‘Study System’, an ‘A’ represents studies in aquatic systems, while a ‘T’ represents terrestrial. In the ‘Sender/Receiver’ column, the first letter presents the organism bearing the eyespot, and the second represents the intended viewer of the eyespot. An ‘I’ represents an invertebrate, while a ‘V’ represents a vertebrate..... 23
- Table 6.1** The current resources available for assessing biological colouration. For more details, see Mason and Bowie (2020) or the original publication..... 80

List of Figures

- Figure 2.1** The global distribution of coral reef fishes with eyespots. While the overall taxonomic and phylogenetic richness of coral reef fish species varies substantially among regions, the proportions of species with and without eyespots are remarkably similar. The total number of species surveyed in each location are listed and have been used to scale each chart accordingly. Black: eyespot-bearing; grey: eyespot-lacking. Throughout all figures, these colours will represent eyespot-bearing and eyespot-lacking species, respectively. 15
- Figure 2.2** The number of species, by family, with eyespots. Only families with >1 species with an eyespot have been plotted. The percentage of species with eyespots is represented by the large number above each bar. The total number of species surveyed in each family is given in parentheses. Note this is not the total number of species within each family. Three families make up 57.1% of all species with eyespots: Labridae (wrasses), Pomacentridae (damsel-fishes), and Chaetodontidae (butterflyfishes). . 16
- Figure 2.3** The evolutionary history of eyespots within coral reef fishes. The internal branches have been painted according to which trait state was estimated to have the higher probability at each node. The concentric rings represent 25 million-year increments. The full phylogeny with the exact character probabilities at each node (obtained from the 1000 averaged SIMMAPS) is available in the supporting information (**Figure A3**). 17
- Figure 2.4** The evolution of eyespots and planktivory in damselfishes. The phylogenetic tree shows the evolutionary history of damselfishes through time. Black lineages within the tree indicate a greater calculated probability of eyespot presence as determined from the 1000 averaged SIMMAPS. Grey lineages indicate a greater likelihood of eyespot absence. Black dots at the tips represent actual presence of eyespots in extant taxa; absence indicates eyespot-absence. Tips denoted by the cyan line indicate planktivorous species, tips lacking cyan represent alternative feeding ecologies (i.e. herbivory, omnivory, etc.). Note the near mutually exclusive nature of planktivory and eyespot-presence. 18
- Figure 2.5** The relationship between feeding ecology and eyespot presence. On the left, the proportion of damselfishes with (black) and without (grey) eyespots based on feeding ecology. On the right, the posterior estimate of the correlation (r) between eyespot absence and planktivory based on 50 million generations of a Bayesian MCMC. The median value of r (0.54) has been highlighted. 19
- Figure 2.6** The total heatmap for all species (**a**). Eyespot heatmaps for active (**b**) and cryptobenthic (**c**) coral reef fishes. The changing colour from red to yellow reflect the frequency of occurrence of eyespots in that location. Yellow has been scaled to represent the location of highest eyespot occurrence in each heatmap. To the right are examples of species within each category: (**b**) *Pomacentrus vaiuli* and (**c**) *Labrisomus nuchipinnis*. Photo credit: Jeffery T. Williams, Smithsonian Institute. 20

Figure 3.1 The diversity of coral reef fishes with eyespots. a) a sandperch, *Parapercis clathrata*, b) an angelfish, *Pygoplites diacanthus*, and c) a pufferfish, *Cathigaster solandri*. Photos with permission from Rick Stuart-Smith (a) and François Libert (b,c)..... 27

Figure 3.2 An example photograph from the Smithsonian Institute’s Division of Fishes Collections. On top is the raw image of *Halichoeres ornatissimus*. The scale bar has been added. In this photograph the fins are exposed, which permits morphological measurements of both the eye and, most importantly, the eyespot. In fishes with folded fins only the presence, not the size, of the eyespot can be recorded. Below are the 8 measurements (both linear and area) of the eye and eyespot features. Photo: 2006 Moorea Biocode/Jeffrey T. Williams, Smithsonian Institution. 30

Figure 3.3 Relationship between the eye area and eyespot area (left) and pupil area and the eyespot ‘pupil’ area (middle). The coloured lines represent the phylogenetic generalised least squares regression (PGLS) lines with 95% confidence intervals. The solid black line represents an isometric growth pattern; where the area of one feature (in this case, the eye) would be equivalent to the area of the other feature (the eyespot). Estimates and 95% confidence intervals (right) of the regression models slope and intercepts for eye/eyespot (red) and pupil/eyespot pupil (blue). Both comparisons have identical slopes but different intercepts indicating that these features scale in the same manner, however the eyespots pupil is consistently larger..... 33

Figure 3.4 The size distribution of individuals with (red) and without (blue) an eyespot based on 250 bootstrapped size estimates. Below are the means and 95% confidence intervals plotted for each iteration. On the right are five individuals of *Halichoeres marginatus*, a species that displays the ‘window’ of eyespot use in coral reef fishes. The number next to each image corresponds to their standard-length measurement which are plotted on the main graph. Therefore, we can see the approximate sizes in which the eyespot is gained (+) and lost (-) marked by vertical dashed lines. Photos: Jeffrey T. Williams, Smithsonian Institution. 34

Figure 3.5 Probability of eyespot occurrence with increasing fish size. 250 bootstrapped binomial glms’s displaying the relationship between standard length and the probability of having an eyespot. Each iteration’s trendline is in black, the mean of these 250 trendlines is in orange. Additionally, the raw 1140 specimen length measurements with their presence or absence (1 or 0 respectively) of an eyespot have been plotted..... 36

Figure 4.1 Four butterflyfish species comprising two species-pairs. Allopatric species a.) *Chaetodon speculum* and b.) *Chaetodon zanzibarensis*; and highly sympatric species. c.) *Chaetodon reticulatus* and d.) *Chaetodon meyeri*. Photos with permission from François Libert..... 42

Figure 4.2 The initial colour calibration technique. a) Collect images of the calibration species; in this example, *Chaetodon fasciatus*. b) Establish colours of interest to be analysed. c) Run colour detection

for each colour. The RGB centre-point and thresholds may need to be altered until images produce similar colour pattern heatmaps. d) Analyse colour areas for each image in a statistical framework, with χ^2 goodness of fit. e) Once stabilised, test the framework with other species to validate among-species applicability. 44

Figure 4.3 The rapid differentiation of colour patterns among species-pairs. a) high levels of differentiation in *C. kleinii* and *C. trichrous* which separated approximately 300,000 years. b) minimum differentiation in *C. speculum* and *C. zanzibarensis*. c) high levels of differentiation in the oldest pair *C. ephippium* and *C. semeion* which diverged 3.96 Ma. Phylogenetic generalised least squares regression (PGLS - blue line) of time of divergence against species-pair colour pattern dissimilarity. The trendline with 95% confidence intervals shows a marginally positive but non-significant slope. Each point represents the mean colour pattern dissimilarity of the 25 individual pairwise comparisons for each species-pair. 49

Figure 4.4 Phylogenetic generalised least squares regression with 95% confidence intervals displaying the relationship between range overlap, range symmetry and species-pair colour pattern dissimilarity. 51

Figure 4.5 Two examples of asymmetric range sizes. a) Peripheral speciation in *C. trichrous* (brown) vs. the widespread *C. kleinii* (yellow). The transparent brown and yellow areas help visualise the total geographic distribution of each species vs. reef-based occurrences denoted by the darker colours. The range area of *C. kleinii* is over 18x greater than the area occupied by *C. trichrous*. Although there is no overlap between these two species, their colour patterns are highly divergent. b) The entirety of *C. ocellicaudus*' range (blue) is within the range of its pair, *C. melannotus* (green), yet they retain similar colour patterns; contrary to theoretical expectations. Photos with permission from François Libert. ... 52

Figure 5.1 The 'faunal colouration' of cryptobenthic fishes at Orpheus Island. The non-metric multidimensional scaling (NMDS) ordination displays the diversity of fish colourations. Stress = 0.12. All individuals that were collected (n = 139) have been plotted. The grey, shaded area is the faunal colouration (the full convex hull area) of all individuals analysed. The species hulls for *Pomacentrus moluccensis*, *Pleurosicya* sp., *Asterropteryx semipunctata*, and *Neopomacentrus bankieri* have been delineated (all species hulls available in **Figure D5**). On the right are the vectors of the most common colours driving the distribution of individuals (and species) within multivariate colourspace. 65

Figure 5.2 The relationship between substratum type and the colour-area of the assemblage colouration, i.e. all species within a single quadrat. A quadrat with high structurally complex coral cover (**a. left**) and a quadrat completely covered in rubble and reef matrix (**a. right**). The linear regressions \pm 95% confidence intervals display the relationship between colour-area and the cover of structurally complex corals (**b. left**) and turf and rubble (**b. right**) per quadrat. The specific quadrat in **a.** has been highlighted

with the arrow in each regression. The assemblage colouration from a given quadrat (**c.** pink and pale green) is compared to the faunal colouration i.e. all individuals collected (grey)..... 67

Figure 5.3 Changes in cryptobenthic fish assemblage colourations over 27 years. **a)** the annual colour-area through time. The dashed line represents the 1998 global coral bleaching event which is followed by a major decline in the colour-area of fishes for multiple years until recovery in 2005. **b)** the decrease in abundance of yellow and green coloured fishes. The negative binomial regression model of the abundance (rounded to nearest whole number per 7m²) tracks the decline in these three, colourful species through time. 69

Figure 6.1 The importance of considering patterns. These two fish species (left – *Dascyllus aruanus* and right – a hypothetical species) possess identical colours. If only colour was measured, no distinctions would be made between these two individuals. When pattern is considered, there are clear differences that can (and do) affect their ecologies..... 76

Figure 6.2 How various photographic properties can alter an organism's appearance. The top row is the same image of *Neamia octospina* (with the background removed) that has been altered in various ways. The middle row shows the RGB values of 100,000 randomly sampled point from each fish. The bottom rows show the number of pixels that fall into 8 major colour categories determined by splitting the RGB colour space into 8 cubes of equal area. **a)** an image in the common .jpg file format displaying extreme colour manipulation performed in-house by the camera. In this example, the subject is extremely red; much more than is typical in life. **b)** the raw image of *N. octospina*, however the image is severely underexposed making the subject appear much darker. **c)** the same subject but overexposed. **d)** properly exposed, and **e)** a properly exposed and colour corrected image; the desired product for all images. The histogram has slightly changed from **d)**, reflecting minor differences in the colour of the fish due to correction protocol. 78

Figure 6.3 Some examples of the alterations that can be made to images prior to analysis. **a)** changing the colours within an image to reflect a viewer's spectral sensitivity. **b)** adjusting an image to reflect a given viewers visual acuity. **c)** cropping a subject and placing it onto a solid-coloured background. **d)** defining a region of interest (ROI) for analysis in the MICA toolbox or placing landmarks. These techniques are not mutually exclusive and can be combined depending on the research question..... 82

Figure 6.4 Modelling the visual acuity of a predatory coral reef fish using AcuityView. On the left is the original image as captured by the camera. On the right is the simulated image according to the visual acuity of a common predatory coral reef fish (*Cephalopholis miniata*). It becomes evident that the small prey fish (*Eviota guttatus*) is harder to detect than is shown in the original image. The distance between the predator and prey fish is assumed to be 1m. Note, the colours have not been altered based on the Coral grouper's spectral sensitivities. 83

- Figure 6.5** What technique should you use to answer your research question? 85
- Figure 6.6** Three different ways to represent colours. a) colours represented in the RGB colourspace. This colourspace is most often used to display colour in computer graphics. b) colours represented as a wavelength distribution which displays the relative amount of light at each wavelength. c) colours represented by how strongly they stimulate various photoreceptors. In this example, the viewer has three photoreceptor types that are sensitive to short (S), medium (M), and long (L) wavelengths (identical to human visual systems)..... 86
- Figure 6.7** The nest of a Killdeer (*Charadrius vociferus*). This bird lays eggs directly on the ground without constructing a nest. Therefore, the eggs rely heavily on camouflage to protect them from potential predators. 87
- Figure 6.8** Different metrics for characterising the colourations of a group of organisms. a) colour area: the area of the convex hull. This approach is sensitive to outliers, i.e. very unique coloured organisms. b) colour spared: the average difference between colourations. c) colour density. The metric identifies the most common colourations found within an assemblage. 88
- Figure 6.9** An example of how to use patternize to test ecological hypotheses. 1) establish a hypothesis to test. In this hypothetical example, anecdotal evidence suggests that populations of butterflies living in more disturbed forests may have different colourations. 2) collect individuals from each location, take photos, and place landmarks. Perform patternize analyses to 3) visualise the data and test hypotheses. Colour patterns for all butterflies photographed were visualised using an ordination. Differences between the two groups (old growth forest vs. disturbed) were tested using a PERMANOVA. A significant difference was found ($p\text{-value} < 0.05$) indicating that there are differences in colouration between the two groups..... 91

Chapter 1: General Introduction

The ecological and evolutionary context of colour

The mosaic of various colours and patterns found in the natural world is striking. Every organism possesses its own unique colouration (i.e. the combination of colours and patterns) that confers various fitness costs and benefits. When comparing the colouration of all organisms within an ecosystem, one can quickly see various themes emerge. Some species have a highly cryptic colouration that closely matches the background of their native environment (Endler 1978; Kelley et al. 2017; Merilaita et al. 2017). Others possess bright colours and patterns that signal their presence to others (Caro and Ruxton 2019). Others fall in-between, showing colourations that combine various aspects of the previous two strategies (Cuthill et al. 2017). Unsurprisingly, these different colourations are often tightly linked to an organism's ecology; reflecting how it behaves and interacts within its environment.

The fitness benefits that colouration can provide are manifold and exist on numerous biological scales. Most fundamentally, colouration allows for the capture of energy from light. This gives plants the ability to photosynthesize (Lambers et al. 2008) and darker coloured organisms the ability to more easily maintain higher body temperatures (Zeuss et al. 2014). At the organismal level, colouration can provide camouflage from predators (Merilaita et al. 2017; Stevens and Ruxton 2019), relay information about an individual's health (Hill et al. 2002), and aid in mate selection and signalling (Reynolds and Fitzpatrick 2007; Kelley et al. 2019). At the population and community level, colouration can help establish and maintain species boundaries (Puebla et al. 2007). This widespread utility makes colouration a critical component of an organism's life history strategy.

Although infinite possibilities of colours and patterns theoretically exist, natural selection favours those that serve specific, and often multiple, functions. Colouration appears to be under constant, strong, selection. Even in environments that lack light, and subsequently colour, entirely (like the abyssal depths of the ocean or deep within caves), selection has favoured the convergent loss of costly yet non-functional pigmentation. Consequently, most organisms in these environments are white or translucent

in colour (Romero and Green 2005; Rogers et al. 2012; Soares and Niemiller 2020). Metaphorically, colours represent a painter's palette, evolution via natural selection – one of the painters.

What, then, are the processes that underpin an organism's colouration? Although a seemingly simple question, the answer is far more complex. Unlike the white and translucent cave-dwelling organisms, we have learned that the colouration of light-experiencing organisms is not simply the product of a single, selective force. As with most traits, multiple forces act upon colouration – each shaping its final appearance in their own specific way (Kelley et al. 2016). Therefore, the colouration of an organism is a compromise between these, often opposing, evolutionary forces. This trade-off was clearly demonstrated by John Endler working on Trinidadian guppies (*Poecilia reticulata*; Endler, 1978, 1980). Endler showed that the 'gaudiness' of a given population of guppies in the wild was directly correlated with the density of co-occurring predators. As predator densities decreased with altitude, i.e. higher up in the mountain streams, the population of male guppies became more colourful – a pattern driven by sexual selection by females which prefer gaudy males (Kodric-Brown 1985). The colouration of these guppies exists on a simple continuum from dull to colourful. The exact position where an individual falls on this continuum is dictated by the trade-off between predation pressure and sexual selection.

For most other organisms, this continuum is far more complex and extends along other axes of interaction. Alfred Russel Wallace, a 19th century naturalist and pioneer in the field of evolution, identified five potential functions that a specific colouration may provide: 1) protective colours, 2) warnings colours, 3) sexual colours, 4) typical colours, and 5) attractive colours (Wallace 1877). Despite being established almost 150 years ago, many of these groups are still used today (Caro 2017), although some have been expanded upon or subdivided to provide higher levels of detail (Caro and Allen 2017; Caro and Ruxton 2019; Caro and Mallarino 2020). While these categories are useful, it is becoming increasingly apparent that an organisms colouration can – and often does – serve numerous functions simultaneously (Marshall 2000b; Cuthill et al. 2017).

In this regard, coral reefs offer an extremely interesting ecosystem in which to study colour. The diversity of colours and patterns found on coral reefs is profound, earning them a reputation as one of

the world's most colourful ecosystems. Interestingly, this diversity of colours and patterns suggests that many of the traditional 'rules' that dictate an organism's appearance, described from other ecosystems, are not as widely applicable on coral reefs. For example, the bright and conspicuous colouration of poison dart frogs (family: Dendrobatidae) serves as a clear advertisement of their noxious composition (Summers and Clough 2001). These frogs contain toxic compounds capable of causing illness or in extreme cases, death for most animals that ingest the frog. Many reef fishes possess the same bright colours found on these frogs (vibrant blues, yellows and reds) but they are not toxic, suggesting that these colours may serve a fundamentally different role in reef ecosystems (Rocha et al. 2020). This notion was highlighted by Marshall (2000b) who showed that the bright yellow and blue colours found on many reef fishes serves two unique functions: signalling and camouflage (Marshall 2000b). Although poison dart frogs and coral reef fishes both use bright yellow as a clear signal to other organisms, the use of bright yellow for camouflage on coral reefs is completely unique. This is just one instance where the rules that dictate colouration on reefs (and more broadly, in aquatic environments, e.g. Kelley et al. 2012) may differ from those in terrestrial systems (Marshall 2017). There are almost certainly numerous processes shaping colouration on coral reefs that have yet to be described, offering much promise in the field of colour research (Marshall et al. 2018b).

Methodological challenges

If we are to ask questions about colouration, its function, and that factors that shape it, we need effective tools to characterise and measure it. Colouration is inherently difficult to study due to its subjective nature. Since humans have highly adept visual systems relative to many other organisms (Caves et al. 2018), we have long been able to comment on and hypothesize about the function that a specific colour pattern may serve for its bearer (Wallace 1877; Caro 2017). However, even in the earliest years of modern natural sciences, it was recognised that we need to remain cautious in how we interpret colouration. Variation within the perceptive abilities among individuals or between taxa prevented consistent, quantifiable, descriptions of colouration (Endler 1990; Caves et al. 2019). Most early studies could only describe obvious patterns (e.g. mottled or banded) and make comparisons with common colours seen in everyday life (e.g. 'cream' coloured; Longley, 1917). But even these are mired in

subjectivity. Indeed, as noted by Longley (1917) when visually assessing the colouration of coral reef fish specimens, “the method is crude; allowance for the personal equation of the observer must be large”.

Accurate quantitative classification of colours first became attainable with the advent of spectrometers. Visible light is broadly defined as the wavelengths (λ) that are detected by most vertebrates, which roughly falls between 400 – 700 nanometres (Kelber et al. 2003). Spectrometers operate by detecting the intensity of reflected electromagnetic radiation at various wavelengths (Johnsen 2016). This method provides the most fundamental measurement of light based on its physical properties: by quantifying the concentration of photons at each wavelength. While this is by far the most accurate method for characterising and measuring colours, it does possess setbacks. Reflectance curves must be remeasured for each specific location on an individual, making it both labour- and equipment-intensive (Stevens et al. 2007). Furthermore, these measurements only inform us about the colour of a specific point on an organism’s body which is assumed to be ecologically or behaviourally relevant (Dalrymple et al. 2015b). Most importantly, spectrometers do not provide any information about patterns, leaving the description of this component up to the viewer (i.e. humans).

Thus, it is critically important to make the distinction between colours and patterns. While colours represent the specific wavelength of light reflected or emitted by a surface (what humans would call red, for example), patterns are the organisation of colours within a spatial context (a red dot for example; Endler 1978). In line with the previous metaphor, colours are the ‘paint’, while an organism’s pattern would be the finished ‘painting’; the exact composition of colours arranged in a spatial context. Indeed, making this distinction and thinking about patterns as a hierarchical tier above colours is necessary when investigating colouration through an ecological or evolutionary lens. How colours are specifically arranged into patterns is critically important in determining how they function for many organisms (Umeton et al. 2019). The term ‘colouration’ is therefore used herein to signify both the colours and the patterns they create. For example, the vertical bands on the banded humbug damselfish (*Dascyllus aruanus*) appears to most successfully reduce predation when they closely match the width of the coral branches in which it lives (Phillips et al. 2017). Similarly, cleaning behaviour on reefs is strongly indicated by the colours blue and yellow, and specifically when these colours are present in horizontal

stripes along the length of the fish (Cheney et al. 2009). Essentially, patterns give colour context. Therefore, considering both the colour and pattern (the colouration) is critical when interpreting the specific function(s) that a certain colouration may serve.

Characterising the wavelength sets clear definitions of what comprises a specific colour (e.g. red being 630 to 700 nm). Patterns, however, are far more abstract. For example, what is the difference between a line, stripe, or band? Humans have established definitions for some of the common and widespread colour patterns (Kelley et al. 2013; Miyazawa 2020) like eyespots, for example (which are studied herein). However, more complex colourations do not conform to such discrete, anthropocentric, classifications and consequently, often lack an obvious ‘category’ to be placed within. Many coral reef fishes exemplify this notion. Parrotfish in the genus *Scarus*, for example, have some of the most complex colourations found on corals reefs (Marshall 2000a) making them far too difficult to categorise simply. Therefore, assessing the often-complex colouration found on many reef fishes requires new and innovative approaches.

In this respect, digital photography makes the objective description of colour patterns far more tenable. As opposed to the point-by-point measurements made using spectrometry, digital photography works by capturing the available light within a scene. This allows for large amounts of information to be recorded in intuitive formats that can be repeated quickly and efficiently. Importantly, images contain information about the spatial arrangement of colours meaning they also capture information about patterns. Digital images therefore offer an exciting medium with which to investigate organismal colours and patterns. There has been a recent surge in the resources available that use image analysis approaches to analyse colourations (Caves and Johnsen 2018; Van Belleghem et al. 2018; Van Den Berg et al. 2019). Recently developed toolkits available in open-source software (Schneider et al. 2012; R Core Team 2020) allow researchers to objectively explore colour patterns in ways that have not been considered previously, opening the door to countless new research questions.

Thesis outline

This thesis uses a range of novel approaches and techniques to investigate the evolutionary and ecological relationships of colour patterns in coral reef fishes. The chapters herein follow a natural progression that gradually transitions from questions that are global in scope, evolutionary in nature, but limited in detail, to questions that are local in scope, ecological in nature, with extremely fine resolution. In my first data chapter, **Chapter 2**, I seek to identify the factors that have shaped the evolution of colouration across the global reef fish community. To circumvent the issue of image accuracy for such a large set of species, I focus specifically on a widespread and functionally important colour pattern: the ocellus or eyespot. This marking strongly resembles a vertebrate eye making it easy to identify on fishes even when image quality is limited. I surveyed over 2,500 species of reef fishes from all global reef locations to identify the evolutionary and ecological factors that shape its occurrence. In **Chapter 3**, I dive into further detail investigating exactly how morphology can shape colouration by again using eyespots as a model study system. However, in this chapter I move beyond the discrete categorisation scheme used in the previous chapter (presence vs. absence) and measure features of the eyespot and relate these to the morphology of their bearers. Importantly, I identify assumed fitness costs associated with possessing this marking to identify when it may no longer serve its intended function.

In **Chapter 4**, I transition to focusing on a specific reef fish family to ask how co-occurrence between sister species cause reef fishes to differentiate in colour. Terrestrial research has demonstrated the concept of reproductive character displacement; a phenomenon in which traits important for reproduction are selected to differentiate when closely related species co-occur. Using an innovative new application that characterises both colour and pattern, I assess whether reproductive character displacement is occurring in butterflyfishes (family: Chaetodontidae), an iconic family of reef fishes found all over the globe. In the final data chapter, **Chapter 5**, I focus on ecological factors that may be responsible for supporting colourful reef fish assemblages and how these relationships might change in response to global environmental disturbances. In this chapter, I investigate the relationship between fish colouration and the composition of the substratum, using complete fish assemblages (photographing

all individuals in-detail) and relating their colouration to the different substratum types where the fishes live (e.g. live branching coral, rubble, etc.).

Finally, in **Chapter 6**, I aggregate all the tools and machinery available to analyse biological colouration. This chapter is essentially a 'how-to' guide that summarises the different approaches I used throughout my dissertation. It addresses 1) the considerations that must be made when analysing colour patterns, 2) the resources currently available for colouration analyses and, 3) some of the questions that can be asked when taking colour pattern research into new and exciting areas of study.

Chapter 2: Drivers of eyespot evolution in coral reef fishes

Published as: Drivers of eyespot evolution in coral reef fishes. *Evolution*. (2021).

2.1 Introduction

The colouration of an organism is often tightly linked to its life history strategy; reflecting how it behaves and interacts with other organisms and its environment (Endler 1992; Caro and Allen 2017). Specific colourations can aid in creating and maintaining species boundaries (Seehausen 1997; Hemingson et al. 2019; Hench et al. 2019), facilitate mate selection (Reynolds and Fitzpatrick 2007), indicate fitness (McGraw et al. 2002), or provide protection from predators through camouflage (Cortesi et al. 2015; Phillips et al. 2017). Across all groups of organisms, coral reef fishes stand out as one of the most colourful and diverse found on the planet (Marshall 2000a; Marshall et al. 2018b). This unrivalled diversity in colouration has garnered the interest of researchers since the dawn of modern ecology. However, due to the intricate relationship between the light environment (i.e. the available light in a scene) and a viewer's perceptive abilities (i.e. what they can and cannot detect or perceive), colouration becomes increasingly difficult to study at broader scales across many taxa (Caves et al. 2019). To overcome this challenge, one of the most promising avenues is to examine specific aspects of colouration at large evolutionary scales (Ortolani 1999; Caro 2005; Dalrymple et al. 2015b; Salis et al. 2018; Wisocki et al. 2019).

The eyespot, or ocellus, is well suited to investigate some of the evolutionary drivers of colouration on coral reefs. From a human perspective, this marking strongly resembles a typical vertebrate eye; with a dark, circular interior surrounded by a lighter, often white, ring (Poulton 1890; Blest 1957). In both terrestrial and aquatic ecosystems, eyespots are widespread with numerous examples in insects, molluscs, crustaceans, birds, and fishes. Eyespots have been shown to provide a range of potential fitness benefits (Stevens and Ruxton 2014), including conspecific communication (Gagliano 2008; Gagliano and Depczynski 2013), enhanced reproductive success (Robertson and Monteiro 2005; Theis et al. 2012) and, most commonly, enhanced survival (Winemiller 1990; Stevens 2005). Despite these advantages, only a minority of fish species have eyespots. This raises the question:

what evolutionary and ecological drivers promote or impede eyespot presence? As one of the most iconic colour patterns involved in predation avoidance, this topic is central to our understanding of the function of colouration in animals.

Although widely studied (Lyytinen et al. 2004; Stevens 2005; Merilaita et al. 2011), relatively few studies have investigated eyespots from a broad phylogenetic or evolutionary perspective (but see Kelley et al. 2013; Kodandaramaiah et al. 2013; Hossie et al. 2015; Ho et al. 2016). Most eyespot research has been experimental, using a small subset of all eyespot-bearing taxa (e.g. Merilaita et al. 2011; Hossie and Sherratt 2013; Olofsson et al. 2015). While these experiments have been invaluable in establishing the functional role of eyespots, numerous broad-scale questions still remain. For example, do eyespots have a geographic or phylogenetic bias in their occurrence? Where are eyespots distributed on the organism's body and, more importantly, does this relate to the ecology and behaviour of the species that bear them? Essentially, are there basic rules that govern when, where, and on who eyespots occur?

Here, we examine the potential factors that determine the evolution and possible function of eyespots in coral reef fishes. Specifically, we aim to determine how widespread eyespots are within coral reef fishes, how often this pattern has arisen and where they occur on the body of these species. Finally, we relate the presence/absence of eyespots, as well as their location, to the ecology of the species to identify what suite of ecological characteristics may favour their occurrence. The overall goal is to shed light on how these various processes have shaped the evolution and ecology of eyespots in one of the most colourful groups of organisms on the planet.

2.2 Methods

Coral reef fish survey

We conducted an extensive survey to determine which reef fish taxa have eyespots within four distinct biogeographic regions (sensu Kulbicki et al. 2013; Cowman et al. 2017): the Tropical Atlantic (specifically, the Caribbean), the Indian Ocean and Red Sea, the Great Barrier Reef and Coral Sea, and the Tropical Eastern Pacific (**Figure 2.1**). Collectively, these four regions contain approximately 42%

of all described coral reef fish species (Kulbicki et al. 2013; Parravicini et al. 2013) and represent a broad subset of all coral reef fishes globally. Additionally, these regions are geographically distinct, allowing us to determine if the development and presence of eyespots are globally ubiquitous or geographically constrained.

Species were placed into one of two categories: eyespot-bearing or eyespot-lacking. We defined an eyespot based on three criteria: 1) the marking is approximately circular or elliptic in shape, b) it has a dark (typically black) interior surrounded by no less than 75% of its circumference by a concentric ring of differing, much lighter colour (typically white), and c) there could be no more than 10 eyespots present on one side of the individual (following Hemingson et al. 2020). Where possible, juvenile life stages were included as some species only possess this marking at certain life-stages. The proportion of species with and without eyespots (at any life-stage) were then compared between realms to identify if eyespots are more or less common in taxa from a given geographic location.

Phylogenetic distribution and ecological relationships

The presence or absence of eyespots was then mapped onto a phylogeny of reef fishes to assess their evolution and phylogenetic signal. The largest published fish phylogeny using both molecular data and fossil calibrations (Rabosky et al. 2018) was trimmed to contain only the coral reef fish species for which eyespot data were collected. Since detailed evolutionary relationships are critical for subsequent analyses based on trait evolution (Rabosky 2015), only species with molecular data were included. This tree, therefore, contains a subset of the species in the eyespot dataset (58%; 1544/2664). This tree contained all consensus list families that characterise coral reefs (Bellwood and Wainwright 2002). Using this coral reef fish phylogeny, we plotted the distribution of eyespots and mapped their evolution using stochastic character mapping following Bollback (2006), within the ‘phytools’ library in R (Bollback 2006; Revell 2012). Additionally, we calculated the phylogenetic signal relating to eyespot presence, by analysing multiple models of discrete character evolution and selecting the most parsimonious based on AICc (model comparison in **Table A1**). The most parsimonious model incorporated the lambda parameter (λ ; Pagel 1999), which gives a robust estimate of the phylogenetic signal for a given trait (in our case eyespots Münkemüller et al. 2012; Molina-Venegas and Rodríguez

2017). If lambda is low (e.g. 0.1), the presence of eyespots is essentially randomly distributed across species within the phylogeny. If lambda is high (e.g. 0.9), it indicates a highly-structured distribution within the phylogeny. Furthermore, the model using the resulting value of lambda (λ) was tested against a model in which lambda was set to 0 (i.e. no phylogenetic signal). These two models were then compared using a likelihood ratio test to determine if there was a significant phylogenetic signal.

To reconstruct the evolution of eyespots, 1000 stochastic character maps (SIMMAP; Bollback 2006) of eyespot evolution were generated (using the ‘ape’; Paradis and Schliep 2019 and ‘phytools’; Revell 2012 libraries in R). The model also estimated different transition rates to and from eyespot-bearing and eyespot-lacking states (specifically, ‘ARD’ in phytools: ‘all rates different’). Furthermore, we generated the Q matrix using the ‘empirical’ method within phytools, which is very similar to the original procedure that first introduced stochastic character mapping (Bollback 2006). Finally, we allowed the model to freely estimate the probabilities of each trait state at the root of the tree, instead of forcing each trait state to have equal probabilities (the default). This was important, since the freely estimated root probabilities (eyespot presence: 8%, eyespot absence: 92%) were markedly different from the default expectation of fixed probabilities (50% – 50%). We then averaged all 1000 SIMMAP iterations to calculate the likelihood of each trait state at ancestral nodes throughout the phylogeny. This approach was used to interpret trait evolution across all species in the molecular phylogeny, as well as specifically focusing on damselfishes.

Previous research has shown that exposure in the water column (the amount of ‘openness’) increases the likelihood of being consumed (Mittelbach 1986; Lester et al. 2020). Therefore, planktivorous species - those that feed exposed in the water column farther away from structural refuges - are presumed to have a higher predation risk than other feeding ecologies (e.g. herbivory). We were curious if this influences the presence of eyespots, which have been shown to provide anti-predatory benefits (Kjærnsmo and Merilaita 2013; Prudic et al. 2014). To explore the potential role of position in the water column (and the implied increase in predation pressure; Motro et al. 2005) on eyespot presence, we quantified if the presence or absence of eyespots in reef fish is linked to specific feeding ecologies. Damselfishes were specifically selected as the focal group because they have a large number

of surveyed species in the phylogeny (147 spp.) and have many species that are planktivorous – a feeding mode that implies high predation risk. (Froese and Pauly 2019). We collected feeding ecology data (a proxy for position within the water column and exposure) for the 147 species of damselfishes present in the molecular phylogeny (i.e. with eyespot data).

To identify any correlations, we used two complementary approaches. First, we used the Bayesian framework of BayesTraits (Meade and Pagel 2019) to compare dependent vs independent models of trait evolution. Since these models only support discrete, binary traits (presence/absence), we classified the damselfish feeding ecology as: planktivorous or non-planktivorous. These groupings were chosen as they represent the largest difference in exposure that individuals would likely incur while feeding. All other possible feeding ecologies (herbivory, detritivory, sessile-invertivory, etc.) represent modes that feed directly on or close to the substratum. We thus applied BayesTraits to assess whether the evolution of eyespots was correlated with the evolution of feeding ecology. We ran both dependent and independent models of discrete trait evolution for 50 million iterations each, sampling parameters every 5,000 iterations. Both models were run using the VarRates option (Venditti et al. 2011) which accounts for heterogeneity in evolutionary rates within the phylogeny. We also used the rjMCMC option with an exponential prior to handle the high number of parameters in the models (Meade and Pagel 2019). After removing 10% of samples as burn in, we assessed convergence through effective sample sizes. Subsequently, we assessed the marginal likelihood of each model through the stepping stone sampler (Xie et al. 2011). The marginal likelihood was then used to compare models through the Bayesian Information Criterion (BIC).

After finding that the dependent model of evolution performed far better than the independent one ($\Delta \text{BIC} > 23$), we applied a quantitative threshold model to quantify the extent of correlated evolution (r) between different discrete traits (Felsenstein 2012). A Bayesian threshold model was generated using the ‘threshBayes’ function within the ‘phytools’ library in R (Revell 2012). This model was run for 50 million generations and sampled at 5,000 generation intervals yielding 10,000 samples per chain (three chains total). The first 10% of each chain was discarded as burn in. Trace plots identified

optimal convergence and mixing, and the effective sample size of both the log likelihood estimate (455) and correlation coefficient (372) were well above generally accepted cut-offs (>200).

Eyespot heatmaps and distribution

Heatmaps were constructed to provide a high-resolution map of eyespot locations across the bodies of coral reef fishes. All species across all families that were identified to have an eyespot were checked for images in a staged, lateral position available in either the Smithsonian Institute's Division of Fishes Collections or Williams et al. (2010). Only high-quality images were included in the heatmap analysis (species included listed in **Table A2**). Using Adobe Photoshop (CC2019), all images were converted to grayscale. Then, for every image, the entire eyespot was manually coloured using the paintbrush tool. We used red, although the specific colour is irrelevant so long as it is not grayscale and is the same colour used in all photos. This yielded a dataset of images in which the fish's body was grayscale, yet the eyespot was coloured. Using 'patternize' (Van Belleghem et al. 2018), a toolkit to compare colour patterns in animals, heatmaps were created that display the distribution of eyespots across the body of fishes. Functions within 'patternize' align images based on morphological landmarks that have been placed using imageJ (Schneider et al. 2012). Thus, the final summarised output displays the distribution of eyespots in a morphologically consistent framework across species. We used 20 landmarks to align the images (following Hemingson et al. 2019, landmarks shown in **Figure A1**) that accurately capture broad morphological variation. This allowed us to compare the distribution of eyespots across the bodies of all species.

There is a connection between the location of an eyespot and its function as deflective eyespots are expected to divert attacks towards them, away from vital body locations (Kodandaramaiah et al. 2013). We were therefore curious if the location of this marking may reflect this difference in coral reef fishes. To classify the location of an eyespot, we divided the body of every fish in half by extending a vertical line upwards from the base of the first anal fin spine and perpendicular to the midline (for details see **Figure A2**). This allowed us to classify if eyespot was located on the anterior or posterior section of the body. This landmark was chosen because it is present in all species surveyed, represents a relatively

consistent half-way split of the body of most reef fishes, and can be easily identified and located across species.

The location of the eyespot was then related to the ecology of the eyespot-bearing species. We classified the species based on a major ecological axis: being cryptobenthic (resting directly on/within the reef substratum) or active swimmers living off the benthos. This is a robust division with clear delineation that can be applied to all reef fish species. Brandl et al. (2018) provide a quantitative definition of cryptobenthic fishes, which are smaller fishes (10% of species in families with <50 mm maximum body length) that are benthic in nature. We utilise this definition to classify species herein but extend it to include highly cryptic and benthic species that may reach lengths greater than 50 mm TL (e.g. *Parapercis clathrata*; list of species classifications in **Table A2**). These alternative habitat-use lifestyles have been shown to be clearly linked to many other differences in life history traits (Koslow 1996). Fish were thus characterised based on two features: (1) having an eyespot in the front or back half of their body and (2) being either cryptobenthic or active. If the eyespot split the dividing line, the location was categorised based on which half possessed the majority of the marking. This generated two sets of binary variables: benthic vs active and eyespot anterior vs posterior.

Since both of these traits are phylogenetically conserved, the correlated evolution of these variables were then analysed following the methods described by Pagel (1994). This method compares competing models in which the evolution of two binary traits are either independent or dependent. Furthermore, the direction of dependence can be specified. We generated and tested three possible dependent models: the first specified that the evolution of eyespot location is dependent upon swimming activity. The second model is the reverse: that swimming activity is dependent on eyespot location. The final model assumes these two traits are co-dependent and have evolved together. The most parsimonious model was selected using AIC and compared to the independent model using a likelihood-ratio test. This was implemented using the 'fitPagel' function in the 'phytools' library in R (Revell 2012).

2.3 Results

In total, 2664 coral reef fish species were surveyed from the four major marine realms. We identified 282 species with eyespots (10.59 %). The Tropical Eastern Pacific displayed a significantly smaller proportion of species with eyespots (5.8%) when compared to the Indian Ocean (9.7%) and the Great Barrier Reef and Coral Sea (9.9%). The Tropical Atlantic, had an intermediate proportion of species possessing eyespots (8.9%) but it was not significantly different from the three other locations (**Figure 2.1; Table A3**).

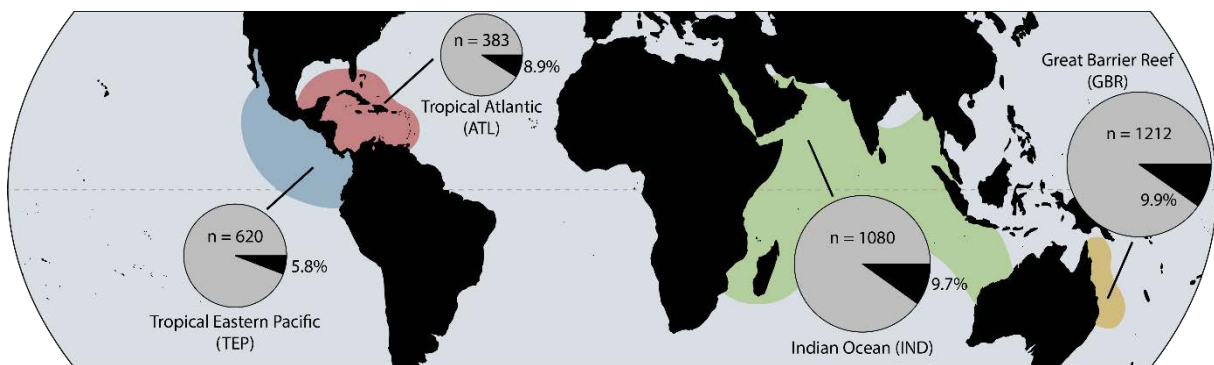


Figure 2.1 The global distribution of coral reef fishes with eyespots. While the overall taxonomic and phylogenetic richness of coral reef fish species varies substantially among regions, the proportions of species with and without eyespots are remarkably similar. The total number of species surveyed in each location are listed and have been used to scale each chart accordingly. Black: eyespot-bearing; grey: eyespot-lacking. Throughout all figures, these colours will represent eyespot-bearing and eyespot-lacking species, respectively.

Phylogenetic patterns of eyespot occurrence

Eyespots were found in 31 reef fish families and have arisen at least eight times in deep evolutionary time (>10 mya based on ancestral reconstruction estimates from the 1000 averaged SIMMAPs). Most of these events occurred between 20 and 60 million years ago. Three families have a particularly high proportion of species with eyespots: Labridae (wrasses, 33.3%, 82/246), Pomacentridae (damselfishes, 23.9%, 42/176) and Chaetodontidae (butterfly- and bannerfishes, 28.7%, 37/129; **Figure 2.2**). Interestingly, other common coral reef fish families have no or very few species possessing eyespots. Only two species of acanthurids (surgeonfishes) and no species of siganids

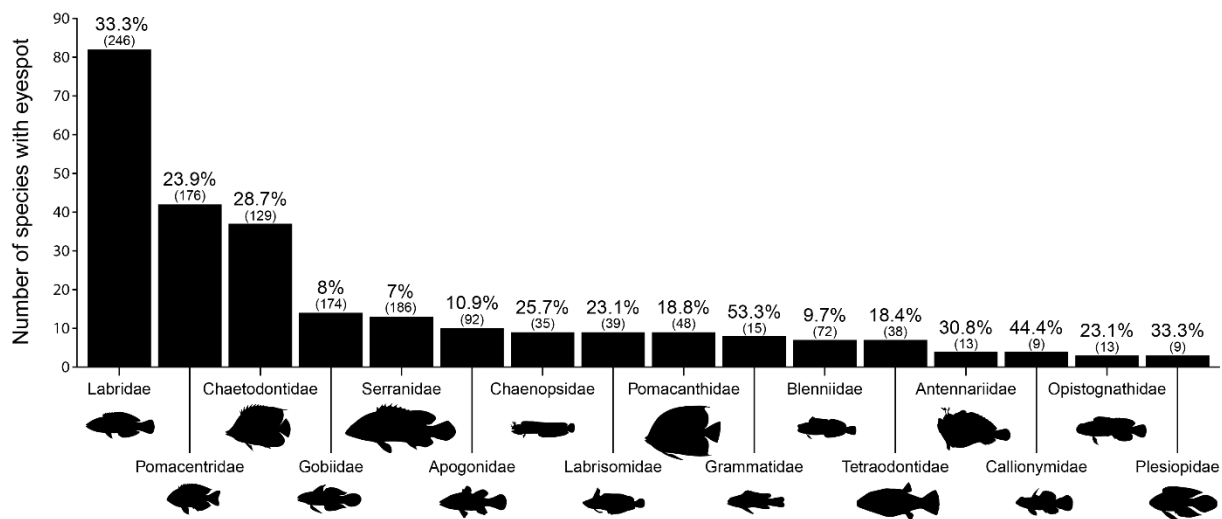


Figure 2.2 The number of species, by family, with eyespots. Only families with >1 species with an eyespot have been plotted. The percentage of species with eyespots is represented by the large number above each bar. The total number of species surveyed in each family is given in parentheses. Note this is not the total number of species within each family. Three families make up 57.1% of all species with eyespots: Labridae (wrasses), Pomacentridae (damselfishes), and Chaetodontidae (butterflyfishes).

(rabbitfishes) have this marking. Analysing the distribution of eyespots throughout the phylogeny showed that eyespots are highly conserved within clades (**Figure 2.3**). The most parsimonious value of lambda (λ), i.e. the strength of phylogenetic signal for eyespots, is 0.93 and significantly differed from 0 (likelihood ratio = 267.025, p-value <0.0001). This demonstrated that having an eyespot is very strongly correlated with a species' position within the phylogeny. Essentially, eyespots were not randomly distributed throughout the reef fish phylogeny and occurred in a highly structured manner, predominantly within specific lineages.

Within these three eyespot-rich families (Labridae, Pomacentridae, and Chaetodontidae), there are further, distinct patterns of presence and absence. At the genus level, eyespots were found to be either very common or notably absent. In pomacentrids, for instance, the genera *Chromis*, *Abudefduf*, and *Amphiprion* have no species possessing eyespots, while in other genera like *Pomacentrus*, *Parma*, *Stegastes*, and *Dichistodus*, eyespots are extremely common (**Figure 2.4**). Investigating the associations between feeding ecology and eyespot occurrence in detail showed a moderate amount of correlated evolution (median $r = 0.54$; **Figure 2.5**). Approximately 44.1% (30/68) of non-planktivorous

pomacentrid species possess an eyespot while in planktivores the marking is extremely rare (1.3%, 1/79).

Eyespot location

The distribution of eyespots across the bodies of coral reef fishes was highly conserved. The location with the most frequent occurrence of eyespots was along the dorsal fin (**Figure 2.6**). Within

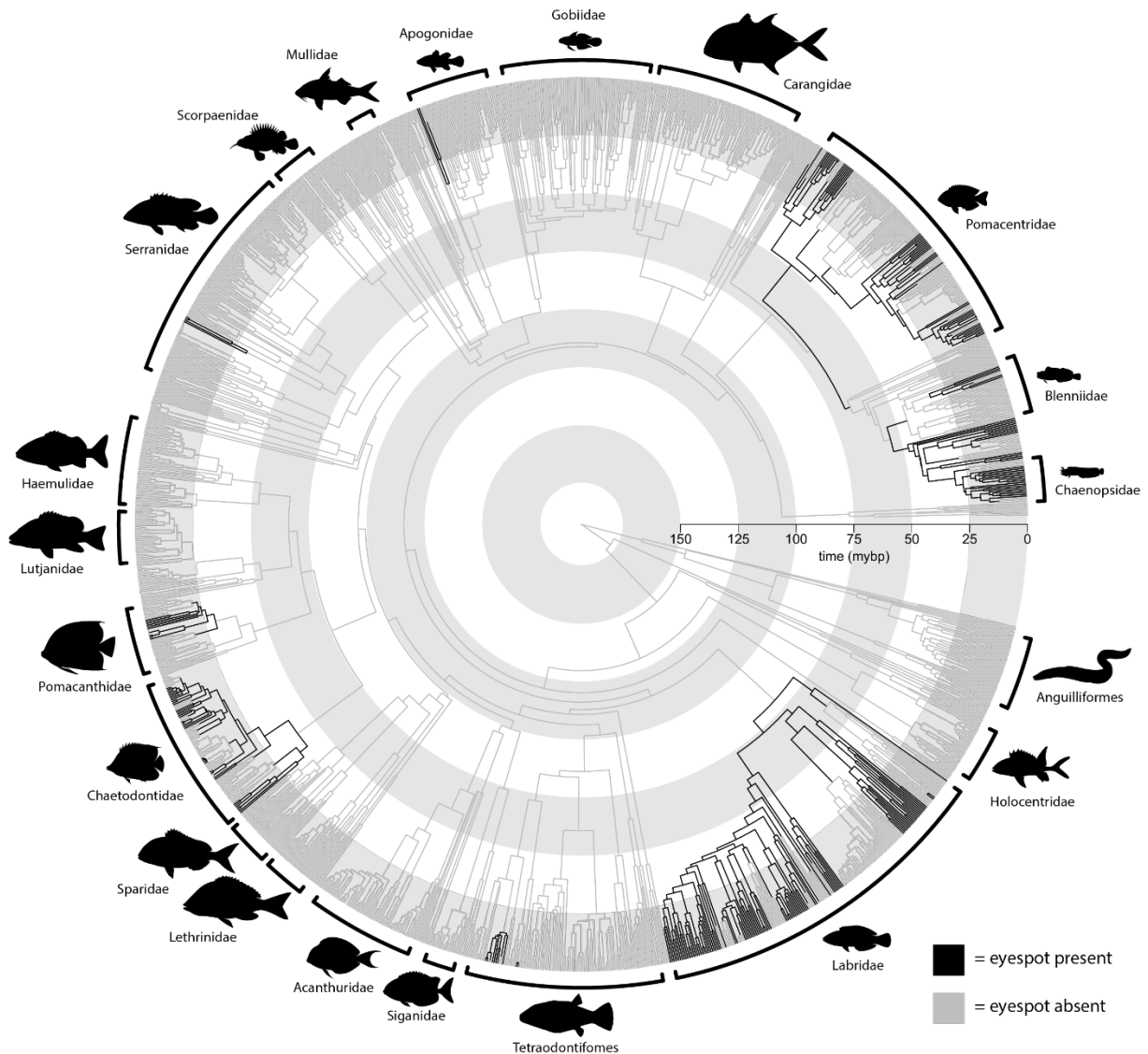


Figure 2.3 The evolutionary history of eyespots within coral reef fishes. The internal branches have been painted according to which trait state was estimated to have the higher probability at each node. The concentric rings represent 25 million-year increments. The full phylogeny with the exact character probabilities at each node (obtained from the 1000 averaged SIMMAPS) is available in the supporting information (**Figure A3**).

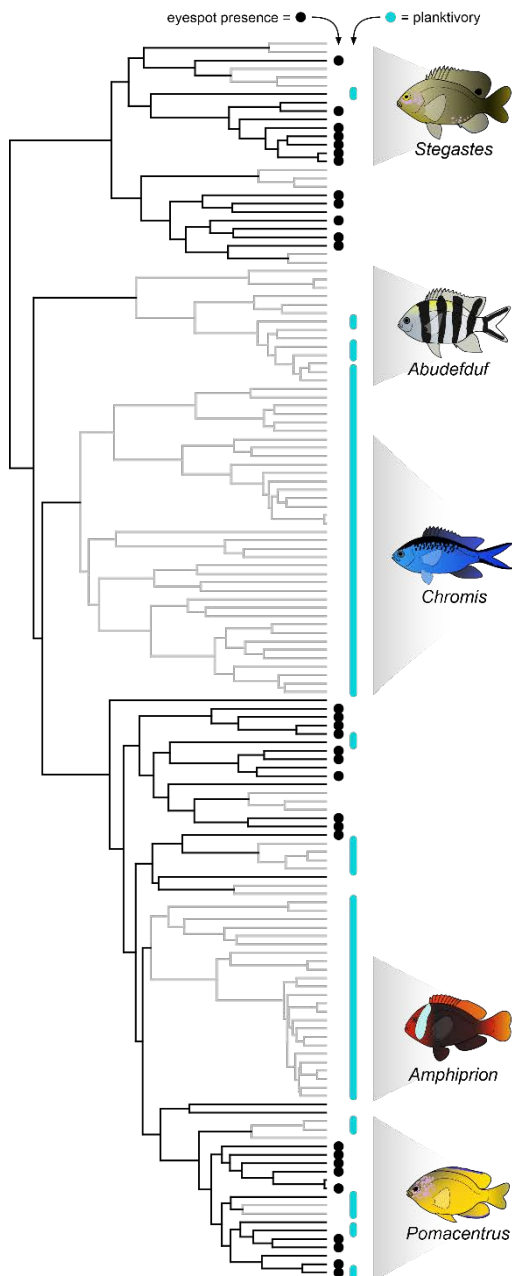


Figure 2.4 The evolution of eyespots and planktivory in damselfishes. The phylogenetic tree shows the evolutionary history of damselfishes through time. Black lineages within the tree indicate a greater calculated probability of eyespot presence as determined from the 1000 averaged SIMMAPs. Grey lineages indicate a greater likelihood of eyespot absence. Black dots at the tips represent actual presence of eyespots in extant taxa; absence indicates eyespot-absence. Tips denoted by the cyan line indicate planktivorous species, tips lacking cyan represent alternative feeding ecologies (i.e. herbivory, omnivory, etc.). Note the near mutually exclusive nature of planktivory and eyespot-presence.

this location, there were two peaks of highest occurrence: one located centrally along the fin and one located along the posterior margin of the fin. The second highest location of eyespot density after the dorsal fin was, surprisingly, located on the operculum; a location close to the real eye. There was significantly more support for models of dependent evolution between activity and eyespot location when compared to the independent model. (likelihood ratio statistic = 8.43, p-value = 0.0148). Furthermore, the most parsimonious of the three dependent models indicated that the location of the eyespot was dependent upon a fish's affinity to the substratum, but critically, not the reverse i.e. activity did not evolve dependent on eyespot location (details of model comparisons in **Table A4**). We can

therefore conclude that the location of the eyespot on the body of a fish is largely driven by its lifestyle. Cryptobenthic species were more likely to have an eyespot located on the operculum, while active, non-cryptobenthic fishes primarily have an eyespot on the dorsal fin.

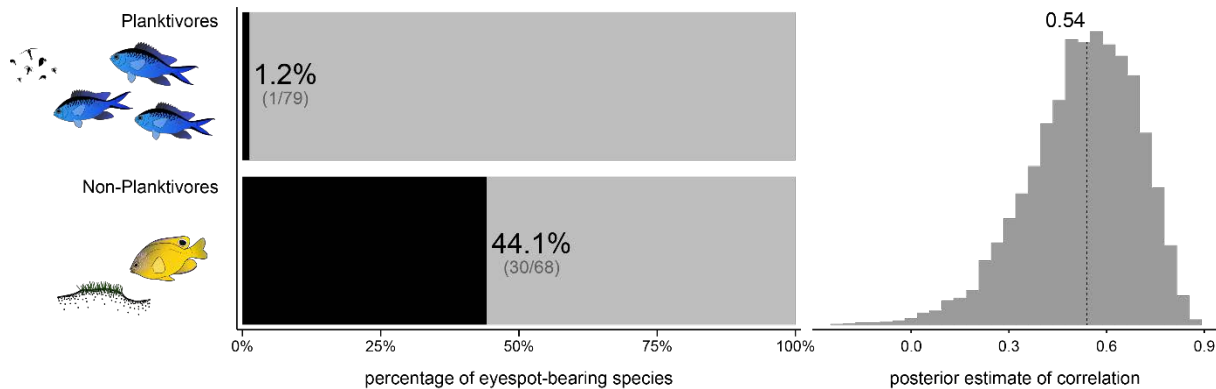


Figure 2.5 The relationship between feeding ecology and eyespot presence. On the left, the proportion of damselfishes with (black) and without (grey) eyespots based on feeding ecology. On the right, the posterior estimate of the correlation (r) between eyespot absence and planktivory based on 50 million generations of a Bayesian MCMC. The median value of r (0.54) has been highlighted.

2.4 Discussion

Eyespots in space and time

Eyespots are common on reef fishes, with approximately one in every ten species possessing this marking. The high levels of visibility associated with clear reef waters (Lewis et al. 1988; Brewin et al. 2010) have likely facilitated the utility of this marking as it functions primarily through vision-based predation. Eyespots have an extremely strong phylogenetic signal, often becoming a defining feature of a given family or genus. Three iconic reef fish families (Labridae, Pomacentridae and Chaetodontidae), collectively account for approximately 57% of all reef fish species with eyespots. Interestingly, there are also families that completely lack eyespots, including the Holocentridae (squirrel and soldierfishes), Carangidae (jacks and trevally), and the Siganidae (rabbitfishes). Holocentrids are nocturnal and Carangids are pelagic, which may explain their lack of eyespots. However, there is no obvious ecological reasons for their absence in Siganids. Nevertheless, it appears that once this colour pattern arises, it has a high propensity to remain in new lineages.

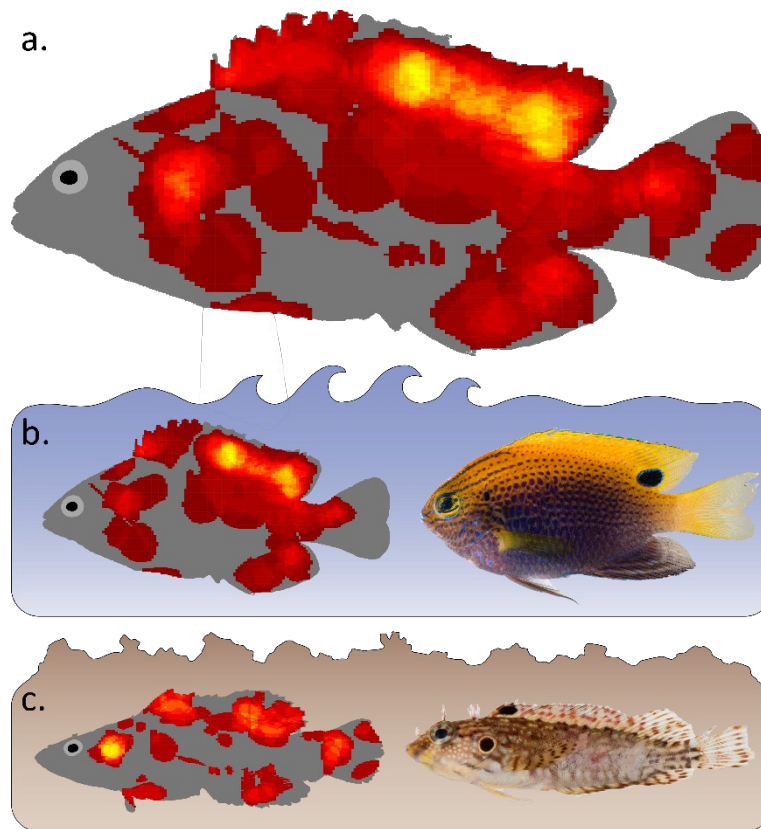


Figure 2.6 The total heatmap for all species (a). Eyespot heatmaps for active (b) and cryptobenthic (c) coral reef fishes. The changing colour from red to yellow reflect the frequency of occurrence of eyespots in that location. Yellow has been scaled to represent the location of highest eyespot occurrence in each heatmap. To the right are examples of species within each category: (b) *Pomacentrus vaiuli* and (c) *Labrisomus nuchipinnis*. Photo credit: Jeffery T. Williams, Smithsonian Institute.

Interestingly, the ancestral state reconstruction estimated eyespot presence as the ancestral condition in the three most eyespot-rich families: wrasses, damselfishes, and butterflyfishes. Therefore, eyespot loss represents the derived character state in these clades. While our methods are sensitive to missing data, incredibly, the timing of estimated eyespot origins agree well with the fossil record. *Paleopomacentrus orphae*, an extinct pomacentrid from the Eocene deposits of Monte Bolca (Bellwood and Sorbini 1996), possessed an eyespot which is evident in the fossilized remains. Furthermore, the location of this marking is consistent with the location of eyespots on many extant damselfish species (Bellwood et al. 2017). It appears that eyespots may have been providing anti-predatory benefits to reef fishes since the Eocene, and probably even earlier (c.f. Cantalice et al. 2020).

Of the four survey locations, the Tropical Eastern Pacific (TEP) was the only one to show a significantly smaller percentage of species with eyespots. Historic vicariance events have isolated the TEP from other tropical marine realms (Bellwood and Wainwright 2002). This time in isolation, with its associated environmental challenges, has led to a more coastal reef fish community containing fewer species in the ‘eyespot-rich’ families (Dominici-Arosemena and Wolff 2006). Nevertheless, in all major reef systems, eyespots are both widespread and present which, unsurprisingly, suggests that they serve a fundamental role that has been consistently selected for on evolutionary timescales.

Ecological links in damselfishes

The absence of eyespots in damselfishes is inextricably linked to a planktivorous feeding mode. Our results indicate that not only have planktivorous damselfish species likely transitioned from alternative feeding ecologies in the past (e.g. herbivory, omnivory, etc., c.f. Siqueira et al. 2020), but that this transition is associated with a concomitant loss of eyespots. Clearly, there is some aspect of the pelagic environment that does not favour eyespots. It is possible that this pattern is being driven by the predation risk associated to a planktivorous feeding mode; one in which individuals are highly exposed and visible to predators (Turner and Mittelbach 1990; Werner et al. 2012). Although eyespots clearly provide anti-predatory benefits to numerous organisms (Kjernsmo and Merilaita 2013; Prudic et al. 2014), they appear to be functionally irrelevant for fishes that occupy highly exposed, open-water habitats given that all but one planktivorous damselfish species lacked this marking (1.1%, 1/79). Interestingly, the one exception, *Pomacentrus nagasakiensis*, although categorised as a planktivore (based on diet), is commonly found associated with the benthos.

Although we were able to demonstrate the link between feeding ecology and eyespot presence in damselfishes, we were unable to do so in wrasses and butterflyfishes because models do not converge, likely due to the low proportion of planktivorous species in these families. Given our damselfish findings, one might logically expect that species incurring the highest predation-pressure would utilise eyespots more frequently. The lack of eyespots on almost all planktivorous damselfishes suggests that there are fitness costs associated with eyespots; they are not a universal solution to predation. Reef fishes

display a clear ontogenetic size threshold above which eyespots are typically lost (75-85 mm TL). This strongly suggests clear selection against this marking in larger fishes (Hemingson et al. 2020). Perhaps eyespots are too conspicuous in open environments and draw an excessive amount of (unwanted) attention (Stevens et al. 2008). Indeed, previous research has highlighted that in some specific contexts, remaining purely cryptic (i.e. not having eyespots) can provide greater anti-predatory benefits than possessing eyespots (Lyytinen et al. 2004; Stevens et al. 2008). Alternatively, eyespots may be a costly feature to maintain in energetic terms (Rodgers et al. 2013). Regardless of the mechanism, the traits that reduce predation in the water column (e.g. deciduous scales, Morgan and Godin 1985; Stevens and Merilaita 2011; Vernerey and Barthelat 2014) appear to be very different to those utilised by more benthic-associated species. This is likely a consequence of the different predatory fish morphologies and behaviours that occur in benthic vs. pelagic environments (Mihalitsis and Bellwood 2019).

Evidence for location-dependent eyespot functions

This same benthic-pelagic axis may also be important in determining where eyespots are located on a fish's body. We found a distinct relationship between the location of the eyespot and how tightly associated a species is with the substratum. Interestingly, the evolutionary models suggest that the level of substratum association determines eyespot location, but eyespot location does not determine substratum association. Essentially, as fish species evolved different ecologies, their eyespots evolved in response to the niche occupied.

A large body of literature on eyespots (with some key findings briefly summarised in **Table 2.1**) has identified that their functionality differs between taxa. From a predation perspective, eyespots have been shown to provide anti-predatory benefits to their bearers through two primary mechanisms (Prudic et al. 2014; De Bona et al. 2015; Kjærnsmo and Merilaita 2017). These are: (1) deflection, by directing strikes away from vital organs like the brain and viscera and towards bodily locations that are more capable of regeneration (Vallin et al. 2011; Kjærnsmo and Merilaita 2013) and, (2) intimidation, by mimicking larger organisms to deter or intimidate potential aggressors and predators (De Bona et al. 2015; Kjærnsmo and Merilaita 2017). We found that eyespots occur in two, primary locations on the

bodies of fishes that likely reflect markedly different functional roles. Therefore, eyespots in reef fishes may have multiple functions, with its function connected to its location on the body. While this is currently a hypothesis based on strong correlations, it may help explain why eyespots have been found to provide different fitness benefits among taxa (Kodandaramaiah et al. 2013).

Table 2.1 *The conflicting evidence of eyespot function. Some highlighted eyespot studies and their summarised findings. In the column ‘Study System’, an ‘A’ represents studies in aquatic systems, while a ‘T’ represents terrestrial. In the ‘Sender/Receiver’ column, the first letter presents the organism bearing the eyespot, and the second represents the intended viewer of the eyespot. An ‘I’ represents an invertebrate, while a ‘V’ represents a vertebrate.*

<i>Hypothesized function</i>	<i>Mechanism</i>	<i>Study System</i>	<i>Sender/Receiver</i>	<i>Support for?</i>	<i>Support against?</i>	<i>Reference(s)</i>
Anti-predation	Deflection	A	-/V	✓		Kjernsmo, Grönholm, & Merilaita, 2016, 2018; Kjernsmo & Merilaita, 2013
Anti-predation	Deflection	T	I/V		✓	Lyytinen, Brakefield, & Mappes, 2003; Vlieger & Brakefield, 2007
Anti-predation	Deflection	T	I/V	✓	✓	Olofsson, Vallin, Jakobsson, & Wiklund, 2010
Anti-predation	Deflection & Mimicry	T	I/V	✓		Olofsson, Wiklund, & Favati, 2015
Anti-predation	Deflection & Mimicry	T	I/V	✓		Halali, Krishna, Kodandaramaiah, & Molleman, 2019
Anti-predation	Mimicry	T	I/V	✓	✓	Vallin, Jakobsson, & Wiklund, 2007
Anti-predation	Mimicry	T	I/V	✓		Hossie & Sherratt, 2012, 2013
Conspecific signalling	Badge of status	A	V/V	✓		Gagliano, 2008; Gagliano & Depczynski, 2013
Conspecific signalling	Cannibalism inhibition	A	V/V	✓		Zaret, 1977
Sexual Selection	Display of fitness	T	I/I	✓		Robertson & Monteiro, 2005
Intimidation	Deception	T	V/V	✓	✓	Deppe et al., 2003
Intimidation	Deception	T	-/V		✓	Belant, Woronecki, Dolbeer, & Seamans, 1998
Intimidation	Deception	A	V/V	✓		Winemiller, 1990
Reproduction	Deception	A	V/V	✓		Theis, Salzburger, & Egger, 2012

In our study system, cryptobenthic species have the highest density of eyespots located on the operculum, a position very close to the real eye. This location does not support the deflective function of eyespots since strikes would be directed towards the viscera or head. Therefore, eyespots in this location are more likely to be functioning through intimidation or predator mimicry (Kjernsmo and Merilaita 2017), or by making prey appear larger to gape-limited predators (Mihalitsis and Bellwood 2017). By contrast, active species most often possess eyespots towards the posterior portion of the dorsal fin. Not only is this location far from vital organs near the head, but fins also have a much higher capacity to fully regenerate (Nakatani et al. 2007). Eyespots found in this location align more strongly with the deflective function; where eyespots divert attacks to less-important body locations allowing the individual to escape relatively unscathed.

The historical debate concerning deflection versus intimidation stems almost completely from terrestrial research; most notably butterflies as a study species (Stevens 2005). Since predatory fishes consume prey whole (Mihalitsis and Bellwood 2017), it is possible that marginal eyespots in fishes may be functioning through an entirely novel deflection mechanism (Kjernsmo et al. 2016). Prey fishes often avoid predation by rapid forward movement away from the predator (their escape response, Eaton and Emberley 1991). In anticipation of this escape response, identification of the head is crucial for successful capture by the predator, with the location of the pupil being a key, identifying feature (hence the use of eye stripes to conceal the pupil; Karplus and Algom 1981; Kelley et al. 2013; Kjernsmo et al. 2016). A false eyespot may therefore suggest the prey fish is facing the opposite direction which would cause the predator to misidentify the escape direction and allow the prey fish to successfully avoid capture. While the eyespot-habitat correlations are strong, a detailed understanding of the mechanistic basis of eyespot function and body location in reef fishes will require a thorough evaluation using experimental trials.

Conclusions

Overall, we show that eyespots have arisen independently on multiple occasions, have probably been providing anti-predatory benefits for over 50 million years, and have become a defining feature of

many fish groups. However, their presence is strongly correlated with the ecology of the organism. In damselfishes, species that live in more exposed environments rarely have eyespots, while species that interact more with the benthos are more likely to possess this marking. This suggests that the anti-predatory function of eyespots may be strictly habitat dependent. Across eyespot-bearing fishes, there is a further separation that may indicate how the eyespot functions in reef fishes. In cryptobenthic reef fishes, the eyespot is most often near the head suggesting a role in intimidation or mimicry. By contrast, active species most often have eyespots on the rear of the dorsal fin, supporting a role in deflection. Regardless of the location, eyespots appear to be a strongly selected and functionally important colour pattern in coral reef fishes.

Chapter 3: Body size determines eyespot size and presence in coral reef fishes

Published as: Body size determines eyespot size and presence in coral reef fishes. *Ecology and Evolution*. (2020). **10** (15). 8144 – 8152.

3.1 Introduction

Many organisms use colouration for differing fitness benefits (Cuthill et al. 2017). Quite often, colouration is tuned to aid in survival (Caro and Allen 2017). One example may be the eyespot or ocellus, a highly conspicuous marking that is believed to resemble the eyes of some vertebrates (Blest 1957). It is comprised of a dark, circular ‘pupil’, surrounded by a pale ring that contrasts against both the pupil and the base colour of the organism. Eyespots are extremely common in nature and are found in numerous taxa from phylogenetically distinct lineages, including insects, molluscs, amphibians, crustaceans, birds, and fishes (Kodandaramaiah 2011; Stevens and Ruxton 2014). Furthermore, eyespots are found on species that have vastly different morphologies, life histories, behaviours and colourations, suggesting a widespread underlying role (**Figure 3.1**; Marshall, Cortesi, de Busserolles, Siebeck, & Cheney, 2018).

The conspicuous nature of eyespots, along with their widespread occurrence, has made them historically appealing to study. Indeed, this marking has received continual research attention since the 19th century (Poulton 1890). Independent studies on different taxa have identified multiple, different, functions of eyespots. These include mate selection and preference (Robertson and Monteiro 2005; Kodandaramaiah 2011), intraspecific competition between juveniles and adults (Gagliano 2008; Gagliano and Depczynski 2013), reproduction (Egger et al. 2011; Theis et al. 2012), and anti-predation benefits (Stevens et al. 2008; Kjærnsmo and Merilaita 2013, 2017).

While extensive in nature, the majority of research has focused on the latter topic, describing how eyespots promote survival through two, primary mechanisms: predator deflection and intimidation. (Lyytinen et al. 2003). Deflective eyespots operate by directing strikes away from vital organs, like the real eyes and head (Kjærnsmo and Merilaita 2013; Prudic et al. 2014). Alternatively, eyespots can



Figure 3.1 The diversity of coral reef fishes with eyespots. a) a sandperch, *Parapercis clathrata*, b) an angelfish, *Pygoplites diacanthus*, and c) a pufferfish, *Cathigaster solandri*. Photos with permission from Rick Stuart-Smith (a) and François Libert (b,c).

function by intimidating potential predators by making the individual bearing them appear larger in size (De Bona et al. 2015). Most research has examined these mechanisms by using experimental approaches, primarily on insects (e.g. caterpillars, butterflies, and moths; Hossie & Sherratt, 2013; Lyytinen, Brakefield, & Mappes, 2003). Often, this entails presenting or manipulating the pattern on a prey item and subjecting it to a model predator species to record the interaction (Prudic et al. 2014; De Bona et al. 2015). These approaches have been particularly informative in describing how the pattern functions and which features may make it successful.

Although these experiments have been supported by field observations (Hossie and Sherratt 2012, 2013) surprisingly few studies have utilised more broad, analytical approaches to describe commonalities in eyespots among many species (but see Ho, Schachat, Piel, & Monteiro, 2016; Hossie, Skelhorn, Breinholt, Kawahara, & Sherratt, 2015). Indeed, several key questions remain: for example, how does the size of the eyespot relate to the size of the real eye, if present? And at what size do eyespots become irrelevant (i.e. when do animals lose them)? These basic questions, albeit critically important, have received relatively little attention (cf. Hossie et al., 2015; Karplus & Algom, 1981). Body size and morphology often strongly constrain the life history traits of many organisms. (Bellwood and Choat 1990; Berumen et al. 2011; Mihalitsis and Bellwood 2017). Therefore, approaching eyespots from a

more general perspective, and analysing these questions across many species, may provide insights into what makes this marking so common and how it may function.

Coral reef fishes offer an ideal group to study this marking. Unlike insects that have a compound eye, reef fishes have an eye with a pupil and iris that the eyespot may resemble. This similarity allows for direct comparison between features of the eyespot and features of the real eye; a comparison not possible in insects. Furthermore, reef fish colouration is highly adaptive (Hemingson et al. 2019) and many species gain or lose eyespots through development. To understand what rules shape the presence of eyespots in reef fishes we ask, 1) how does the eyespot compare to the eye in size and 2) at what body size are eyespots typically gained or lost in coral reef fishes? In doing so, we shed light on the processes that may shape eyespot use in one of the world's most diverse and colourful group of vertebrates.

3.2 Methods

Defining an eyespot

For reef fishes, we defined an eyespot based on three criteria. 1) The entire eyespot needs to be approximately circular or elliptic in shape. 2) It has a dark (typically black) interior circle or ellipse that is surrounded by no less than 75% of its circumference by a concentric ring of differing, much lighter colour (typically white). 3) There could be no more than 10 eyespots present on an individual. These criteria were chosen to ensure that the pattern is as a distinct marking that is visually conspicuous against rest of the fish's colouration. Strict criteria are necessary since there is a broad spectrum of markings present on coral reef fishes. Establishing these criteria allow us to focus on the species with a consistent eyespot form to determine what influences their presence and appearance.

Image sourcing and data collection

Bony fishes from four geographically distinct ecoregions were surveyed for the presence of eyespots (The Great Barrier Reef and Coral Sea, the Red Sea and Indian Ocean, the Caribbean Sea, and the Tropical Eastern Pacific; Cowman, Parravicini, Kulbicki, & Floeter, 2017; Kulbicki et al., 2013). Collectively, these locations encompass approximately 45% of all currently described coral reef fish

species. To assess the taxa present in these ecoregions, we surveyed multiple species identification guides, including published ID books, as well as online databases like FishBase (www.fishbase.com) and Reef Life Survey (www.reeflifesurvey.com). After identifying which species have eyespots, fish images were sourced from the Smithsonian Institute's Division of Fishes Collections, supplemented by images from Williams et al. (2010). Images in this database or publication contain standard length (SL) and/or total length measurements (TL) which permit further measuring of morphological features (e.g. the eye, etc.). Furthermore, photographs of specimens in these collections have been photographed in a standardised manner, with the left side of the fish photographed, typically, shortly after death. However, not all individuals had their dorsal, anal, and caudal fins fully exposed which dictated whether the eyespot could be measured (see **Figure 3.2**). Therefore, this catalogue yielded two datasets which contained different information; each of which were used for different analyses. The first dataset contained length measurements of all eyespot-bearing species in which the presence or absence of the marking could be identified (n species = 167, n samples = 1140). For example, if the specimen photographed was in too poor of condition to allow for measurement (a consequence of preservation or the manner in which the individual was collected) but the presence/absence of an eyespot could be determined, its length and presence/absence was recorded. The second dataset contained only the images of specimens in high resolution of excellent preservation quality which permitted detailed measurements of the eyes and eyespot (n species = 140, n samples = 354). This data set was used to make direct comparisons between the size of the eye and the size of the eyespot.

Morphological measurements and comparisons

We were curious if there is a distinct relationship between the size of the eyespot and the size of the eye. To test this, we measured four different features on both the eye and the eyespot. These four measurements were: 1) the maximum width of the eye, 2) the maximum width of the pupil, 3) the area of the eye, and 4) the area of the pupil (**Figure 3.2**, further detail in **Figure B3**). These four features were measured using ImageJ (Schneider et al. 2012) and were repeated on the matching features of the eyespot (e.g. the maximum width of the eyespot's pupil). Each matched feature between the eye and eyespot were then compared using phylogenetic generalised least squares (PGLS) regression analyses

due to the non-independent nature of species data (the details of the phylogenetic tree used are described in the following section). Since the linear and area measurements measure the same features in alternative ways, only the area PGLS regression results are presented in the main text (linear regression results were identical and are presented in the supplemental material **Figure B2** and **Table B1**). In all analyses, we used the measurements of the eye as the explanatory variable, and the measurements of the eyespot as the response variable. For species with more than one eyespot, measurements were taken of the largest eyespot. All measurements were converted into millimetres (mm) or mm^2 .

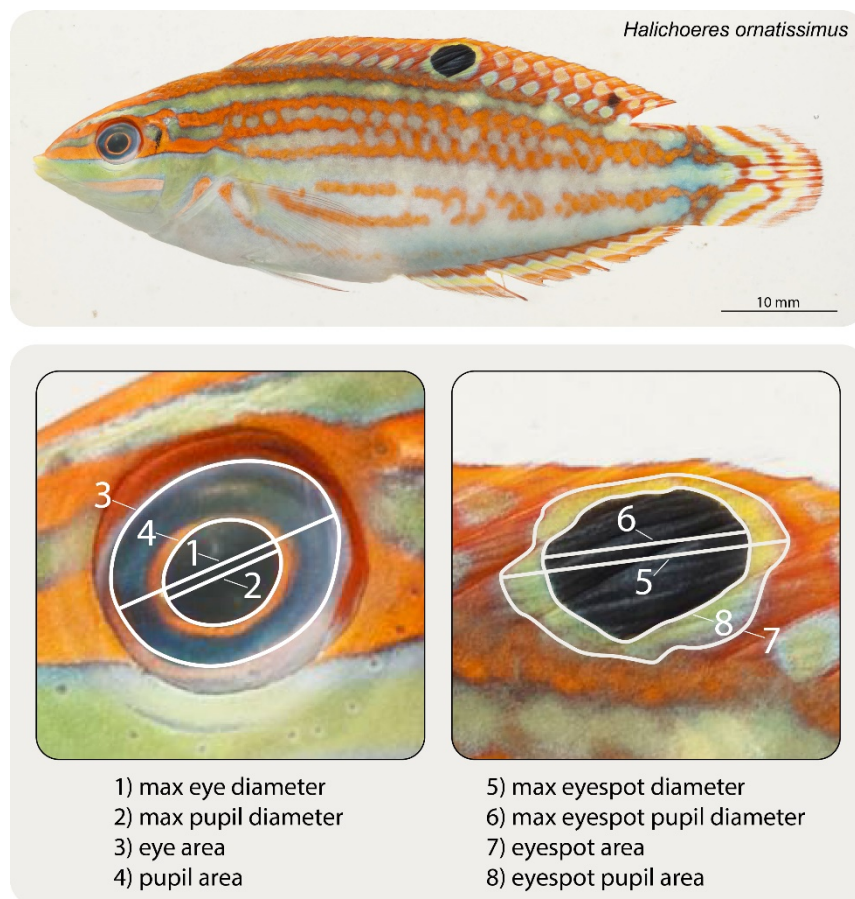


Figure 3.2 An example photograph from the Smithsonian Institute's Division of Fishes Collections. On top is the raw image of *Halichoeres ornatissimus*. The scale bar has been added. In this photograph the fins are exposed, which permits morphological measurements of both the eye and, most importantly, the eyespot. In fishes with folded fins only the presence, not the size, of the eyespot can be recorded. Below are the 8 measurements (both linear and area) of the eye and eyespot features. Photo: 2006 Moorea Biocode/Jeffrey T. Williams, Smithsonian Institution.

Phylogenetic backbone construction

To account for non-independence due to shared evolutionary history (Felsenstein 1985), a topology of all species included in this study was constructed using the most recent and comprehensive published phylogeny of coral reef fishes (Rabosky et al. 2018). Missing species were inserted based on previously published phylogenetic hypotheses (Betancur-R et al. 2017). Replicate tips for each species were added to the tree depending on the number of images with measurable features available for each species. For example, five images of *Chrysiptera biocellata* were available that permitted measurements of the eye and eyespot. Therefore, four additional tips (since one tip was already present during the initial construction of the phylogeny) were added to the tree. These replicated tips have a branch length of zero, meaning each of the individuals within a species (e.g. *C. biocellata* #2 and *C. biocellata* #5) have the same phylogenetic distance to all other species. In doing this, we could add as many replicates for individuals within a species as there were images available, without letting species with many images drive relationships. This backbone was then incorporated into phylogenetic generalised least squares (PGLS) regression analysis to account for phylogenetic nonindependence (phylogenetic tree available in **Figure B1**).

Estimating size distributions and eyespot transitions

We utilised two separate statistical approaches to investigate the size at which fish have eyespots, and consequently, at what sizes this feature is lost. The first dataset (containing only eyespot presence/absence and standard length, $n = 1140$) was divided into those fish with or without an eyespot. This yielded two separate datasets: one containing the size measurements of fish with eyespots (n species = 140, n samples = 586; 51.4%), and one containing the sizes of fishes that had or will have eyespots (n species = 115, n samples = 554, 48.6%). This is essentially the ecosystem perspective on eyespots: regardless of phylogeny, i.e. at what size do fishes have eyespots and at what size do they not? To generate the size distribution of eyespot-bearing and eyespot-lacking individuals, a bootstrapping procedure was utilised that sampled one size measurement per species. This approach was used to account for variation in image sample-sizes among species and more importantly, the variation in the size of individuals at which eyespots are lost or gained, i.e. the size range where species may be

transitioning from having an eyespot to losing it, or vice versa. This bootstrapping procedure is important since eyespots are gained or lost during ontogeny, but the size at which this happens differs for each individual within a species. These distributions were compared using a generalised linear model incorporating a gamma distribution which best accommodates the error structure of the data. The explanatory variable was eyespot presence or absence and the response variable was the standard length (SL). This test was run for each iteration of the resampled dataset (250 times). Essentially, this approach tests if the size of individuals with eyespots is significantly different to those without.

This dataset can also be used to ask the question “what is the probability that a fish has an eyespot at a given size”? To answer this, we modelled the probability of possessing an eyespot at various standard lengths. This was done by using a binomial regression in which eyespot presence and absence were modelled as 1 or 0 (the response variable) and regressed against standard length (the explanatory variable). This was also run for 250 iterations. Additionally, the 50-50 point were calculated for each iteration. This is defined as the size in which the probability of having an eyespot is equal to the probability of not having it. All statistical analyses were conducted using the ‘stats’ and ‘nlme’ packages in R (Pinheiro et al. 2019; R Core Team 2020)

3.3 Results

Morphological relationships

The eyespot’s total area and the eyespot’s ‘pupil’ area are significantly related to the area of the real eye and real pupil, respectively (**Figure 3.3**; all summary statistics in **Table B2**). The eyespot and the eye were almost identical in area. The slope was significant, indicating that the larger the individuals eye size, the greater in size of the eyespot. The slope was significantly greater than 1 which was likely driven by a few outliers of individuals which had the largest eyes recorded. However, since this relationship did not have an intercept significantly different than zero it indicates a consistent scaling between the size of the eyespot and the size of the real eye (**Figure 3.3**). Essentially, the size of the eyespot is almost identical to that of the real eye.

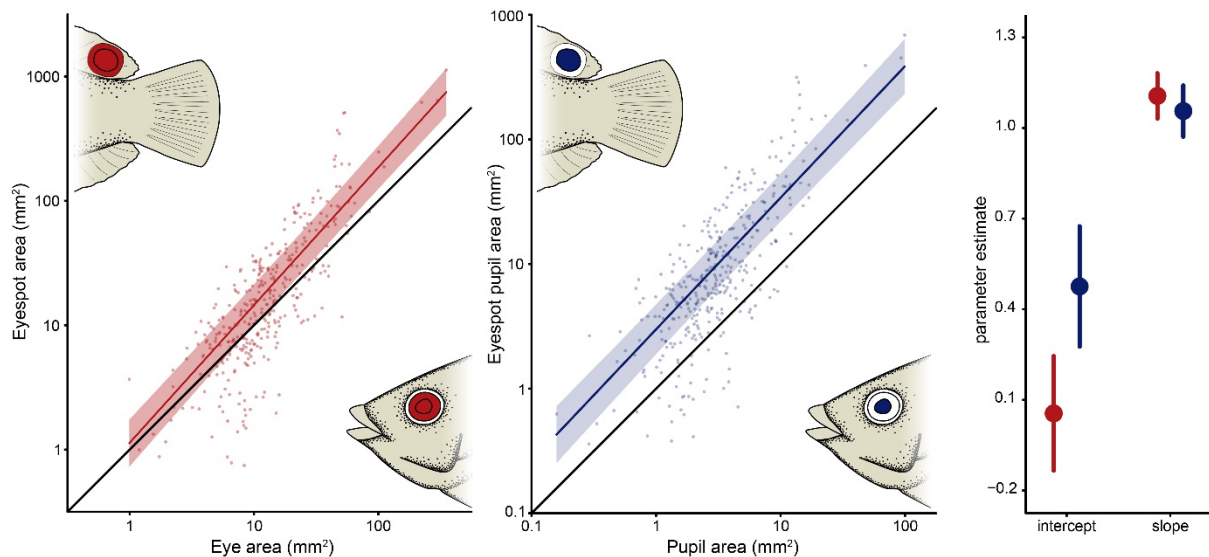


Figure 3.3 Relationship between the eye area and eyespot area (left) and pupil area and the eyespot ‘pupil’ area (middle). The coloured lines represent the phylogenetic generalised least squares regression (PGLS) lines with 95% confidence intervals. The solid black line represents an isometric growth pattern; where the area of one feature (in this case, the eye) would be equivalent to the area of the other feature (the eyespot). Estimates and 95% confidence intervals (right) of the regression models slope and intercepts for eye/eyespot (red) and pupil/eyespot pupil (blue). Both comparisons have identical slopes but different intercepts indicating that these features scale in the same manner, however the eyespots pupil is consistently larger.

The real pupil area and the eyespot’s ‘pupil’ area were also significantly related with a slope that is not significantly different than 1. However, this relationship’s intercept was significantly greater than zero and the confidence intervals were completely separated from the isometric line. In this case, the eyespot’s ‘pupil’ is consistently four times larger, on average, than the real pupil. When we compare the slope and intercept estimates from both models (the eyespot to eye and the eyespot pupil to the real pupil), it is evident that the slopes are not significantly different, but the intercepts are (**Figure 3.3**). Thus, in fish of all sizes, the overall size of the eyespot is remarkably similar to that of the eye, but the size of the eyespot’s pupil is about four times larger.

Size distributions and eyespot loss

The size distributions of fishes with eyespots ($n = 586$; 51.4%) were significantly smaller than those without ($n = 554$, 48.6%; **Figure 3.4**). This pattern was consistent across all 250 iterations (median

p-value = 0.0007, mean p-value = 0.002; histogram of all p-values in **Figure B4**), indicating that even whilst accounting for individual variation, there were still pronounced differences. Individuals that possessed an eyespot were significantly smaller than the individuals of the same species which no longer had this marking. The variation within each iteration was low since most curves followed the same general trajectory; there was little influence of sampling differences among species.

Furthermore, the standard length of an individual could significantly predict the probability of having an eyespot, with the highest probabilities occurring at the smallest sizes (**Figure 3.5**). All 250

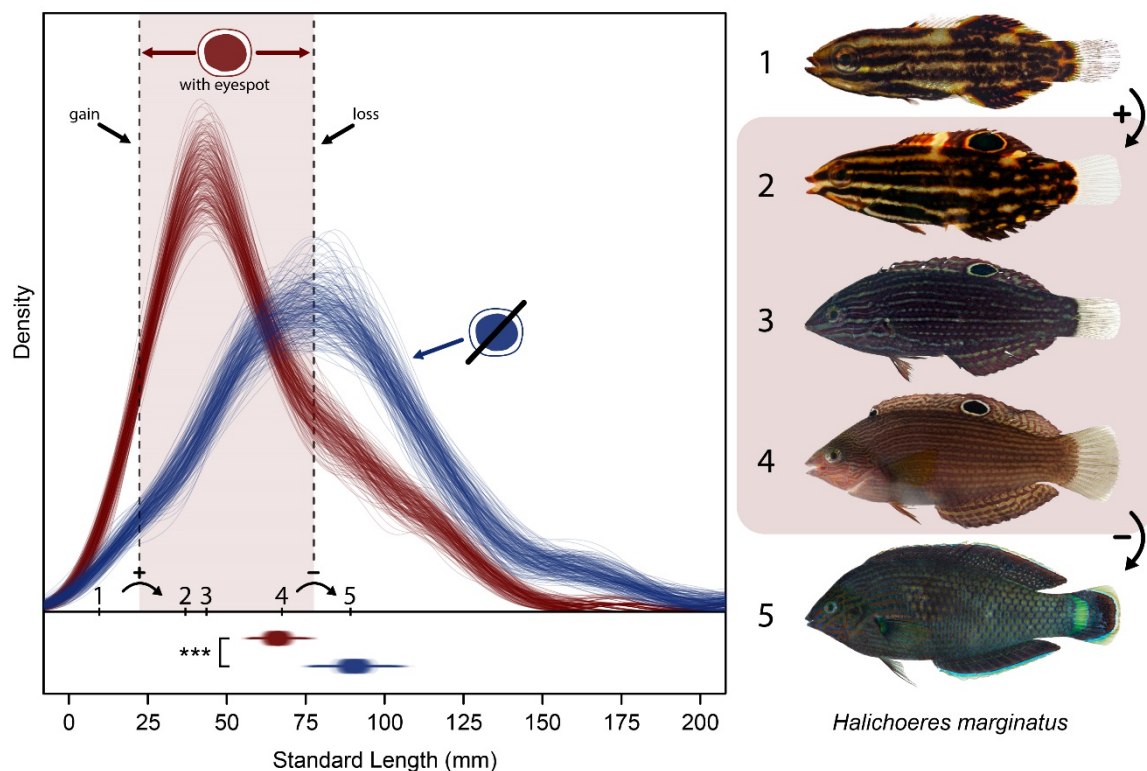


Figure 3.4 The size distribution of individuals with (red) and without (blue) an eyespot based on 250 bootstrapped size estimates. Below are the means and 95% confidence intervals plotted for each iteration. On the right are five individuals of *Halichoeres marginatus*, a species that displays the ‘window’ of eyespot use in coral reef fishes. The number next to each image corresponds to their standard-length measurement which are plotted on the main graph. Therefore, we can see the approximate sizes in which the eyespot is gained (+) and lost (-) marked by vertical dashed lines. Photos: Jeffrey T. Williams, Smithsonian Institution.

iterations of the binomial glm were significant (both mean and median p-value < 0.001; histogram of p-values in **Figure B5**). The size in which a fish was equally likely to have/not have an eyespot (50-50 point) ranged from 75 mm to 85 mm (SL) depending on the iteration (mean: 79.77 mm, median: 79.51

mm; **Figure B6**). We can interpret this range of standard lengths as the sizes at which the costs of an eyespot outweigh the benefits.

3.4 Discussion

Eye size induced constraints on eyespot size

The morphological regressions provide direct clues to the features that may determine eyespot size and structure in coral reef fishes. Since the area of the eyespot is approximately equivalent to the area of the eye at all fish sizes, eye size appears to strongly constrain the maximum effective size of eyespots. Essentially, it appears that the eyespot is not free to become as large as possible; it is strongly linked to fish size and presumably must be of a realistic size. Such size constraints have been demonstrated previously in reef fishes, especially in ecological and morphological features (Schmitz and Wainwright 2011b; Mihalitsis and Bellwood 2017), but not with colouration. However, within this constraint, the eyespot's 'pupil' is consistently and significantly larger than the real pupil. This suggests that the eyespot's pupil is responding to different selective pressures and may be responsible for drawing attention to this marking since the overall size of the eyespot is consistent with the real eye. Experimental studies are needed to explore this hypothesis and the extent to which pupil-based conspicuousness could play a role in an eyespot's ability to grab attention (c.f. Kjærsmo, Grönholm, & Merilaita, 2018). Interestingly, the outer ring appears to be critically important in the anti-predatory function of eyespots, as purely black, circular markings do not deter predators to the same extent (Winemiller 1990). So, in reef fishes, eyespots do appear to resemble the overall size of the real eye, but the eyespot typically possess an exaggerated pupil which may aid in grabbing the attention of predators.

Furthermore, the presence of eyespots appears to be an 'all or nothing' phenomenon. In coral reef fishes, eye size displays negative allometry, that is, for a given increase in body size, the eye does not increase in size to a similar extent (Howland et al. 2004; Goatley and Bellwood 2009; Schmitz and Wainwright 2011a). Eyespots show similar, negative allometry (non-significantly different, **Figure B7 Table B3**), tracking an identical decrease in the relative eye size as body size increases. This suggests that to be effective eyespots must match eyes or be avoided entirely.

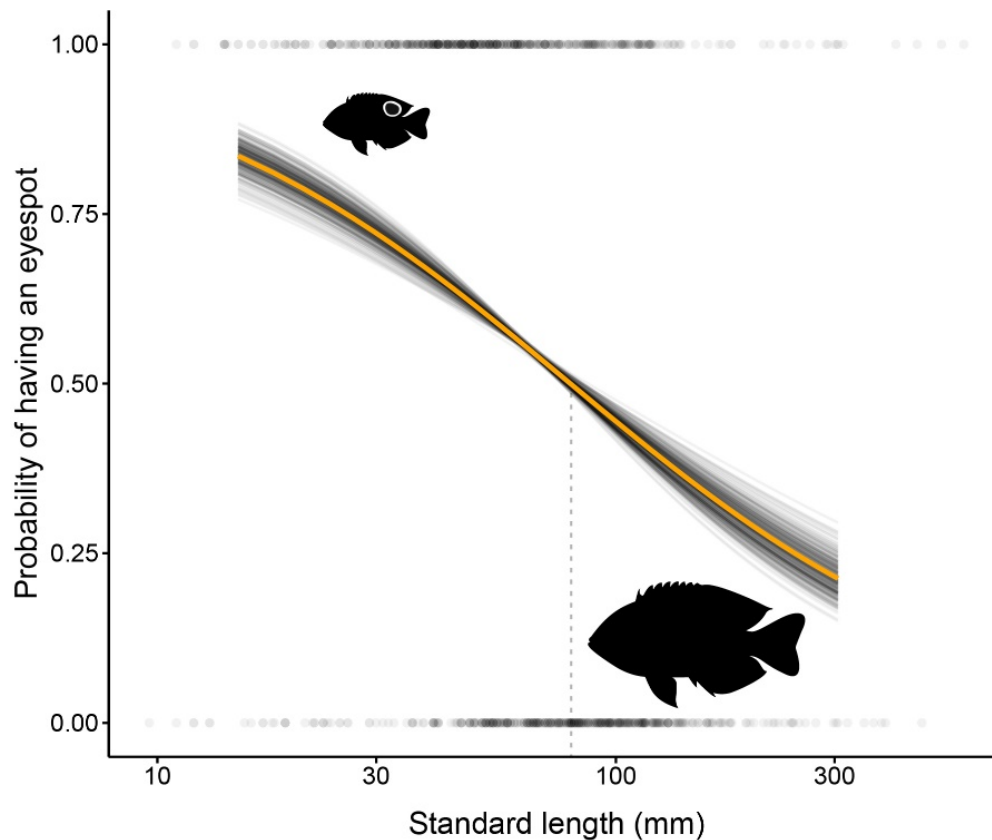


Figure 3.5 Probability of eyespot occurrence with increasing fish size. 250 bootstrapped binomial glms's displaying the relationship between standard length and the probability of having an eyespot. Each iteration's trendline is in black, the mean of these 250 trendlines is in orange. Additionally, the raw 1140 specimen length measurements with their presence or absence (1 or 0 respectively) of an eyespot have been plotted.

The notion of body size constraints on eyespot size have been found in caterpillars, butterflies and freshwater fishes (Kodandaramaiah et al. 2013; Hossie et al. 2015; Ho et al. 2016; Kjærnsmo et al. 2018). A lower limit based upon the size of the real eye makes ecological sense from a predation perspective. If attention is to be brought away from the real eye, logically, the eyespot would need to be realistic if not larger (Ho et al. 2016; although eye concealment may mitigate this relationship – Kjærnsmo, Grönholm, & Merilaita, 2016). The upper limit remains more difficult to explain. Possibly, the upper limit reflects the size range of predators most likely to consume a prey of a given size. Restricting the upper limit may most effectively deter predators that are most likely to consume the individual (Kjærnsmo and Merilaita 2017).

Reduced presence with increasing size

The widespread and relatively rapid loss of an eyespot with growth suggests a marked decrease in their benefit during development. There appears to be a distinct ‘window’ of eyespot effectiveness in coral reef fishes between 30 to 60 mm SL. Interestingly, a similar phenomenon has been described in caterpillars, with eyespots only benefitting species that are larger in size (Hossie et al. 2015). In this caterpillar example, eyespots were actually a detriment to smaller caterpillar species, increasing their probability of being attacked/eaten. A comparable scenario may operate in coral reef fishes. Many small coral reef fishes in the families Gobiidae and Tripterygiidae do not have eyespots although these families are particularly speciose. Furthermore, the majority of species within these families do not reach lengths greater than 50 mm, making them some of the smallest fishes on coral reefs (Brandl et al. 2018). They are therefore of a size that is subjected to some of the highest predation rates on reefs (Goatley and Bellwood 2016). In this case, having purely cryptic colouration probably provides the most effective solution to avoiding predation at these smaller sizes (Lyytinen et al. 2004; Cortesi et al. 2016). An eyespot would presumably draw the attention of predators, as in the caterpillar experiment.

The widespread loss of eyespots at 50 – 85 mm SL in multiple phylogenetically distinct lineages of reef fishes suggests that this loss is driven by strong selective pressure (Stevens 2005). Of the samples surveyed herein, only 3.58% of individuals possessed this marking above 150 mm SL. Interestingly, the size at which fishes start to lose eyespots coincides with a significant decrease in the mortality rates of fishes on coral reefs. Previous research has shown that 43 mm total length is an important transition point in mortality rates for fishes on coral reefs (Goatley and Bellwood 2016). Above this size threshold, predation pressure decreases substantially. The presence of an eyespot appears to reflect this threshold since eyespot presence decreases rapidly past this critical size. This narrow size window of eyespot presence (between 30 and 60 mm SL) offers support for the suggestion that eyespots in fishes may be functioning primarily as anti-predatory mechanisms, amongst other mechanisms (Gagliano and Depczynski 2013).

The consistent eyespot loss through development strongly suggests that their presence (and consequently, function) is strictly size-dependent. If there were no costs in maintaining eyespots, they

would in theory persist throughout the lifetime of many species. Since this is clearly not the case, there must be consequences for maintaining this feature through adulthood. Transitioning from prey to predator may operate in some species, i.e. increasing crypsis as an adult. However, many reef fish species with eyespots as juveniles are not piscivorous as adults (e.g. all damselfishes and butterflyfishes; many wrasses). Clearly, there are strong selective pressures that constrain the presence of eyespots to moderately sized individuals. Investigating the fitness costs of eyespots for fishes offers a promising future avenue of research.

Herein, we identify the factors that determine eyespots size and form in coral reef fishes (matching eye size and maximising the pupil) as well as evidence supporting a threshold associated with body size (the systematic acquisition then loss of eyespots through ontogeny). We show that eyespots have constraints that dictate how large the eyespot can become as well as the size of fishes that can utilise these markings. Our data highlights how certain factors can shape the appearance of an animal's colouration, since an eyespot is clearly for small, not large, reef fishes.

Chapter 4: The influence of range overlap and symmetry in shaping the evolution of reef fish colouration

Published as: Colour pattern divergence in reef fish species is rapid and driven by both range overlap and symmetry. *Ecology Letters*. (2018). **22** (1). 190 – 199.

4.1 Introduction

Signals that relay information about identity, like colouration, are important for the creation and maintenance of species boundaries. Often, these signals are heavily shaped by selective pressures. In particular, sexual selection can have a profound influence on the colouration of species (Panhuis et al. 2001; Gray and McKinnon 2007). Numerous studies on birds, freshwater fishes, lizards and frogs have documented a choice for mates based on various aspects of colouration and pattern (Seehausen 1997; Figuerola and Green 2000; Reynolds and Fitzpatrick 2007; Bastiaans et al. 2014). Given enough time, this gradual selection pressure can shape the colouration of a species over evolutionary timescales and subsequently lead to the diversification of lineages (Seehausen et al. 1999). While sexual selection is well described in species that are sexually dichromatic (i.e. when males and females are visually different), active selection for certain visual attributes in the opposing sex can also occur in species that are sexually uniform in colour but exhibit assortative mating (Puebla et al. 2007; Whitney et al. 2018).

Assortative mating can occur when an individual chooses a mate based on preferences for phenotypes that are similar to their own. Albeit more gradual, this process can also influence colouration and may lead to the divergence and reinforcement of colour patterns in separate lineages (Mavárez et al. 2006; Puebla et al. 2007; Reynolds and Fitzpatrick 2007). This process can be expedited if lineages develop in sympatry because they would have the potential to interact through the entirety of their divergence (Barluenga et al. 2006). This form of selection requires rapid differentiation of the phenotype and significant reinforcement, if that phenotype is to persist through time (Kondrashov and Mina 1986; Kondrashov and Kondrashov 1999; Marshall et al. 2002).

The species recognition hypothesis posits that signals, like colour pattern, are important in species identification by conspecifics (Ryan and Rand 1993). Therefore, colour patterns are expected to be more different in closely-related species that co-occur geographically (i.e. exhibit a high degree of sympatry).

It is hypothesized that differences in colouration prevent hybridisation amongst sympatric species. If the signals are not sufficiently divergent, regression of the signal takes place and the species does not diverge. This concept of increased signal divergence in sympatric vs allopatric taxa has been widely documented, especially in studies focusing on mate song/call (Höbel and Gerhardt 2003; Seddon 2005; Lemmon 2009) and colouration (Reynolds and Fitzpatrick 2007; Martin et al. 2010; Doutrelant et al. 2016).

However, one aspect of how species distributions influence signal divergence that has received far less attention is the effect of range size. Termed “range symmetry” by Barraclough & Vogler (2000), it is defined as the relative difference in the total range area of two species. Range symmetry is necessary to include when analysing the extent of overlap because it gives context to the influence that genetic changes may have within a population (Barraclough and Vogler 2000). Genetic changes are more influential in populations with restricted size, thus allowing for quicker rates of differentiation in genotype and phenotype. One may therefore hypothesise that small range species with extensive overlap would display the greatest colour differentiation. Indeed, range symmetry has been shown, in some groups, to be a critical component that supports barriers to gene flow and drives signal diversification (Seddon and Tobias 2007; Malay and Paulay 2010). Therefore, the interplay of both range overlap (i.e. allopatry vs sympatry) and range symmetry (i.e. peripatry) is likely to contribute to resultant patterns of signal diversification, especially in taxa with highly variable range sizes such as reef fishes.

Coral reef fishes exhibit exceptional signal diversity and possess some of the most complex and intricate colours and patterns found in the natural world (Marshall 2000a). However, due to the attenuation of light in water, aquatic environments dictate different colour pattern assembly rules when compared to terrestrial systems (Levine and MacNichol 1982; Marshall 2017). For example, blue and yellow are extremely common on coral reefs (Marshall et al. 2003), yet quite rare in terrestrial environments. For reef fishes, these colours serve a dual purpose of camouflage and signalling, depending on the context (Marshall 2000b). This combination of extreme colour diversity and differing rules makes coral reef fishes a prime study group to explore how signal divergence arises in marine ecosystems.

Historically, the study of colour patterns has proved challenging due to difficulties in objectively quantifying an organism's visual appearance (Endler 1990). Colour quantification became possible with the advent of high-resolution spectrophotometers, which measure light reflectance at various wavelengths. However, studies incorporating patterns have had to rely on categorisation schemes based upon human constructs (cf. Kelley *et al.* 2013). While informative, they retain a level of human-induced bias. Research has shown that it is critically important to consider both colour and pattern when interpreting the function of an organism's appearance (Phillips *et al.* 2017). Fortunately, recent advances in image-analysis techniques permit us to objectively describe colour patterns based on both colour and location (Van Belleghem *et al.* 2018). We are now able to quantitatively compare organisms in terms of both their colours and patterns simultaneously. Herein, colours and patterns are collectively termed colouration or colour patterns.

Our goal, therefore, was to use high-resolution digital colour photographs of reef fishes to quantify colour patterns and explore how they are influenced by evolutionary processes. The genus *Chaetodon* was selected for study as they: 1) do not exhibit sexual dichromatism, 2) possess high levels of recent diversification and, 3) possess strongly contrasting colour patterns that are highly variable among species but highly conserved within species. This allows us to not only examine the role of colouration in the evolution of species that are sexually uniform in colouration, but to also test if trends observed in terrestrial and freshwater systems (Seehausen and Schluter 2004; Seddon 2005; Lemmon 2009) hold true for the marine environment. Specifically, our goals are: 1) to examine how colour patterns change over evolutionary time, 2) to investigate the relationship between the extent of sympatry and colour pattern differences among recently diverged species-pairs; and 3) to examine the effect of range size symmetry on the extent of colouration differences between species-pairs. Terrestrial systems predict that colour patterns will diverge with increasing sympatry (Martin *et al.* 2010; Doutrelant *et al.* 2016), a pattern which may be further accentuated by large differences in range size (Seddon and Tobias 2007). This will be the first study to quantitatively evaluate this pattern in a marine ecosystem.

4.2 Methods

Study group: *Chaetodon*

Butterflyfishes (Family: Chaetodontidae; **Figure 4.1**) are a family of fishes found in tropical and temperate reef environments. The genus *Chaetodon* contains 89 nominal species (Eschmeyer et al. 2018) of iconic tropical and sub-tropical reef fishes. This genus is relatively well known, with high resolution taxonomically, near-complete phylogenies and well documented distributions, many of which span the Indian and Pacific Oceans. Their high lateral body compression gives them ample body area to display bold colour patterns. Interestingly, the majority of species are comprised of three primary colours: yellow, black and white (with the occasional different accent colour). Colour patterns are highly conserved within species but vary remarkably between species. Chaetodontids possess three peaks in their spectral sensitivities which are centred around 430, 490 and 530 nanometres (Losey et al. 2003; Marshall 2017); corresponding to blues for the two shorter wavelengths and green/yellows for the longer wavelength. It is likely that species within this family can detect the colour patterns of other

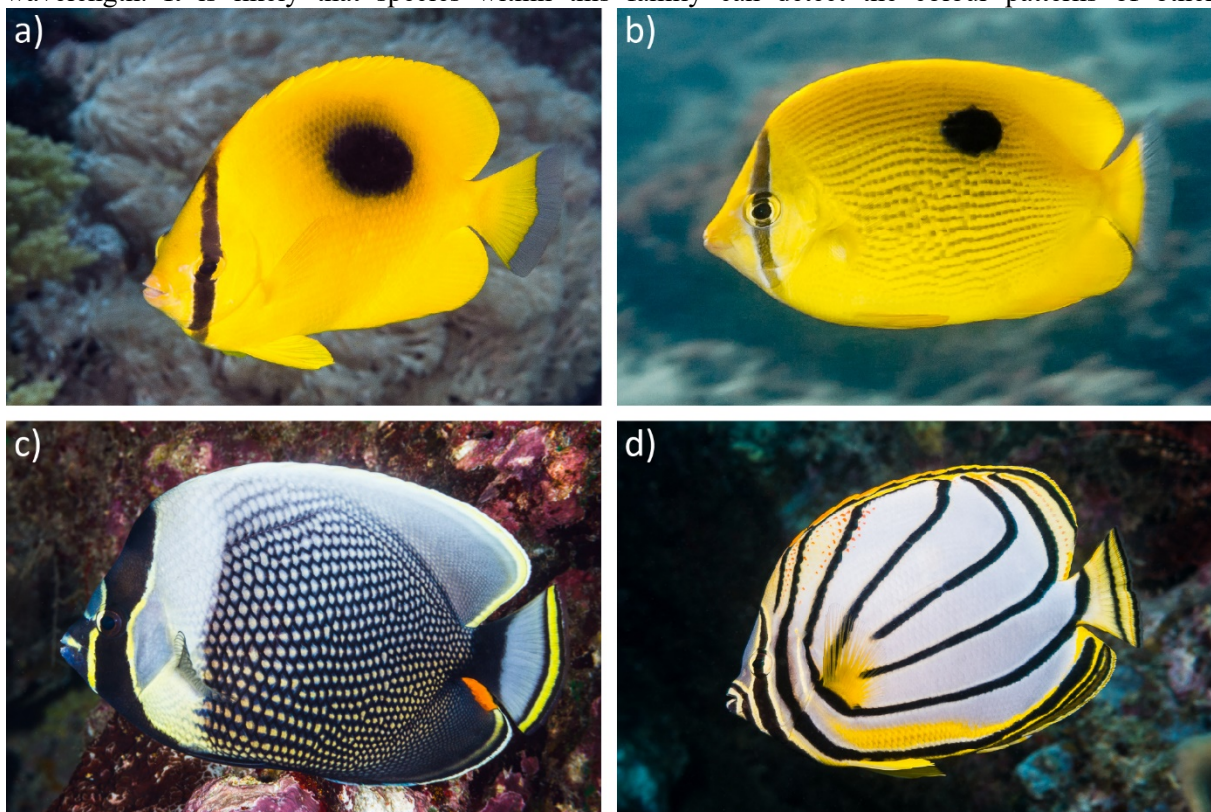


Figure 4.1 Four butterflyfish species comprising two species-pairs. Allopatric species a.) *Chaetodon speculum* and b.) *Chaetodon zanzibarensis*; and highly sympatric species. c.) *Chaetodon reticulatus* and d.) *Chaetodon meyeri*. Photos with permission from François Libert.

chaetodontids, supporting the notion that colour patterns are influential in species recognition. These factors identify butterflyfishes as a promising group in which to study the evolution of signal divergence.

Species-pair approach

For identifying species-pairs, we used a published chaetodontid phylogeny with > 77% taxa represented (69 of 89 *Chaetodon* species) sampled from four mitochondrial and four nuclear gene regions (Cowman & Bellwood 2011). We identified 22 distinct species-pairs. A species pair was defined as two species who share a single common ancestor that is not shared with any other taxa based on our phylogeny. Of the 22 distinct species pairs, all current molecular and morphological information indicates that at least 17 of these pairs also represent direct sister-species. We utilised species-pairs as our sampling unit because they are the simplest group for comparisons and offer insights into the most recent divergence events. Only one species-pair was not included in the analyses as images could not be sourced that were of sufficient quality (*C. robustus* and *C. hoefleri* pair), therefore 21 species-pairs were analysed. Five images were used for each of the 42 focal species providing a sufficient number of replicates to accurately capture colour pattern variation within species (Dalrymple et al. 2015a), as well as any variation that may arise due to image quality.

Image sources, selection criteria and colour calibration

Images were compiled from various online image databases (Reef Life Survey, Fishes of Australia, FishBase, etc; all image details are listed in the Supporting Information). For initial selection, images were required to be in lateral view with adequate illumination to reveal the whole body. This meant the majority of photographs were taken using flash photography, the remainder being in well-lit positions. It must be noted that Chaetodontidae are exceptionally stable with regards to colour. Colour patterns are based largely on three, dominant colours in distinct, bold, blocks. It was this stability that was part of the reason for selecting *Chaetodon* for this study. For more variable coloured species, standardised photographs are likely to be particularly important.

A colour calibration procedure was performed using “patternize” (Van Belleghem et al. 2018) to establish the working RGB (Red, Green, Blue) centre points and thresholds for the colours of interest (yellow, black, white, and ‘other’, i.e. not yellow, black or white; **Figure 4.2**). These colours were chosen as they are the dominant colours found on most species within this family (Marshall et al. 2003). The fourth category, ‘other’, was incorporated to allow for variation due to other colours while preventing a single unique occurrence of one colour to bias dissimilarity calculations. *Chaetodon fasciatus* was chosen for initial colour calibration as it clearly exhibits the three focal colours: yellow, black and white. Five images were analysed from different sources, each representing varying degrees

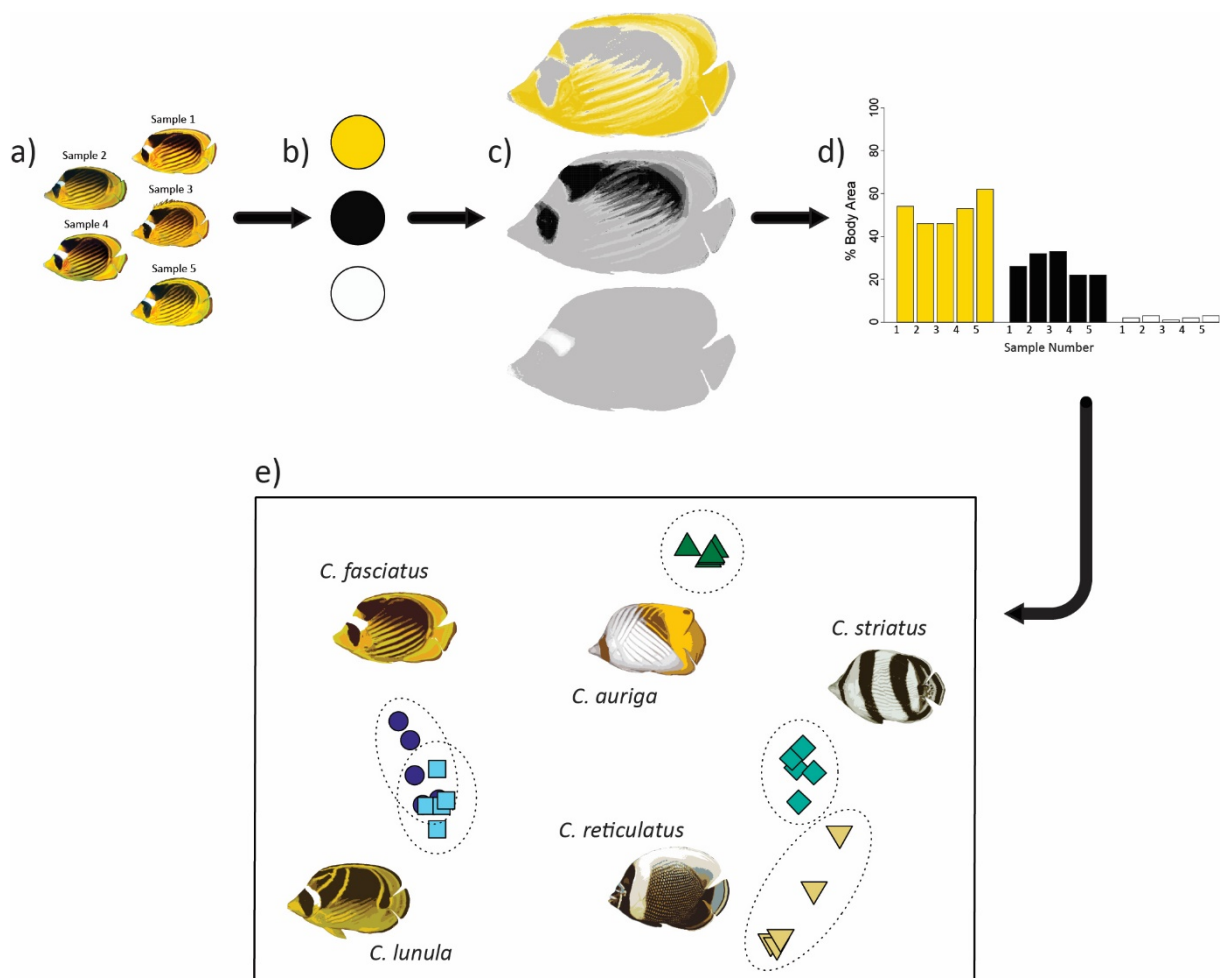


Figure 4.2 The initial colour calibration technique. a) Collect images of the calibration species; in this example, *Chaetodon fasciatus*. b) Establish colours of interest to be analysed. c) Run colour detection for each colour. The RGB centre-point and thresholds may need to be altered until images produce similar colour pattern heatmaps. d) Analyse colour areas for each image in a statistical framework, with χ^2 goodness of fit. e) Once stabilised, test the framework with other species to validate among-species applicability.

of image quality. Colour values (the RGB centre point) and cut-offs (the RGB offset) were procedurally increased until images produced statistically identical colour areas and colour heatmaps (**Figure 4.2c** and **4.2d**; RGB values and cut-offs are given in Supporting Information **Table C1**). When using these centre points and offsets, all five photos of this species produced non-significantly different images ($\chi^2 = 8.0795$; p-value = 0.4393). These working values were then validated using multiple species to test their effectiveness in detecting between-species variation in colour patterns (**Figure 4.2e**). The principal coordinates analysis displaying five test species, with five test images each, shows strong species-level congruence (**Figure 4.2e**) except in *C. fasciatus* and *Chaetodon lunula*, which are a visually similar species-pair.

Colour-pattern quantification

Images were analysed for presence and distribution of yellow, black and white at 250,000 locations across each image using the package “patternize” in R (Van Belleghem et al. 2018). After images were aligned using morphological landmarks (landmarks given in Supporting Information, **Figure C1**), colour detection was run on each image. The presence of yellow, black, white and ‘other’ colours were recorded based on our predetermined RGB and offset values. Patternize works by subdividing an image into a predetermined number of blocks. The greater the resolution requested by the user, the smaller in size and the greater the number of these blocks (**Figure C2**). Each block is effectively a variable that corresponds to a column in a data matrix, the rows being each image that is analysed. The value within each column for a specific image is either 1 or 0 depending on whether the colour being assessed is present or absent within each specific block. The algorithm moves procedurally from block to block, recording the presence or absence of the specified colour. The path it takes from block to block throughout the image is specific and occurs in the exact same manner for every subsequent image analysed. Since all images have been pre-aligned, meaning the morphological landmarks between them coincide, the order of blocks represents a specific pathway across the body. For example, if a colour is present in block 417 on image 1, but absent in block 417 on image 2, we know that the colour occurred on fish 1 but not in the same morphological location on fish 2. In our analysis, we specified a resolution that sub-divides each image into 250,000 blocks. Therefore, the result

of our detection protocol was a matrix of 250,000 columns (these being the 250,000 blocks) and 210 rows (210 rows = 210 images analysed = 5 for each of the 42 species).

However, *patternize* can only record the presence of one single colour at a time. Therefore, the colour detection protocol was run three times, once for each of the three colours of interest. Whichever blocks received absences (i.e. they didn't have yellow or black or white) across all three colours matrices were coded as our fourth 'other' colour category. Each colour matrix was converted to a unique alphabetic identifier that represents which colour it was told to detect (Y for yellow, B for black, etc). These were then combined to form a full colour-pattern matrix. The alphabetic identifier allows each colour to have an even contribution to the multivariate analyses, as numeric values would contribute uneven weights based on their size (full details in **Figure C3**). The full colour pattern matrix was analysed using Gower's dissimilarity measure due to its compatibility with categorical data (Gower 1971). This measure generates a dissimilarity value for each pair-wise comparison of every image to every other image. This value ranges from 0, where images are completely identical, to 1, where images are completely different. Since we used five images for each species, there were 25 pairwise comparisons for each of the recently diverged species-pairs that were assessed. Therefore, a total of 525 individual species-pair comparisons were recorded. Each of the 25 comparisons per species-pair were averaged, yielding a mean dissimilarity value representative of difference between colour patterns of each species-pair.

Photograph ground-truthing

To ensure the colour pattern dissimilarity between species-pairs was not a product of image quality, the mean within-species, between species-pairs and random-pair dissimilarities were compared using a one-way ANOVA with Tukey's HSD post hoc tests. If our methods accurately capture variation between species, the mean within-species colour pattern dissimilarity should be substantially lower than the mean colour pattern dissimilarity between species-pairs or between random-pairs. Furthermore, we tested the influence of geographic location on colouration on a focal species to ensure it did not differ depending on the location in which the individual was photographed.

Statistical Analyses

Mean species-pair colour pattern dissimilarity values were compared using phylogenetic generalised least-squares models in R (package ‘nlme’, Pinheiro *et al.* 2018). To account for non-independence of species due to shared evolutionary history, a phylogenetic correlation structure was incorporated into the model. Since each observation represents the mean relative colour pattern difference between a species-pair, the tips of the phylogeny were collapsed to the node that represents the divergence of each species-pair. Therefore, our working groups (i.e. the tips on our phylogeny) were the nodes of each pair (**Figure C4**).

Three variables were used to explain variation in species-pair colour pattern dissimilarity. The first was time of divergence, defined as the estimated time (Ma) when each species-pair diverged. These values were based on fossil-calibrated, mean ages in Cowman & Bellwood (2011). This was chosen as a form of null hypothesis testing which follows the assumption that colour patterns are merely a product of genetic drift and mutations. The second and third variables were range overlap and range symmetry. Species’ range size and location data were compiled from the IUCN Red List website (IUCN 2017). Range overlap and range symmetry between species-pairs were calculated following the methods established in Barraclough & Vogler (2000). Range overlap is defined as the area of overlap between two species divided by the area of the species with the smaller range. This value spans from 0 to 1. Range symmetry is defined as the range of the smaller clade divided by the total area of both clades. This value spans from 0.5, where ranges are equal in size, to approaching 0 where ranges are vastly different in size. Range overlap was subsequently multiplied by 100 to yield a percentage, and all explanatory variables were mean-centred to reduce the effects of collinearity. Models were generated that incorporated all possible combinations of variables and their interactions while simultaneously accounting for phylogeny (PGLS). The best fitting model was then chosen using AICc and AICc weights (Akaike 1987; Wagenmakers and Farrell 2004). All analyses were conducted in R (R Core Team 2018).

4.3 Results

Photographic ground truthing

The mean within-species colour pattern dissimilarity was significantly lower than the mean between species-pair and mean random-pair colour pattern dissimilarities, with values of (mean \pm 95% C.I.) 0.1648 ± 0.0061 , 0.2340 ± 0.0062 and 0.2862 ± 0.0056 respectively (all significantly different, Tukey's HSD post hoc test; details in **Figure C5**, **Table C2**). This validated the colour pattern quantification method as it displayed its ability to discern similar images (i.e. of the same species) and separate them from different images (i.e. compared to other species). Additionally, it shows that a species-pairs' colour patterns are not generated via random processes, as they possessed colour pattern dissimilarity values significantly lower than the values observed when comparing random-pairs (i.e. a random comparison of two images from different species). We also found no geographic location effect on colour patterns within a species (**Figure C6**, summary statistics **Table C3**).

Time of divergence effect

Time of divergence was not deemed an important predictor of colour pattern dissimilarity between species-pairs, indicating no influence of evolutionary time on species-pair colour pattern divergence (model selection criteria in **Table C4**). While there is a slight positive relationship when only time of divergence is analysed, this relationship is non-significant (p-value = 0.1351, $R^2 = 0.0907$; **Figure 4.3**, summary statistics **Table C5**). All models incorporating time of divergence as a predictor were not suited for describing colour pattern dissimilarity between species-pairs.

The youngest species-pairs reached mean colour pattern dissimilarity within 1 million years; subsequently this level of dissimilarity is maintained. Four of the five highest species-pair dissimilarities were achieved in less than 1 million years. In extreme examples (e.g. *C. kleinii* and *C. trichrous* which possess the second highest dissimilarity between any pair), colour pattern differences were achieved in just over 300,000 years (highest posterior density interval = 0.0381 – 0.6883). Conversely, the third oldest pair, *C. plebeius* and *C. bennetti*, (mean age = 3.30 Ma; HPD interval = 2.217 – 4.49 Ma) are the

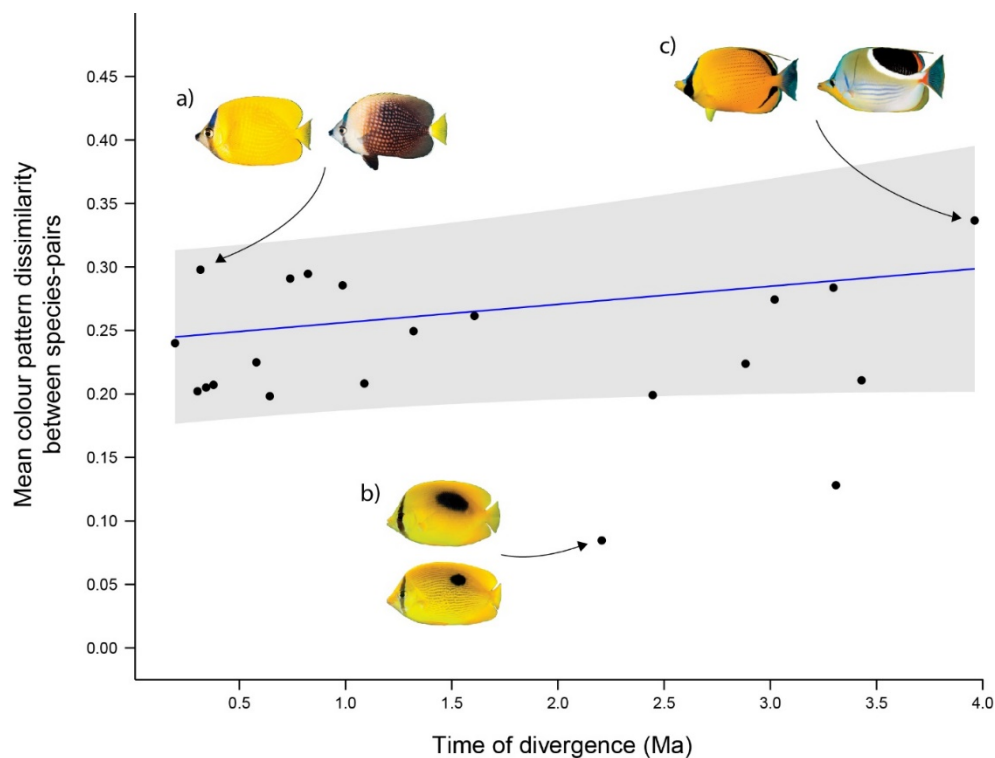


Figure 4.3 The rapid differentiation of colour patterns among species-pairs. a) high levels of differentiation in *C. kleinii* and *C. trichrous* which separated approximately 300,000 years. b) minimum differentiation in *C. speculum* and *C. zanzibarensis*. c) high levels of differentiation in the oldest pair *C. ephippium* and *C. semeion* which diverged 3.96 Ma. Phylogenetic generalised least squares regression (PGLS - blue line) of time of divergence against species-pair colour pattern dissimilarity. The trendline with 95% confidence intervals shows a marginally positive but non-significant slope. Each point represents the mean colour pattern dissimilarity of the 25 individual pairwise comparisons for each species-pair.

second most similar of all pairs. It appears that differences in colour pattern can occur rapidly, in the youngest of species-pairs, with no significant influence of time thereafter.

Range effects

Like time of divergence, there was no significant effect of only range overlap or only range symmetry. However, the model incorporating range overlap, range symmetry and their interaction was, by far, best suited for describing colour pattern dissimilarity between species-pairs. Only the interaction between range overlap and range symmetry was found to be significant (p-value = 0.0129, $R^2 = 0.349$; **Figure 4.3**, summary statistics in **Table C6**). It appears there is a trade-off between the influence of

range overlap and range symmetry on colour pattern dissimilarity between species-pairs. When ranges are of similar size (symmetry ≥ 0.4 , $n = 4$), there is an increase in colour pattern difference with an increase in range overlap, i.e. species-pairs become more visually different within increasing sympatry (**Figure 4.4a**). However, if species-pairs have drastically different range sizes (symmetry ≤ 0.1 , $n = 5$), there is an inverse relationship, i.e. colour patterns between species-pairs become more similar with increasing sympatry (**Figure 4.4c**).

4.4 Discussion

We found that colour pattern dissimilarity between species-pairs is significantly related to the interaction between range overlap and range symmetry. Butterflyfishes species-pairs that overlap more in their geographic range tend to have larger differences in colour patterns, but only when their ranges are symmetric (i.e. of similar size). At the mean level of range symmetry (symmetry > 0.1 and < 0.4), colour patterns are equally similar regardless of overlap. At extremely asymmetric range sizes, the pattern is reversed – highly overlapping species-pairs have the lowest colour pattern difference.

When species-pair ranges are symmetric, our results are in broad agreement with much of the literature that has quantified signal divergence in terrestrial organisms (Seddon 2005; Bothwell et al. 2015; Doutrelant et al. 2016). Furthermore, we show that this relationship also holds for the full organismal colouration, incorporating both colour palette and patterns, for an iconic group of coral reef fishes. However, we found a surprising, and previously undescribed, reversal when species-pairs with highly asymmetric ranges are included in the analyses. Additionally, colour pattern differences appear to arise shortly after species diverge regardless of the extent of sympatry.

Colour patterns and time

The rate at which species-pairs diverge in colour pattern is extremely fast when compared to morphological traits (Floeter *et al.* 2018). Since species-pairs must have diverged from the same common ancestor and chaetodontids lack colour polymorphisms, colour pattern dissimilarity at the time

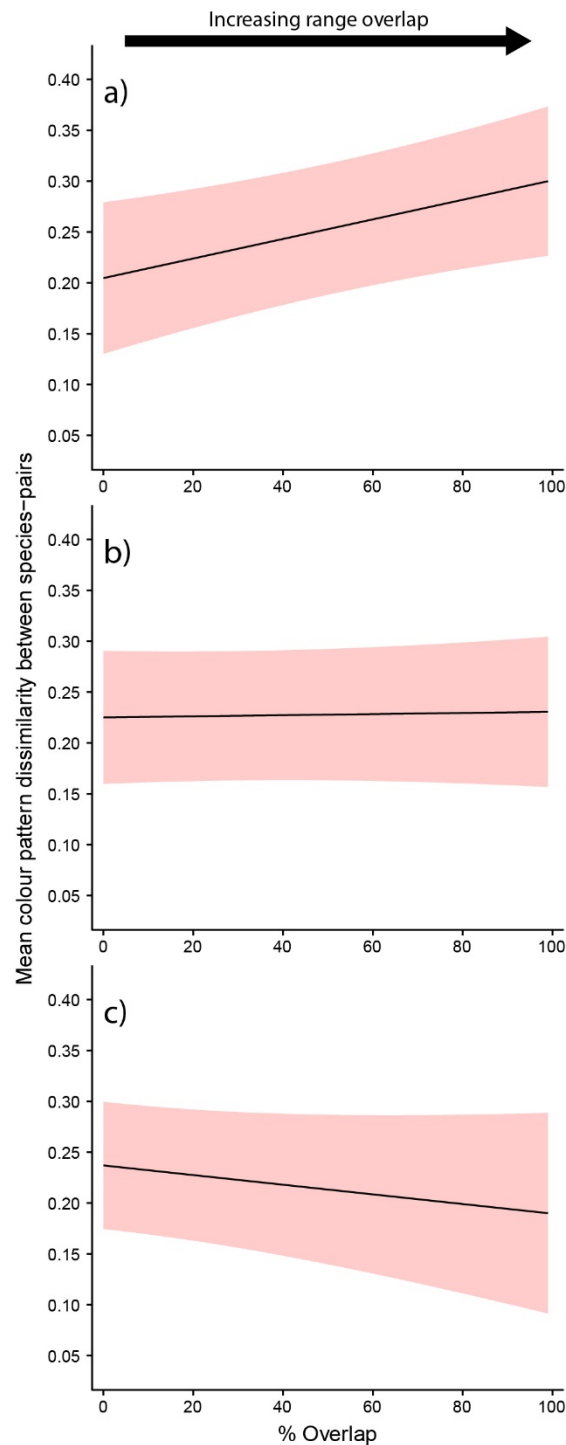


Figure 4.4 Phylogenetic generalised least squares regression with 95% confidence intervals displaying the relationship between range overlap, range symmetry and species-pair colour pattern dissimilarity.

of divergence must be near to zero. Yet, in just over 300,000 years, rapid divergence in colour patterns can occur. We observed some of the youngest species-pairs achieving greater colour pattern differences than the average difference of all species-pairs analysed. Similar rapid colour differentiation between

species-pairs has been reported in African cichlids (1 -2 million years, Smith & Kornfield 2002; Kocher 2004). However, these are mouth-brooding, site-attached cichlids restricted to specific lakes. To see comparable changes in pelagic-spawning, reef fishes with geographic ranges spanning one- to two-thirds of the global tropics was most unexpected.

Furthermore, there was no significant relationship between the difference observed between species-pair colour patterns and their time since divergence. Therefore, colour patterns are not merely a product of genetic drift and mutations. While time may influence colour patterns for some species in this matter, colour patterns are not exclusively driven by this phenomenon. Colour pattern divergence in birds has been shown to have the same disjunct relationship (Cooney et al. 2017). Two different bird

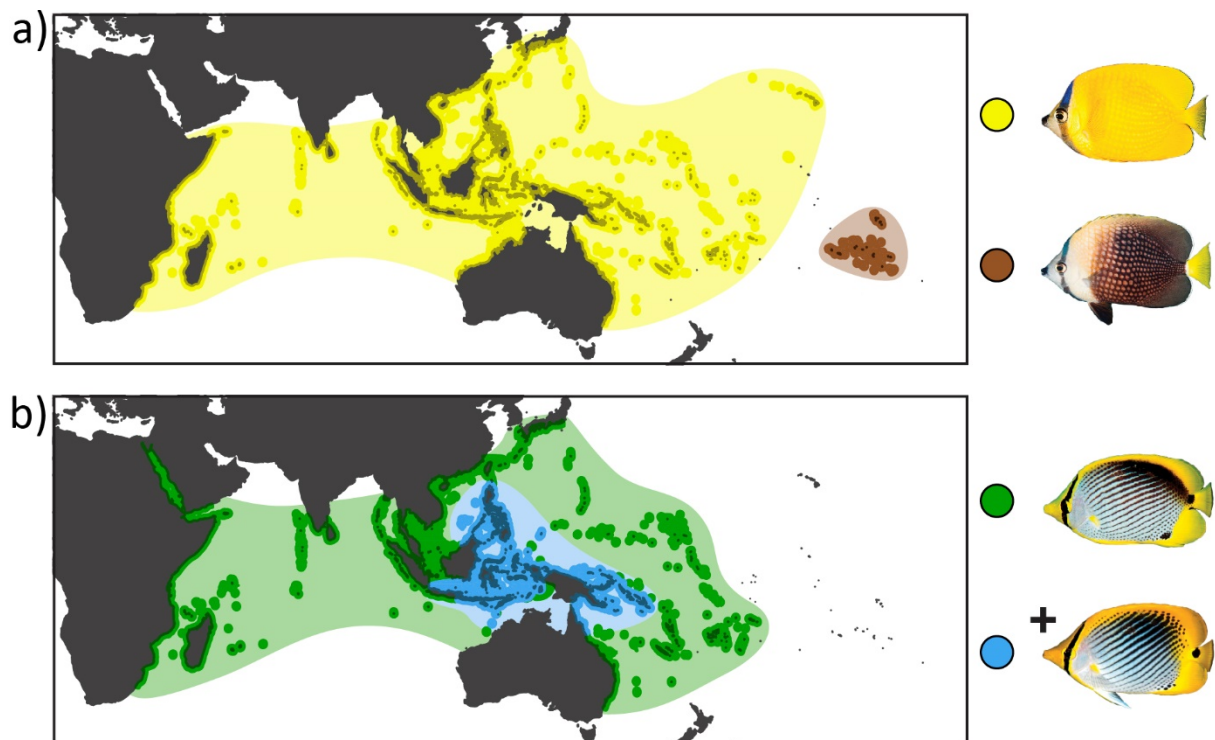


Figure 4.5 Two examples of asymmetric range sizes. a) Peripheral speciation in *C. trichrous* (brown) vs. the widespread *C. kleinii* (yellow). The transparent brown and yellow areas help visualise the total geographic distribution of each species vs. reef-based occurrences denoted by the darker colours. The range area of *C. kleinii* is over 18x greater than the area occupied by *C. trichrous*. Although there is no overlap between these two species, their colour patterns are highly divergent. b) The entirety of *C. ocellicaudus*' range (blue) is within the range of its pair, *C. melannotus* (green), yet they retain similar colour patterns; contrary to theoretical expectations. Photos with permission from François Libert.

datasets measuring the level of dichromatism between male and females of the same species displayed a similar slightly positive but non-significant relationship with time. While this does not represent the same scenario as that studied herein, (as one is comparing colour divergence between species and the other between sexes), both display a general disconnect between colouration and time.

The ability for colour patterns to evolve rapidly may be a key factor underpinning the vast taxonomic diversity in coral reef fishes. Often, colouration is the only factor differentiating closely related species (McMillan *et al.* 1999). While these new colour-forms increase the visual complexity and perceived taxonomic diversity of coral reef ecosystems, they often contribute little to their functional diversity (Bellwood *et al.* 2017). Evolution of certain morphological aspects (e.g. teeth, gut, etc.) are often tightly linked to ecology (Bellwood and Choat 1990; Berumen *et al.* 2011). Colour patterns, however, may be more neutral in that there are potentially multiple options that can meet the basic evolutionary requirements allowing lineages to differentiate. Whether a diverging lineage develops spots or stripes may be irrelevant; the only important feature is that this colour pattern is sufficiently different from its congener. In effect, colour patterns may be an extreme evolutionary example of many-to-one mapping (Wainwright *et al.* 2005) where numerous alternatives may deliver the same functional outcomes.

Species ranges and their relationship to colour patterns

Of the three explanatory variables investigated herein, geographic range overlap was by far the most likely to predict colour pattern dissimilarity. A pattern which is consistent with previous studies (Martin *et al.* 2010). Evolution offers diverging lineages two options: 1) to increase signal divergence thereby making species identity more easily distinguishable, promoting speciation, or 2) fail to increase signal divergence and regress back into the original form (Templeton 1981). *C. reticulatus* and *C. meyeri* are a prime example of colour pattern differentiation coinciding with overlap (**Figure 4.1c** and **4.1d**). These two species co-occur throughout much of their ranges and, presumably through reinforcement, have vastly different colour patterns. This relationship between co-occurrence and signal divergence has

been shown repeatedly in frogs, birds and lizards, based on evidence from both sound and colour (Höbel and Gerhardt 2003; Seddon 2005; Bastiaans et al. 2014).

Maximizing signal divergence where species co-occur is likely to be critically important for chaetodontids due to their heavy reliance on pair formation and strong territoriality (Roberts and Ormond 1992). Some species maintain territories that they aggressively defend to ensure dietary resources; often the level of aggression is dependent on the dietary speciality of the species (Righton and Mills 2006). In this context, having highly contrasted signals would make ecological sense, to prevent unwarranted aggression from species that may have different dietary needs. Additionally, having bold and brightly contrasting colour patterns that are highly differentiated from heterospecifics would permit effective visual communication over large distances (Marshall et al. 2003; Marshall 2017) whether defending areas or locating a partner. The common colours found on most individuals within this family further optimise conspicuousness thus enhancing the signals strength. Black and white are the most contrasted of all colours, while yellow is highly contrasted with blue, the ambient background colour found in coral reef ecosystems. Together, the use of these specific colours, and the strength of social/territorial structure, puts the divergence of these signals into perspective. Interestingly, defensive morphological traits in chaetodontids, like the dorsal and anal fin spines, have been shown to follow axes driven by their pairing tendency and foraging strategies (Hodge et al. 2018). It appears that colour patterns may be reflecting a similar relationship.

What was most surprising was the reversal of this relationship in species-pairs with highly asymmetric ranges. Asymmetry is commonly associated with peripheral speciation (Rocha et al. 2008; Hodge et al. 2012; Gaither et al. 2015). Often, this equates to allopatry (specifically, peripatry). In our study, this is exemplified by the non-overlapping species-pair *C. kleinii* and *C. trichrous* (**Figure 4.5a**). *C. trichrous* is endemic to French Polynesia, while *C. kleinii* possess an extremely broad distribution over 18 times greater than that of *C. trichrous*; spanning the entirety of the Indian and western Pacific Oceans. This pair possessed the second highest mean dissimilarity value between any pair, providing an example of large colour pattern changes likely associated with asymmetric peripatric speciation.

However, we found that when species-pair range sizes are highly asymmetric, yet also highly overlapped, there is a decrease in colour pattern dissimilarity (**Figure 4.4c**). Theory would predict that these highly overlapped, highly asymmetric species would have the most differentiated signals of all species-pairs that were analysed. This was not the case. There are a few potential explanations for the maintenance of these non-geographically delineated colour patterns. Firstly, fine-scale patterns may play a key role (Grether et al. 2015). For example, the spot on the caudal peduncle that differentiates *C. ocellicaudus* from *C. melannotus* (**Figure 4.5b**) could be important in species identities. Alternatively, UV-reflective colouration may be important (Siebeck 2004), although this is unlikely given the spectral sensitivity of chaetodontids (Losey et al. 2003; Marshall 2017). These minor colouration components and how they relate to the recognition of conspecifics warrants further attention. Secondly, and possibly more likely, other non-visual methods of species recognition may be more influential (McMillan *et al.* 1999), like sound (Bowen et al. 2013; Tricas and Boyle 2014) and smell (Boyle and Tricas 2014). Indeed, repeated hybridization in colourful reef fish, i.e. those with highly differentiated colour patterns (Yaakub et al. 2006; DiBattista et al. 2012), including chaetodontids, points to the potential limitations of species boundaries based exclusively on colour (Gaither et al. 2014). Lastly, these species may be occupying different specific habitats within their shared geographic range. While at the global scale they appear to co-occur, there may be partitioning at the localised scale. Investigating more specific patterns of co-occurrence and overlap may shed light on the lack of colour patterns differentiation in species with shared geographic ranges.

Future Directions

By incorporating both colour and pattern, we can begin to explore the functional basis of organismal colour patterns. This new method of colour pattern quantification (Van Belleghem et al. 2018) shows great promise and offers a first step towards more holistic colour pattern analyses. Our quantification of both colour and pattern in butterflyfishes revealed clear trends in the evolution of colour with rapid differentiation and the influence of geographic range components. We show support for the traditional paradigm of increased divergence in visual signals with increasing range overlap, but

only when range sizes are symmetric. The most surprising trend is a reversal of this relationship when ranges are highly asymmetric.

Our findings contribute to an increasing body of evidence that suggests that the evolution of colouration, in relation to species distributions, may be quite conserved; operating consistently across numerous terrestrial and aquatic ecosystems (Puebla et al. 2007; Martin et al. 2010; Bothwell et al. 2015). However, it is remarkable that butterflyfishes should exhibit such similarity to terrestrial species, especially as they arise in organisms with geographic ranges that span over half the global tropics.

Chapter 5: Fish communities on coral reefs are becoming less colourful

5.1 Introduction

There is often a strong link between an organism's appearance and the environment in which it lives (Green et al. 2019; Hulse et al. 2020). Specifically, the local biotic and abiotic factors of an ecosystem strongly shape how and what function colouration serves (Endler 1992; Phillips et al. 2017). Whether the goal is to conceal one's appearance from predators or to remain conspicuous to attract mates, the characteristics of the surrounding environment must be considered (Endler 1978; Marshall 2000b). Interestingly, profound changes to the environment can induce equally profound changes in an organism's appearance and colouration (Seehausen et al. 1997; Fuller 2002; Camacho et al. 2020).

Historically, researchers have approached colouration from an individualistic perspective, i.e. focusing on the individual or species, rather than on communities. This has often meant treating every organism's colouration as independent samples and using analyses that describe how these may be similar or different to one another (Hemingson et al. 2020). While informative, it has left the field with a limited understanding of how communities use colour as a collective whole. Ecologists have used taxonomy (Warwick and Clarke 1991; Öhman et al. 1997; Hemingson and Bellwood 2020), morphology (Hulse and Wainwright 2002; Mihalitsis and Bellwood 2019; Su et al. 2019) and more recently traits and functions (Villéger et al. 2008; Hemingson and Bellwood 2018; McWilliam et al. 2018), to describe the multidimensional nature of community data. However, colour as a community-level trait has received little attention although it is one of the most conspicuous features of many ecosystems, including coral reefs.

From a community perspective, the diversity of colours found on coral reefs is striking (Alieva et al. 2008; Lapshin et al. 2015). The benthos on healthy coral reefs is dominated by numerous different colourful organisms, primarily corals. Intermittent patches of differing substratum types create a visual mosaic that is unrivalled by most other ecosystems. Fishes that inhabit coral reefs are equally, if not more, diverse in their colouration, and have consequently received much research attention (Marshall,

2000b; Marshall, Cortesi, de Busserolles, Siebeck, & Cheney, 2018). These complex and unique colours and patterns have been linked to a broad range of functions, from camouflage (Cortesi et al. 2015; Tyrie et al. 2015; Phillips et al. 2017), to communication (Cheney, Grutter, Blomberg, & Marshall, 2009; Hamilton III & Peterman, 1971; Marshall, 2000a), and maintaining species boundaries (Choat, Klanten, Van Herwerden, Robertson, & Clements, 2012; Hemingson, Cowman, Hodge, & Bellwood, 2019). Indeed, we have learned much about how colouration may function in various reef fish groups. However, we lack a broader understanding of the extent to which environmental factors may shape fish colouration on coral reefs, especially at a community or assemblage level.

The relationship between fish colour and environment may be further altered by the drastic transitions occurring on coral reefs due to climate change. Human-induced stressors are severely impacting coral reef ecosystems, causing a transition from coral-dominated to alternative reef states (Nyström et al. 2000; Bellwood et al. 2004; Morais et al. 2020). Contemporary reefs are becoming increasingly characterised by non-coral substrata including turf algae, macroalgae, and coral rubble (Graham et al. 2015; Bellwood et al. 2019a). Marked changes have already been documented, in both the taxonomic structure of fish assemblages (i.e. what species are present, Bellwood, Hoey, Ackerman, & Depczynski, 2006; McClure et al., 2019) and in their traits (Richardson et al. 2018) or functional characteristics (Morais et al. 2020), following disturbances and environmental change. But how has this impacted fish colouration on reefs?

Herein, we utilise a novel image-analysis approach to characterise the colouration of entire fish assemblages; the ‘assemblage colouration’. We then relate this directly to the environment in which the assemblage was collected. Furthermore, using a dataset that has tracked reef fish assemblages over 27 years, we determine if assemblage colouration has changed in response to large-scale disturbance events. Specifically, we ask: 1) does reef fish colouration relate to the benthic configuration of the immediate, local environment? Essentially, does benthic composition shape the diversity of colours in resident reef fishes? And 2) have large-scale environmental disturbances (mass bleaching events) affected colour diversity through time? These questions will shed light on the role of environmental factors in shaping

the vast diversity of colours observed in coral reef fishes and how robust they are to environmental change.

5.2 Methods

Method development and habitat relationships

This study is comprised of two major components: in the first component (*Part A*) we developed a framework for measuring and quantifying the colouration of an entire fish assemblage: the ‘assemblage colouration’. This was then used to examine how the local habitat characteristics (e.g. branching coral cover) correlate with the assemblage colouration measured as multidimensional ‘colour space’. The second component (*Part B*) applies this assemblage colouration approach to a 27-year time series that encompassed all four global bleaching events. This component aims to analyse how the assemblage colouration may have been impacted by major environmental disturbance events.

Part A - quantifying ‘assemblage colouration’

We wanted to measure and quantify the collective appearance of an entire fish assemblage; namely its ‘assemblage colouration’. To do this, we first needed an approach that quantifies the full colouration of an organism, that is, measuring both the number of different colours present as well as their relative amounts on every individual. To do this, we used the *colordistance* library in R (Weller and Westneat 2019). Briefly, *colordistance* quantifies colouration by measuring the number of pixels on an image that fall within specified regions of the RGB colourspace. This procedure essentially creates a ‘colour thumbprint’ for every image by recording the relative amount of each colour in each image (for more details, see Weller & Westneat, 2019).

These ‘thumbprints’ can then be compared using standard multivariate techniques because, when combined, they are simply a matrix of specific colours and their relative amounts on every image. To display similarities and differences between colourations, they can be visualised using a non-metric multidimensional scaling (NMDS) ordination. This NMDS plot displays the summarised, full colouration of numerous organisms. Within the plot, each organism’s colouration becomes a point.

Points that are closer together have similar colourations; points farther apart have very different colourations.

With a biplot of colourations, we can now ask questions relating to the ‘assemblage colouration’, defined herein as the ‘collective colouration of a group of organisms from a single location’. Herein, we use two separate metrics to measure space use in the NMDS ‘colour space’; both of which have been well established in the literature: convex hulls and multivariate dispersion (Mouillot et al. 2013a). The convex hull is the smallest possible polygon in two-dimensional space that encompasses all points within a specified group. In our scenario (analysing colouration), this effectively represents the area encompassed by the most uniquely coloured species within an assemblage. The second metric, dispersion, measures the spread of points within this multivariate space – typically the average distance of all points from the centroid. A higher average dispersion means the colouration of organisms in that assemblage is, on average, more different looking. Details of these two metrics can be found in **Figure D1**. From here on, these metrics will be referred to as ‘colour-area’ (the convex hull) and ‘colour-spread’ (the multivariate dispersion). Furthermore, we establish one overarching measure of colour: the ‘faunal colouration’ i.e. the ‘collective colouration of all organisms surveyed’. While the assemblage colouration represents the colouration of distinct, sampling units (herein quadrats described in the following sections), the faunal colouration is the full colouration of all sampling units combined (all quadrats). Ultimately, these steps allow us to 1) characterise the full colouration of an individual, 2) compare them between individuals to note similarities and differences, and 3) quantify the assemblage colouration of a local assemblage and to compare this to the potential colouration of the total fauna.

Study group

We focus on small, site-attached reef fishes. This includes damselfishes (Pomacentridae), small wrasses (Labridae), butterflyfishes (Chaetodontidae), and groupers (Serranidae), as well as cryptobenthic reef fishes. Cryptobenthic reef fishes (Brandl et al. 2018) are small bodied, morphologically or behaviourally cryptic fishes that are a key component for the functioning of coral reef ecosystems (Brandl et al., 2019). These fishes are characterised by high site-fidelity and limited

movement (Nash, Welsh, Graham, & Bellwood, 2015) which allows for direct comparison with the habitat in which they live. Thus, this group of fishes offers an ideal assemblage with which to study the relationship between substratum types and fish colouration. For the sake of brevity, the general term ‘cryptobenthic’ is used herein to include all the previously mentioned groups of fishes.

Substratum and fish surveys

Fishes and benthic images were collected from three sampling sites at Orpheus Island (18.6161°S, 146.4972°E) in the mid-section of the Great Barrier Reef. Specific sampling locations were chosen to encompass varying levels of the six focal substratum types: structurally complex hard corals, massive and encrusting hard corals, soft corals, rubble, turf algae-covered reef matrix, and sand (**Figure D2**). The cover of each substratum type varied significantly between sites (**Table D1**) highlighting that a wide diversity of benthic configurations was surveyed.

At each sampling location, a 1m² PVC quadrat was placed onto the substratum. The quadrat was then photographed directly from above using a Nikon Coolpix W300; capturing the entire 1m² quadrat in planar view. The quadrat was then enclosed in a 2mm mesh mosquito net and anchored to the benthos using a chain to completely seal off any gaps (image of collection technique in **Figure D3**). Two divers each applied 250 mL of diluted clove oil solution (a mixture of 15% clove oil and 85% ethanol) from hand operated spray bottles. The spraying continued until the netted area was completely exposed to the diluted clove oil solution. The mixture was left for approximately five minutes to ensure all fishes within the quadrat were anesthetized. Both divers carefully examined the quadrat collecting all fishes using forceps until no new fishes were found after approximately 3-5 minutes of intense searching. Following the dive, the fishes were placed in an insulated cooler filled with ice. Ethical and permitting permission allowed a total of 12, 1m² quadrats to be sampled, which yielded a total of 139 fishes. Average abundance per quadrat was 11.6 individuals (range: 4 – 20) and average species richness was 6.25 species (range 4 – 9) per quadrat.

Photography, image processing, and analysis

The fish were immediately transported back to the lab and photographed. Photographs were taken using a Nikon D200 in *raw* format with the same camera settings (ISO: 400, f-number: 9, shutter speed: 1/40 to 1/80). Specimens were submerged in a petri dish of saltwater on a white background, laid on their side and photographed laterally while illuminated with a white LED dissection lamp (mounted at 45° to avoid reflection). To ensure all photos were colour-standardised, a colour standard slate (the X-Rite ColorChecker Passport) was included next to the fish in all photos. This small slate contains 24 different colour patches which cover most of the visible light spectrum, including white and black. This was later used to standardise all photos.

Images were generally slightly under-exposed, so the exposure was increased by 1 exposure value in Adobe Lightroom (CC2019) to ensure the photographs accurately reflect each fish's true colours in life. Since all fish were photographed using the same camera settings, increasing exposure on all photos applies the same correction to all images thus keeping them standardised. Once completed, all images were exported as *.jpg* files then colour standardised (Bergman and Beehner 2008) using the 'colorChecker' function in the *patternize* library in R (Van Belleghem et al. 2018; R Core Team 2020). This function detects the RGB (red, green, blue) values in each patch on the colour standard within every image and compares it to the known RGB values of each patch as determined by the manufacturer. The algorithms within the function then make corrections to the various colour channels to rebuild each image to match the known colour values as close as possible. These steps ensure the colouration is accurate and standardised between specimens.

After colour standardisation, images were imported back into Adobe Photoshop (CC2019) to remove the background. The fish in each image was cropped using the selection tool and pasted onto a solid, bright green background (specific RGB values: 64, 255, 0). This background colour is ignored when the colour detection protocol is run. It is therefore necessary to choose an extremely saturated colour not present in any of the fishes' colours. The colouration was then analysed using the aforementioned procedure in *colordistance* (Weller and Westneat 2019). We chose to partition each axis of the RGB colourspace into 6 sections (double the default number dictated by *colordistance*) which

yielded a total of 216 possible colour categories that a pixel could fall within (6 sections per axis \times 3 axes = 216). We utilised the chi-squared distance in *colordistance* to generate the colouration dissimilarity matrix. The dissimilarity matrix was then visualised using a NMDS and the colour-area and colour-spread were then measured for the fish assemblage within each quadrat.

The relative cover of the six focal substratum types were measured in each quadrat using ImageJ (Schneider et al. 2012). Some substratum types were combined to generate more comprehensive substrate groups based on different ecological hypotheses. For example, assuming that live corals may be important for colouration the category ‘live coral cover’ = ‘structurally complex hard coral cover’ + ‘massive and encrusting hard coral cover’ + ‘soft coral cover’.

Species richness was found to have a significant and positive effect on both colour-area and spread (**Figure D4** and **Table D2**). Therefore, the residuals from this analysis were used in the subsequent analyses as the dependent variable to account for the confounding effect of richness. Multiple regression models were generated in which the explanatory variable was the cover of different substratum types and the response variable was species-standardised colour-area and colour-spread. The most parsimonious models were chosen using AICc and AICc weights. Furthermore, each variable’s predictive power (R^2) was calculated to explore the substratum types (or combinations) that best explain variation in colour-area and spread.

Part B – Temporal variation and disturbance effects

We then examined if the assemblage colouration of cryptobenthic reef fishes was impacted by major environmental disturbances, most notably, mass coral bleaching events. To assess this, we quantified the colour-area of cryptobenthic fish assemblages in annual samples from Orpheus Island, Australia spanning 27 years. We utilised a long-term dataset of cryptobenthic fish assemblages in the same location and using the same technique as outlined above. This dataset started in 1993 (described in Bellwood et al., 2012, 2006), and encompasses all global bleaching events and multiple major cyclones that have severely impacted the reefs surrounding Orpheus Island. This includes the first

recorded global mass coral bleaching event in 1998 that was responsible for a complete shift in the structure of local cryptobenthic fish assemblages (Bellwood et al. 2006).

The fish abundances in this dataset were used to calculate assemblage colourations through time. Simply put, the colouration NMDS plot (displayed in **Figure 5.1**) created in *Part A* was used as a ‘key’ to calculate colour-areas based on the abundances present in the long-term monitoring dataset (for specific details, see the Supporting Information, **Figure D7**). Using this approach, we could recreate each year’s cryptobenthic assemblage colouration and quantify changes through time and in response to disturbances. A generalised additive model (gam) was used to visualise changes in the colour-area between years since relationships may be non-linear. Given the exceptional focus of humans on ‘desirable’ or ‘attractive’ yellow-coloured fishes (Tribot et al., 2018, 2019), we also examined the relative abundance through time of species that occupy the yellow-green component of the faunal colouration.

All analyses were conducted in R (R Core Team 2020). The specific libraries used were *patternize* (Van Belleghem et al. 2018) and *colordistance* (Weller and Westneat 2019) for image analysis, *dplyr* (Wickham et al. 2020) for data manipulation, *mgcv* (Wood 2011), *betareg* (Cribari-Neto and Zeileis 2010), *emmeans* (Lenth 2020), and *vegan* (Oksanen et al. 2019) for model fitting and testing, and *ggplot2* for visualisation (Wickham 2016).

5.3 Results

Part A: visualising reef fish colourations

The NMDS of fish colouration could accurately discern differences between species and among individuals within species with a high degree of accuracy (**Figure 5.1**, stress = 0.12). The distribution of colourations followed three primary axes: those comprising large amounts of dark colours (e.g. blacks and dark browns), those comprising large amounts of light colours (light browns and greys), and those with predominantly yellows. The edges of the full convex hull, the faunal colouration, were defined by species with unique appearances defined by ‘bright’ colours, like *Gobiodon histrio*, *Paragobiodon xanthosoma*, *Neamia octospina*, and male *Enneapterygius atrogulare*. The convex hulls of each species

generally occupied their own, distinct, areas in the NMDS with limited overlap between species (**Figure D5**).

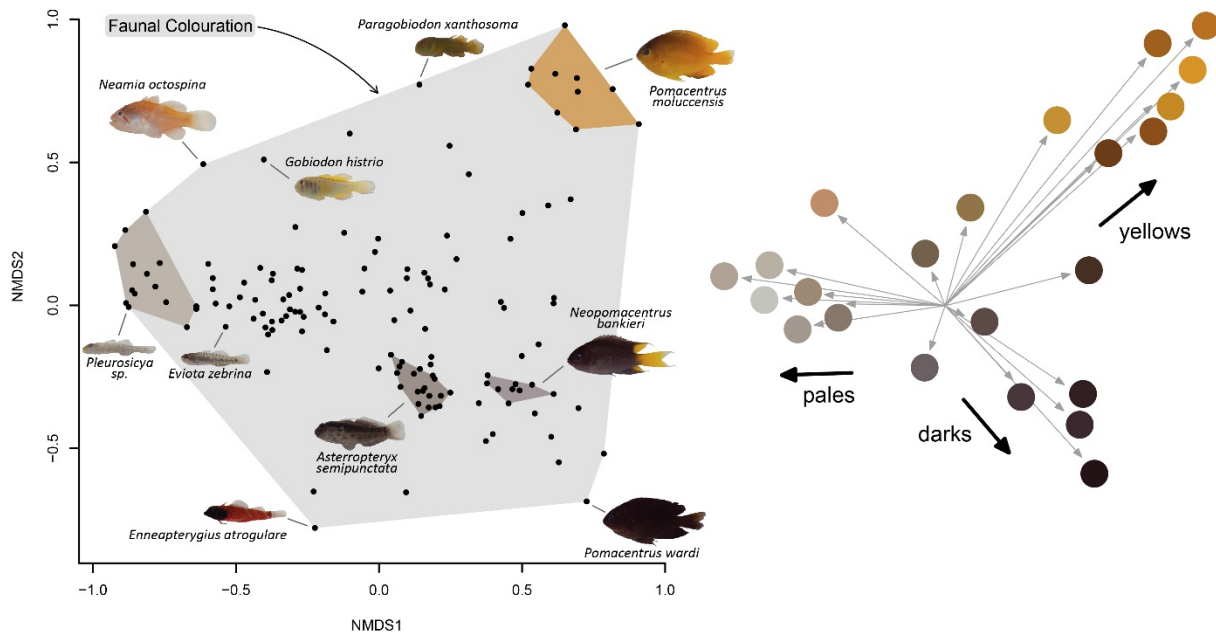


Figure 5.1 The ‘faunal colouration’ of cryptobenthic fishes at Orpheus Island. The non-metric multidimensional scaling (NMDS) ordination displays the diversity of fish colourations. Stress = 0.12. All individuals that were collected ($n = 139$) have been plotted. The grey, shaded area is the faunal colouration (the full convex hull area) of all individuals analysed. The species hulls for *Pomacentrus moluccensis*, *Pleurosicya sp.*, *Asterropteryx semipunctata*, and *Neopomacentrus bankieri* have been delineated (all species hulls available in **Figure D5**). On the right are the vectors of the most common colours driving the distribution of individuals (and species) within multivariate colourspace.

Habitat relationships

The colour-area and colour-spread of each assemblage colouration differed markedly among quadrats (**Figure D6**). The least colourful quadrat (quadrat 12) only occupied 3.6% of the area of the full faunal colouration. The quadrat with the largest assemblage colouration (i.e. the most colourful quadrat; quadrat 9) occupied over half of the full faunal colouration (52.6%) and was almost 15 times larger in area than the least colourful quadrat. On average, assemblage colourations occupied approximately a quarter of the area of the full faunal colouration ($26.7\% \pm 4.4$ [standard error]). Colour-spread yielded almost identical results among quadrats (details in **Appendix D**).

There were strong, significant, linear relationships between the cover of certain substratum types and the assemblage colourations of cryptobenthic fishes. Structurally complex coral cover (structurally complex hard coral cover and soft coral cover combined) was the best factor to explain assemblage colouration areas (adjusted $R^2 = 0.67$, p -value < 0.001 , **Figure 5.2a**, **Table D3**) and the second-best factor to explain colour-spread (adjusted $R^2 = 0.43$, p -value $= 0.012$, **Figure D8**, **Table D4**). In both models, structurally complex coral cover displayed significant and positive relationships with both metrics (**Table D5**). Inversely, the total cover of rubble & turf-covered reef matrix was the best model to explain colour-spread (adjusted $R^2 = 0.43$, p -value $= 0.012$, **Figure D8**, **Table D4**) and the second best to explain colour-area (adjusted $R^2 = 0.64$, p -value $= 0.001$, **Figure 5.2b**, **Table D3**). For both metrics, turf & rubble cover displayed significant negative relationships. Our results were strongly supported by additional permutation tests which assessed the robustness of our findings (**Figure D9**). Simply put, as structurally complex coral cover increases, so does the total range (area) and difference (spread) of colours present in cryptobenthic fish assemblages. Inversely, as rubble and turf area increase, there is a contraction of colour-area and fishes begin to have more similar colourations. It is important to note that these relationships are after accounting for known differences in species richness among quadrats.

The different substratum types showed considerable variability in their ability to predict colour-area and spread. Complex coral cover and turf & rubble area were the two best fitting variables with R^2 values > 0.60 . All other substratum types goodness-of-fit values (R^2) decreased gradually in their ability to predict species-standardised colour-area and spread (**Figure D10**). Interestingly, the worst predictor was massive & encrusting coral cover, possessing an R^2 of 0.03 for both colour-area and spread. Both relationships were non-significant.

Temporal changes

Applying the above assemblage colouration approach to the time-series, we found that the assemblage colour-area occupied by cryptobenthic fishes varied substantially from year-to-year throughout the 27-year sampling period (**Figure 5.3a**). The largest change was a drastic decrease in

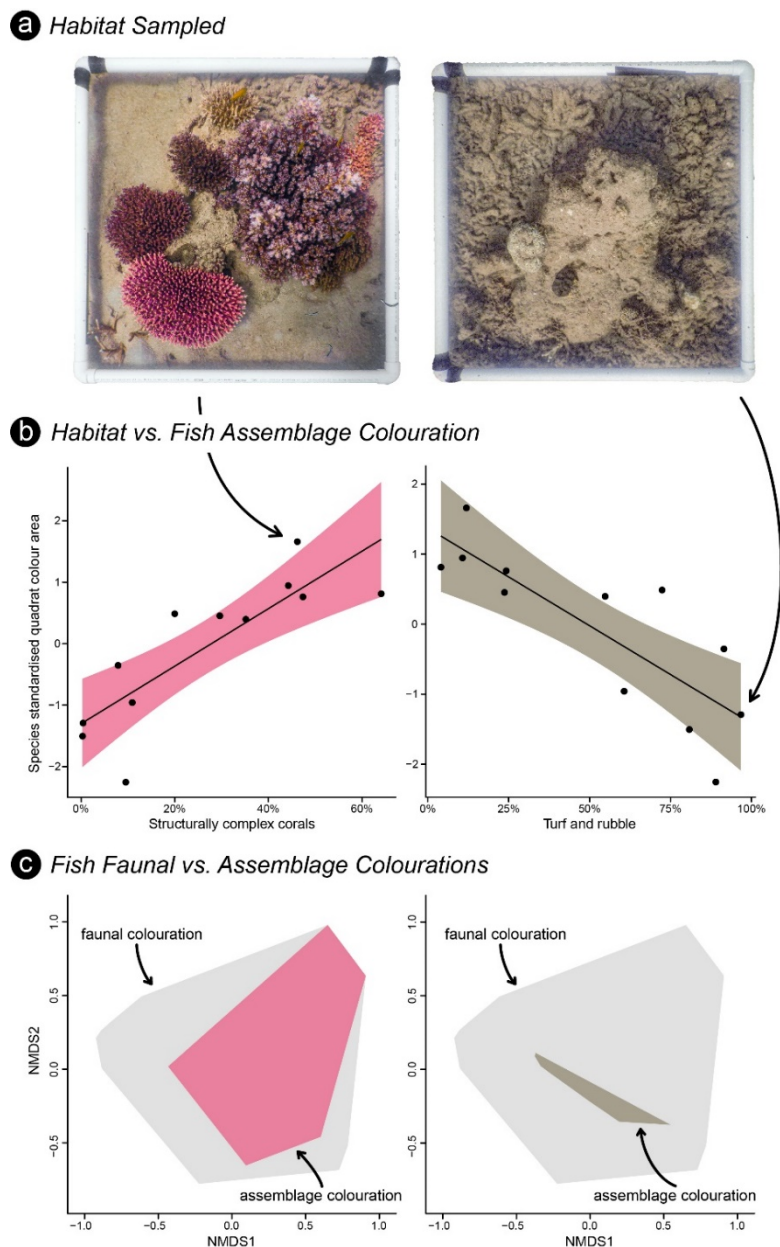


Figure 5.2 The relationship between substratum type and the colour-area of the assemblage colouration, i.e. all species within a single quadrat. A quadrat with high structurally complex coral cover (**a**. left) and a quadrat completely covered in rubble and reef matrix (**a**. right). The linear regressions \pm 95% confidence intervals display the relationship between colour-area and the cover of structurally complex corals (**b**. left) and turf and rubble (**b**. right) per quadrat. The specific quadrat in **a**. has been highlighted with the arrow in each regression. The assemblage colouration from a given quadrat (**c**. pink and pale green) is compared to the faunal colouration i.e. all individuals collected (grey).

colour-area following the 1998 mass coral bleaching event. This bleaching event was responsible for a >30% decline in colour-area. The following five years (2000 – 2004) showed a gradual recovery back

to pre-bleaching levels. Interestingly, if these five, post bleaching and recovery years are removed from the analysis, the best fitting gam model actually becomes a non-significant linear model (**Figure D11, Table D6**). This further suggests that there is a consistent, baseline assemblage colouration inherent to cryptobenthic fish assemblages at Orpheus Island, and that this baseline was severely impacted by the '98 bleaching event.

Although assemblage colouration areas appear to have recovered to pre-'98 bleaching levels, the extreme parts of this area are being supported by increasingly fewer individuals, especially in the area occupied by yellow and green fishes. *Pomacentrus moluccensis*, *Gobiodon histrio*, and *Paragobiodon xanthosoma* are the only predominantly yellow and/or green fishes and consequently, they are the only species that constitute the top right-hand 'yellow' section of the colour-area (representing approximately 29% of the faunal colour-area; **Figure D12**). The abundance of these three focal species has decreased significantly over the last 27 years. A negative binomial regression had a significant and negative relationship ($R^2 = 0.39$, $p\text{-value} < 0.01$, **Table D7**) between the year surveyed (explanatory variable) and the annual abundance (response variable; **Figure 5.3b**). Prior to the 1998 bleaching, the average abundance of these three species was 18.1 ± 3 individuals per 7m^2 . Post bleaching, there was over a 70% decline to just 4.8 ± 1 individuals per 7m^2 .

5.4 Discussion

There is a clear relationship between the substratum type and the colouration of the associated cryptobenthic fish assemblage. As the cover of structurally complex corals increases, so does the diversity of colours present on fishes that reside in and around them. Conversely, as the cover of turf and rubble increases, the diversity and spread of colours contracts to a more generalised, uniform appearance. Furthermore, long term data suggests that assemblage colourations respond negatively to major environmental disturbance. Although the total colour-area has recovered in recent times, this colour-area is becoming increasingly fragile; with outlying areas supported by fewer and fewer individuals every year. This is particularly marked for the more attractive yellow species. These findings provide direct evidence that the state of the reef benthos is critically important for supporting the

diversity of colours seen on the fishes that live on reefs, and that Anthropocene reefs are becoming less colourful and ‘attractive’ in terms of fish colours.

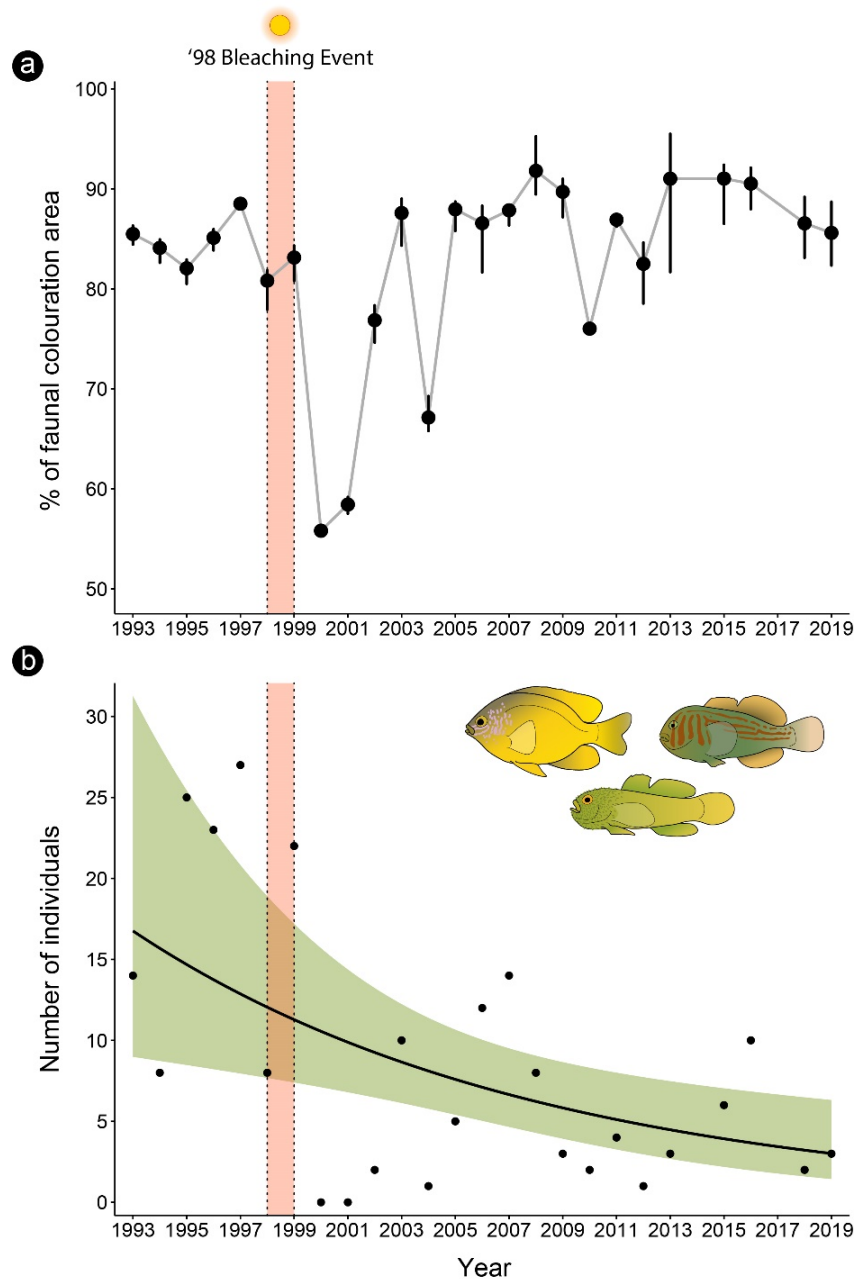


Figure 5.3 Changes in cryptobenthic fish assemblage colourations over 27 years. **a)** the annual colour-area through time. The dashed line represents the 1998 global coral bleaching event which is followed by a major decline in the colour-area of fishes for multiple years until recovery in 2005. **b)** the decrease in abundance of yellow and green coloured fishes. The negative binomial regression model of the abundance (rounded to nearest whole number per $7m^2$) tracks the decline in these three, colourful species through time.

A new paradigm: 'assemblage colouration'

The use of assemblage colouration – the colour composition of an entire local assemblage – enable us to analyse the full, multivariate nature of colouration and offers much promise for future studies. Using concepts developed by community ecologists (Villéger et al. 2008; Mouillot et al. 2013b) the notion of assemblage colouration moves beyond individual colouration to consider the measurement and description of a full group of organisms, in concert. Furthermore, differences can be observed between species as well as between individuals within a species. Our analysis revealed clear differences between the colouration of both individuals and species with a high level of accuracy (demonstrated by the low stress values; Rabinowitz, 1975). The vectors from the NMDS also show the specific colours most responsible for driving the distribution of colourations within an assemblage allowing for further inferences to be made about important colours. The colourations of fishes we collected followed three primary axes: darks, pales, and yellows. Interestingly, these three colour axes are the same principal colour axes in other reef fish groups (Hemingson et al. 2019).

'Assemblage colouration' through space and time

In recent times, coral reefs have changed profoundly. Human-induced stressors, especially global warming due to climate change, have caused widespread reconfiguration of coral reefs (Graham et al. 2015) with the loss of many temperature-sensitive coral taxa such as branching *Acropora* spp. and soft corals (Hughes et al. 2017). These species are often the first to bleach and die when exposed to increased temperatures. Future reefs are likely to have increased cover of algal turfs and rubble and a higher relative cover of temperature-resistant coral species such as massive *Porites* (Bellwood et al., 2019). Our evidence strongly suggests that turf & rubble dominated reefs are likely to support smaller colour-areas, but critically, that encrusting and massive coral types, like massive *Porites*, do not mitigate against this effect since they displayed no significant relationship with colour-area or spread. Unfortunately, this means that the corals that are most capable of surviving the immediate impacts climate change are unlikely to maintain the diversity of colours currently supported by coral reefs. Fish assemblages on future reefs are likely to be a duller version of their previous configurations.

In this context, the long-term data from Orpheus Island enables us to directly test the impact of the first recorded mass bleaching event on fish colours – a bleaching event that had a major influence on fish assemblages at this location (Bellwood et al. 2006). We found that the assemblage colouration of reef fishes responded quickly to large scale environmental disturbance. The assemblage colouration showed a clear decline in response to the severe bleaching event that occurred in 1998. During this event, there was widespread coral mortality responsible for marked decreases in the amount of live coral cover present on impacted reefs (Bellwood et al. 2012). This event also triggered significant changes to many of the fish communities present on impacted reefs (Booth and Beretta 2002; Bellwood et al. 2006). However, our data show a recovery of the assemblage colouration in the following five years, returning to the ambient, pre-bleaching levels. This may be a product of the gradual recovery of coral abundance following the bleaching event (Bellwood et al. 2012).

While this initially offers hope that the colouration, and the underlying attractive appearance of reefs is resilient to coral loss, a more detailed look into the make-up of the fish assemblage highlights the need for caution. The 1998 bleaching event was responsible for profound changes in the cryptobenthic and site-attached fish assemblages at Orpheus Island (Bellwood et al. 2006, 2012). Although most species are still present in samples, the abundance of various species have changed markedly. This is particularly evident in the abundance of the only yellow and green fishes collected in our quadrats: *P. moluccensis*, *G. histrio*, and *P. xanthosoma*. These three fish species are responsible for occupying a large and unique portion of the yellow-green colour-area; an area that is of direct aesthetic interest to humans (Bellwood, Hemingson, & Tebbett, 2020; Tribot et al., 2019). While these species are still present, they have declined in abundance by two-thirds over the last 30 years. Unfortunately, the total assemblage colouration does not reflect this decline until it is too late (colour-area is maintained until the last outlying individual is lost). Ongoing declines (exacerbated by further disturbance events) are likely to lead to a complete loss of these brightly coloured species and consequently, to large losses in the assemblage colouration. Thus, the assemblage colouration post-bleaching is becoming increasingly vulnerable to future disturbance and change.

Implications for future reefs; a social-ecological perspective

Many of the aesthetic values humans place on coral reefs are associated with the diversity of forms, shapes, and colours (Marshall et al., 2019; Tribot et al., 2016). It has recently been shown that research on coral reef fishes is biased (likely unknowingly) towards brightly coloured, yellow fishes which are studied more frequently than expected, even after accounting for local abundance and species richness (Bellwood et al. 2020). Furthermore, brightly coloured, yellow reef fishes are given greater aesthetic value when compared to duller and darker-coloured species (Tribot et al., 2018). Many brightly coloured reef fishes are often highly coral-associated, like the three species described herein. The continual decline in coral cover on reefs (Bellwood et al. 2004; Bruno and Selig 2007) is likely to negatively impact many of these species. Outside of their more fundamental values like the provision of consumable protein, humans place great value on the aesthetic properties and recreation that coral reefs provide (Costanza et al., 1997; Marshall et al., 2018). Reefs have already experienced precipitous declines in value which is unrivalled by any other ecosystem (Costanza et al. 2014). Loss of these colourful species may underpin a broad range of human responses, including grief (Curnock et al. 2019).

So, are degraded coral reefs less colourful? At a small spatial scale, the absence of structurally complex corals results in a smaller colour-area, so yes. Over a 27-year period, there was a marked decrease in the assemblage colouration following the '98 bleaching event, so initially - yes. And despite the recovery of assemblage colouration long-term, the abundance of yellow and green coloured fish which are 'attractive' has fallen by two-thirds – so again yes. In all three cases, reefs do appear to be becoming less colourful and thus, likely less attractive to humans.

Conclusions

We demonstrate that the colouration of reef fishes has an intrinsic link to the environment in which they live. High coral cover facilitates a broad diversity of colourations. As structurally complex coral cover is lost and replaced by turf algae and rubble, the colouration of fish assemblages become increasingly restricted. Crucially, this loss of colour occurs both spatially and temporally, in response to severe coral bleaching events. Our findings suggest that reefs may be at a critical transition point and

might be poised to become much less colourful in the coming years. The loss of these colourful fishes may not have a huge impact if we are assessing reefs through a functional or ecological lens (Tribot et al. 2018; Bellwood et al. 2019b), but in a human context, these aesthetic changes represent the loss of an important and culturally significant, ecosystem service (Marshall et al. 2018a; Pert et al. 2020).

Chapter 6: A practical guide to analysing colours and patterns in biology: integrating theory, principles, and practice

6.1 Introduction

Understanding the role of colour has remained a central focus in evolutionary and ecological studies. An organism's colouration (the combination of both colours and patterns) often has an intrinsic link to its life history strategy; dictating how it behaves and interacts within its environment. Colouration can facilitate species boundaries (Puebla et al. 2007; Hemingson et al. 2019), aid in mate selection (Hill 1990), or provide crypsis from predators (Endler 1980). Therefore, colouration is critical to the success of both the individual and the species. Researchers and naturalists alike have been fascinated with the intricacies of animal colouration since the times of Darwin and Wallace (Darwin 1859; Wallace 1877; Caro 2017). However, the physical properties that create colouration can make it a difficult subject to study (Endler 1978). How light behaves and interacts within an environment is extremely context dependent. Furthermore, how this light is then perceived by a viewer makes this seemingly simple field rather complex (Endler 1990).

Darwin and Wallace would be impressed with the progress that has been made in objectively quantifying organismal colouration (Endler 1978, 1990). Historically, descriptions of colouration were both context and viewer dependent, which, as noted by Longley (1917), "...is crude; allowance for the personal equation of the observer must be large". The advent of spectrometers allowed for more physical descriptions of light, and consequently colour, to be made. These instruments operate by detecting the intensity of electromagnetic radiation at various wavelengths, giving a measure of reflectance via a wavelength distribution (Endler 1990; Johnsen 2016). While this is by far the most accurate method for characterising the colour of an object, it does possess setbacks. Reflectance spectra must be remeasured for each specific colour of interest (Marshall et al. 2003), making it both labour and equipment intensive. Additionally, and more importantly, they fail to provide any objective description of patterns, leaving this to the interpretation of the viewer.

Patterns are quite simply the arrangement of colours in a spatial context. Due to their abstract nature and unlimited possibility of combinations, their objective description has historically remained even more difficult than the evaluation of colours. Yet patterns remain critically important when considering the visual appearance of an organism and its functional implications (Phillips et al. 2017). Patterns provide camouflage (Umeton et al. 2019), aid in selection for mating purposes (Kodric-Brown 1985; Eakley and Houde 2004), and facilitate warning colouration (Maan and Cummings 2012; Caro and Ruxton 2019). Quite simply, patterns give colour context. Therefore, it is often critical to consider both colour and patterns when assessing an organism's visual appearance (termed colouration herein, i.e. the combination of colour and patterns).

However, it is becoming increasingly apparent that most organism's visual systems are substantially different from our own (Osorio and Vorobyev 2005, 2008). An organism's vision can differ in either the colours they perceive (Kelber et al. 2003) or how detailed they visually resolve their environment (Caves et al. 2018). Since colouration provides a medium by which signals are sent, research investigating these signals often needs to account for how this signal is received (Endler 1992; Caves et al. 2016). Through dedicated research, we are beginning to have a more nuanced understanding of the specific visual capabilities of many organisms (Losey et al. 1999, 2003; Osorio and Vorobyev 2008). Incorporating this aspect into research is allowing us to better understand the complex trade-offs in the roles of colours and colour patterns.

The study of biological colour is currently benefitting from the combination of eloquent and informed research design and brute-force computing. Through the advent of open-source programming languages, like R, many new, freely available computational resources have arisen in recent years. These new resources are incredibly powerful and allow researchers to ask and answer questions that previously were not possible. However, each technique or application possesses its own strengths and weaknesses, answers specific questions, and requires time to learn and master.

Herein, I present an overview of the recent tools that have become available and the steps necessary to effectively quantify and interpret full organismal colouration (colours + patterns). The goal of this review is to provide a starting point for researchers entering the field of biological colouration.

First, it details some key considerations that need to be addressed when photographing organisms. It then provides an overview of what resources are available to measure and characterise colours and colour patterns from digital images. Finally, it demonstrates how these various techniques can be brought together and describes their potential applicability and future directions for holistic colour pattern studies. The tools and resources covered will primarily focus on image analysis techniques, as these are the methods that have seen the most recent growth. My overall aim is to provide a resource for beginners and experts alike to help design, develop, and conduct studies on biological colouration using new techniques in a rapidly growing field.

Colours or patterns: which to study and why?

An organism's colouration is comprised of two components: individual colours and pattern. Colours are the specific wavelengths of light reflected or emitted while patterns are how these colours are arranged spatially on a surface or object; i.e. their spatial geometry (Endler 1978). Without pattern, colours often lack context, and consequently would likely not serve their intended function for many organisms (i.e. camouflage; Phillips et al., 2017; Umeton, Tarawneh, Fezza, Read, & Rowe, 2019). The nature of the research question being asked strongly determines if patterns need to be considered when analysing colouration (**Figure 6.1**). As a rule of thumb, questions involving physical, chemical, or biological properties of colour often do not require the inclusion of pattern. For example, analysing how well a certain shade of black absorbs light to assess thermoregulation does not need pattern data.

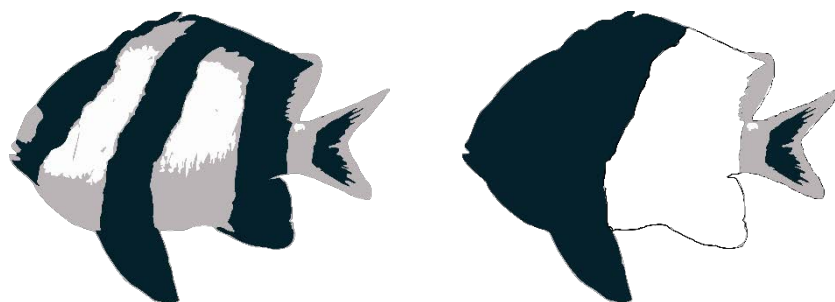


Figure 6.1 The importance of considering patterns. These two fish species (left – *Dascyllus aruanus* and right – a hypothetical species) possess identical colours. If only colour was measured, no distinctions would be made between these two individuals. When pattern is considered, there are clear differences that can (and do) affect their ecologies.

However, behavioural and ecological questions often need to include pattern as they typically involve how organisms are perceived by others or how well they match their environment (e.g. Tyrie, Hanlon, Siemann, & Uyarra, 2015). For example, how easily a prey species can be detected by a predator would need to include both colour and pattern since the predator would be viewing the prey in its entirety against a background (Green et al. 2019).

6.2 Methodological Approaches

Digital images are the primary means of obtaining full organismal colours and patterns for analysis. Digital images allow for large quantities of information to be collected in intuitive formats that are easily visualised. However, their ease of collection can lead to simple yet significant problems unless care is taken from the outset. Many so called ‘point-and-shoot’ cameras (entry level cameras) automatically alter photographs; either by adjusting the colour, contrast, or white balance in a permanent and irreversible manner. Often these cameras increase the ‘saturation’ of the photo which boosts the colours to make the image appear more vibrant (**Figure 6.2**). While this processing may make photographs look more appealing to the human viewer (more colourful and brighter), they do not accurately represent the true colouration of the organism or scene. Furthermore, these in-camera transformations make it almost impossible to recreate the native light environment in which the photograph was captured (Stevens et al. 2007; Akkaynak et al. 2014).

Quite obviously, these transformations are detrimental when the goal is to quantitatively compare colour patterns between subjects or images in a standardised manner. It is therefore paramount that the camera being used is capable of shooting in a ‘raw’ format. *Raw* is a colloquial term that refers to uncompressed image file formats. This format is the closest a camera can get to capturing a ‘true’ representation of a scene or object. The widely used *.jpeg* file type is a compressed format, meaning some of the image data is deliberately discarded to reduce file size. Although these changes are not often noticeable to the naked eye, it makes this file type unfavourable for image science (Akkaynak et al. 2014). For a comprehensive guide to using digital cameras to study biological colouration, see Stevens et al. (2007) and White et al. (2015).

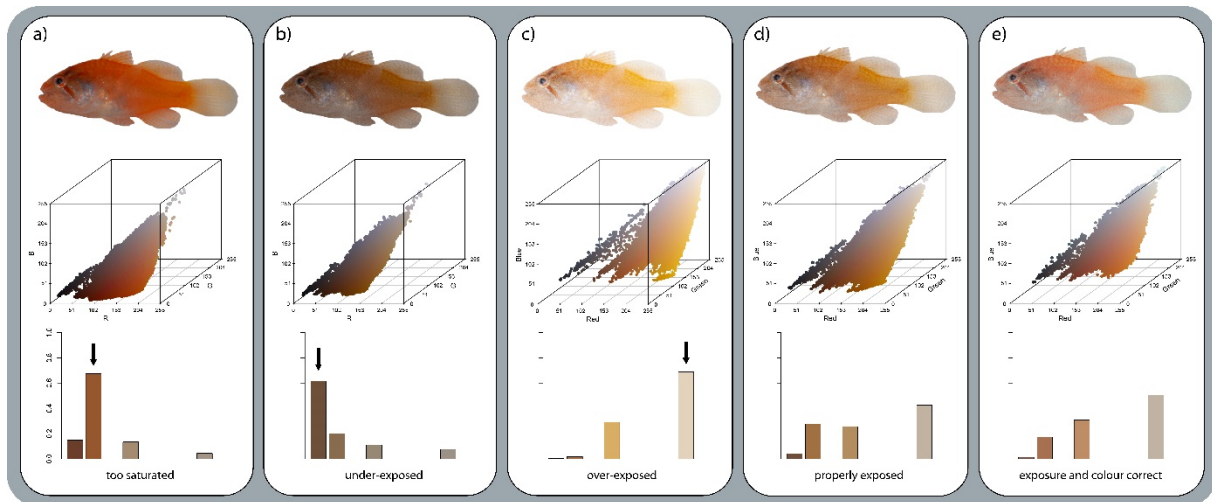


Figure 6.2 How various photographic properties can alter an organism's appearance. The top row is the same image of *Neamia octospina* (with the background removed) that has been altered in various ways. The middle row shows the RGB values of 100,000 randomly sampled point from each fish. The bottom rows show the number of pixels that fall into 8 major colour categories determined by splitting the RGB colour space into 8 cubes of equal area. **a)** an image in the common .jpg file format displaying extreme colour manipulation performed in-house by the camera. In this example, the subject is extremely red; much more than is typical in life. **b)** the raw image of *N. octospina*, however the image is severely underexposed making the subject appear much darker. **c)** the same subject but overexposed. **d)** properly exposed, and **e)** a properly exposed and colour corrected image; the desired product for all images. The histogram has slightly changed from **d)**, reflecting minor differences in the colour of the fish due to correction protocol.

Standards are used to ensure colour consistency between images. Grey and colour standards are small slates that contain patches of different colours that intentionally vary in their brightness and hue. Grey standards only contain a neutral grey colour of known reflectance whereas colour standards contain multiple colour patches designed to cover the full visible light spectrum (**Figure 6.3**). The standard is included in the image alongside the subject being photographed. Afterwards, the standard is used to adjust/correct the colours within an image to accurately resemble the colours of the subject in life. To work effectively, standards need to be the same distance from the camera as the subject and receive the same amount of light. Including a colour standard in every image is the most reliable way to ensure colour consistency between images. The most popular commercially available colour standards are the X-Rite ColorChecker Passport and ColorGauge Analyzer which work well in biological applications

(Bergman and Beehner 2008; Westley et al. 2013). These standards come with software to aid in the colour correction process, however libraries within R (*patternize*; Van Belleghem et al., 2018) offer freely-available functions to correct images using either of these standards.

Platforms for analyses

Currently, there are multiple software platforms that conduct biological colour pattern analyses. The most supported platforms are R (R Core Team 2020) and ImageJ (Schneider et al. 2012) which are both freely-available and open-source. Each platform has unique packages/addons that have been designed to meet specific needs. Depending on your research question, it may be necessary to use multiple platforms for their unique applications. Generally speaking, the add-ons and tools available in ImageJ are strictly for processing or measuring images prior to any statistical analyses. For example, converting an image of a flower to mimic how it would be seen by a Bumble bee both in terms of spectral sensitivities and acuity (Van Den Berg et al. 2019). ImageJ has the advantage of providing a graphical user interface (GUI) which makes it relatively easy to navigate. Most of the resources in R involve assessing and comparing images, after processing (Caves and Johnsen 2018; Van Belleghem et al. 2018). R's strength is that further statistical analyses on the colour data (like a generalised linear model) are relatively easy. Matlab and Python have the same functional capabilities of R and ImageJ (if not more) but lack many of the user-friendly packages and addons. Using these platforms will require a much greater proficiency and knowledge of programming as most functions will need to be written manually. A current list of available methods, their description, and platforms on which they are available is listed in **Table 6.1**.

An overview of the resources available

Following is a brief summary of the current resources available for colour pattern processing and analysis. The resources have been categorised largely based on whether they: **A**) are used for image processing prior to measurements and analysis, **B**) aim to compare only the colours within and between images, or **C**) analyse both colour and pattern within and between images. It is important to note that within each of the three categories (**A**, **B**, and **C**), there are techniques that either do or do not analyse

Table 6.1 The current resources available for assessing biological colouration. For more details, see Mason and Bowie (2020) or the original publication.

Technique/Approach name	Description	Resource Provided	Platform/Language	Reference
Overall Pattern Contrast	Overall comparison of colour pattern differences	-	-	Endler and Mielke 2005
Adjacency Analysis	Assess transitions between different colours along a 'transect' across the image being studied	-	MatLab or R (not explicitly stated)	Endler 2012
Boundary Strength Analysis	Combines geometry of pattern edges with receptor-noise estimates of boundary intensity	-	Matlab or ImageJ	Endler et al. 2018, van de Berg, 2019
NaturePatternMatch	Program to compare patterns between images.	Stand-alone program	c++	Caswell-Stoddard et al. 2014
PAVO & PAVO 2.0	Analyzes spectral data and performs k-means clustering on image colouration. Has capacity for plotting in different colourspaces, visual modelling, measuring colour distances and performing adjacency and boundary strength analyses.	R package - 'pavo'	R	Maia et al. 2019
Quantitative Colour Pattern Analysis (QCPA)	Provides a wide suite of functions available for the processing and interpretations of images explicitly from the viewers perception. Includes visual modelling, Local edge intensity analysis, colour adjacency and boundary strength, and visual contrasts	MICA toolbox plugin	ImageJ	van de Berg et al. 2019
Patternize	Objectively analyses both colour and pattern to quantify colour pattern variation between individuals	R package - 'patternize'	R	Van Belleghem et al. 2018
ColorDistance	Objectively analyses colour variation between individuals. Supports multiple different dissimilarity measures as well as colour spaces	R package - 'colordistance'	R	Weller and Westneat 2019
PAT-GEOM	Measures specific aspects of pattern, including shape, directionality, and distribution, amongst others	PAT-GEOM plugin	ImageJ	Chan et al. 2019
AcuityView	Renders images based on the visual acuity of a given observer.	R package - 'acuityview'	R	Caves and Johnsen 2018
Sea-thru	Algorithms to reconstruct near-accurate colouration of images taken underwater. Importantly, it does not require the use of a colour standard.	Script	Python	Akkaynak et al. 2019
Colourvision	Modelling of various photoreceptor sensitivities and plotting in colourspace	R package - 'colourvision'	R	Gawryszewski 2018
Color Inspector 3D	Program that displays image colours in colourspaces as specified by the user	Program and ImageJ plugin	ImageJ and Java	Barthel 2007

colouration explicitly from a visual perspective. This means some techniques deliberately model how a certain colour or pattern would be perceived by a viewer (dependent entirely on their visual capabilities). For example, modelling how well a human can see the text in a book at 1 metre away will yield different results when compared to a Wedge-tailed Eagle (*Aquila audax*), given that the visual acuity (how well it resolves detail) of an Eagle is greater than ours. Your research question will dictate whether you need to use descriptive colour analyses or visual-based colour analyses.

A) Image processing prior to measurement and analysis

The first step for most colour-based research questions will involve processing and manipulating images in various ways to prepare them for analyses (**Figure 6.3**). If colour or grey standards have been included in the images, then the image's colours can be adjusted to ensure the lighting is standardised between all photos. This is particularly important if images are taken outdoors or underwater where cloud cover, time of day, and depth can greatly impact the available light spectrum (Stevens et al. 2007; Bergman and Beehner 2008; Akkaynak 2019). Images containing the XRite ColorChecker Passport or the Image Science Associates ColorGauge can be adjusted within the R package *patternize* using the function 'colorChecker' (Van Belleghem et al. 2018). Alternatively, if the approach is based more in visual-modelling (i.e. what organisms see and perceive), images can be reflectance normalised if a grey standard was included using the Multispectral Image Calibration and Analysis (MICA) toolbox (Troscianko and Stevens 2015).

Once images are colour-accurate, further changes can be made to mimic how certain organisms may perceive the scene or subject photographed within each image (Troscianko and Stevens 2015). These are made by adjusting either: **a)** the colours present, and/or **b)** the level of detail based on the visual acuity of the viewer. Every organism possesses their own unique suite of photoreceptor cells which gives them the ability to perceive certain colours (Kelber et al. 2003; Osorio and Vorobyev 2008). If your research question involves specifically what colours an organism can perceive, colours within an image may need adjusting (**Figure 6.3a**). These image transformations can only currently be made

using the MICA toolbox (Troscianko and Stevens 2015; Van Den Berg et al. 2019) and require knowledge of the spectral sensitivities of the taxon whose vision is being modelled.

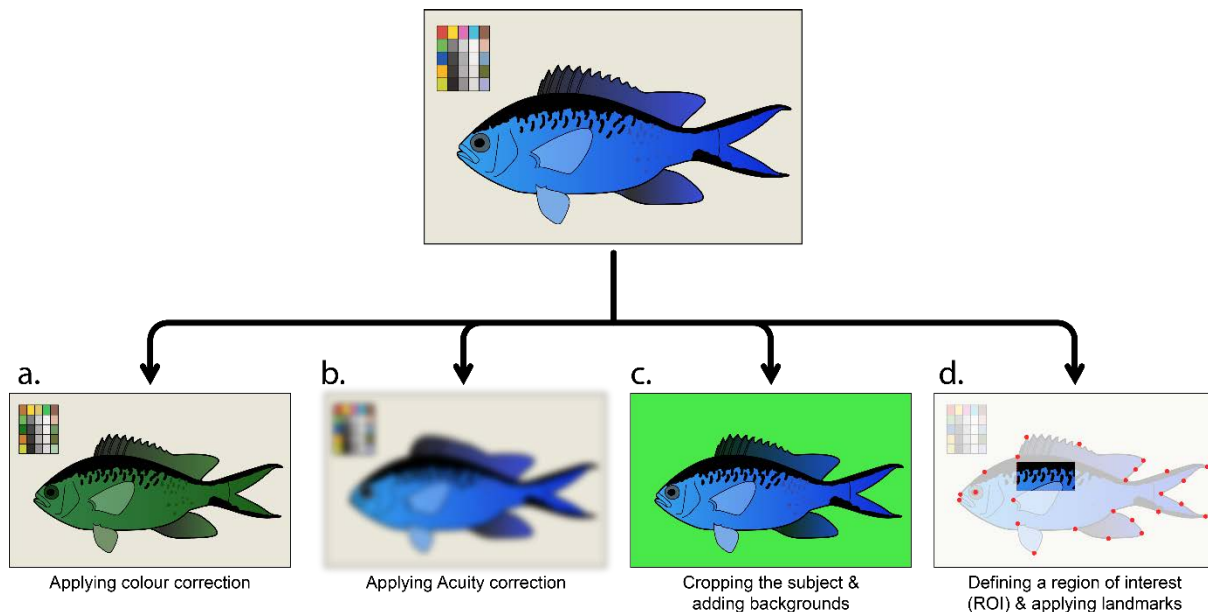


Figure 6.3 Some examples of the alterations that can be made to images prior to analysis. **a)** changing the colours within an image to reflect a viewer’s spectral sensitivity. **b)** adjusting an image to reflect a given viewer’s visual acuity. **c)** cropping a subject and placing it onto a solid-coloured background. **d)** defining a region of interest (ROI) for analysis in the MICA toolbox or placing landmarks. These techniques are not mutually exclusive and can be combined depending on the research question.

Visual acuity is defined as how well an organism can resolve details from a scene. Most organisms have visual acuities much worse than our own (Caves et al. 2018). Therefore, if perception is an important component of the research question, then visual acuity may need to be incorporated into the analysis. Perhaps your research question involves how well a predatory coral reef fish (e.g. *Cephalopholis miniata*) can detect a prey fish species (e.g. *Eviota guttatus*). Adjustments can be made to the images of the prey fish species to more accurately reflect how well the predator fish can perceive the prey (**Figure 6.4**).

There are multiple applications available that provide these acuity adjustments. *AcuityView* is an R package that can provide acuity modelling (Caves and Johnsen 2018). The user needs to specify the **a)** viewer’s visual acuity (the unit is typically cycles per degree) and, **b)** the distance between the subject

in the image and the viewer. *AcuityView* uses a fast Fourier transformation to remove details that a viewer would not likely resolve. While this is effective, it is not meant to mimic what an organism is actually seeing, but more accurately represent the level of detail it may perceive. The MICA toolbox provides further application of acuity modelling by more accurately mimicking what an organism would actually perceive (Troschianko and Stevens 2015). The MICA toolbox also uses a Fast-Fourier transformation to remove details from an image. However, the MICA toolbox can further apply a Receptor Noise Limited model to recreate sharp edges between elements in the photo (Van Den Berg et al. 2019). Thus, the final image has reduced detail while maintaining sharp borders between elements within the image.

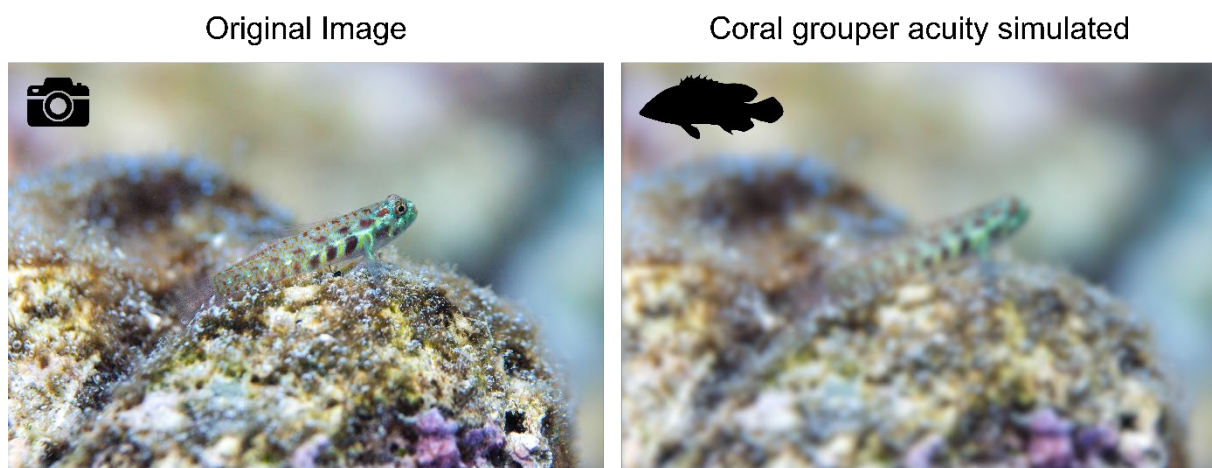


Figure 6.4 Modelling the visual acuity of a predatory coral reef fish using *AcuityView*. On the left is the original image as captured by the camera. On the right is the simulated image according to the visual acuity of a common predatory coral reef fish (*Cephalopholis miniata*). It becomes evident that the small prey fish (*Eviota guttatus*) is harder to detect than is shown in the original image. The distance between the predator and prey fish is assumed to be 1m. Note, the colours have not been altered based on the Coral grouper's spectral sensitivities.

Finally, images may need to have the subject cropped out or outlined to facilitate further analyses. Cropping the subject is most easily done in Adobe Photoshop using the selection tool. Some analyses need the subject to be placed onto a solid-coloured background which is then subsequently ignored from the calculations. If this is required for your research question, it is imperative to use a colour that is not found on any of the subjects being analysed as it will be discarded. Using a highly saturated colour (i.e. bright, neon green) is the most effective as these colours rarely occur in nature (**Figure 6.3c**).

Alternatively, your research question may only be concerned with a specific aspect of an image. For these cases, you may need to designate a region of interest (ROI) which essentially is a boundary or outline (**Figure 6.3d**). Inside this boundary, the colours and patterns are analysed; outside, they are ignored. Last, your analysis may require the placement of landmarks to align images during analysis (Van Belleghem et al. 2018). Landmarks can easily be placed in ImageJ using the ‘point’ tool (**Figure 6.3d**). After placing the landmark points of interest on a given image, the x and y coordinates of all points can be exported and saved as a spreadsheet.

B) Comparing only colours within and between images

The largest methodological decision is whether pattern (i.e. the spatial arrangement of colours) needs to be explicitly considered (**Figure 6.5**). Most of the ‘traditional’ image analysis techniques generally do not account for pattern. These techniques often require the user to specify what colours within an image are to be measured; for example, measuring the colour of throat patches within a group of birds. While useful, these ‘patch-measuring’ approaches do not consider the amount of a given colour on an organism, so discretion is advised when interpreting the behavioural or ecological significance of the results (e.g. Dalrymple et al. 2015b).

The most simplistic method to characterise colours on a computer is by recording their colourspace triplet value. This triplet value is the combination of three numbers that correspond to that specific colours x, y , and z coordinates within a given colourspace. The most common computer-based colourspace used is RGB (red, blue, green, **Figure 6.6a**) whose three axes (x, y, z) are meant to loosely imitate the three peak spectral sensitivities of humans (blue – short wavelengths, green – medium wavelengths, and red – long wavelengths). While useful to work within, distances in this colourspace are not representative of perceptual distances, that is, how different we as humans would perceive two or more colours (see **Figure E1** for details). To overcome this limitation, the CIELab colourspace was intentionally designed so that Euclidean distances between colours reflect their perceptual difference in life. CIELab’s colourspace uses lightness (L), differences along a red – green axis (a) and differences along a blue – yellow axis (b). Weller & Westneat (2019) provide a more detailed description of different

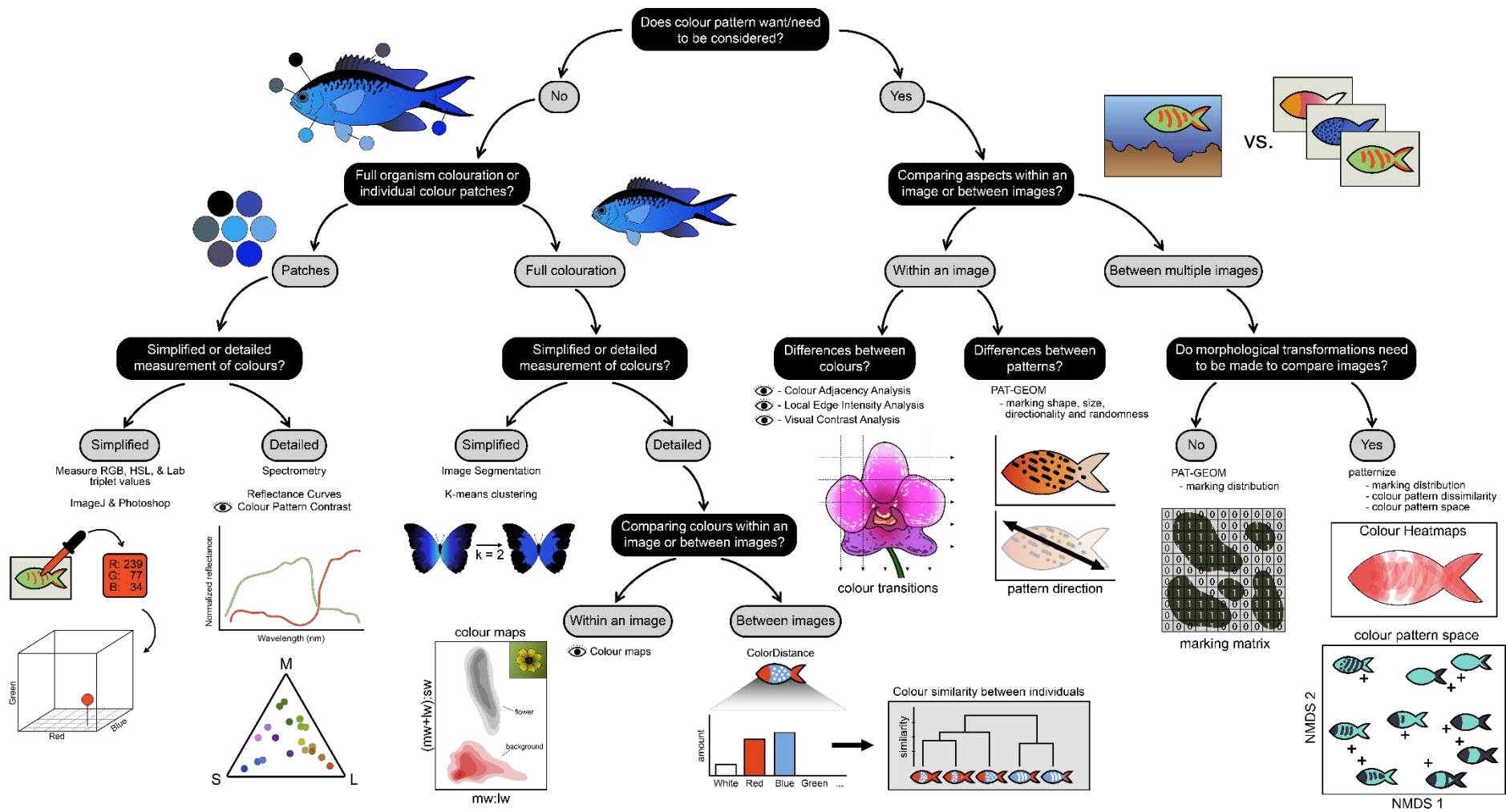


Figure 6.5 What technique should you use to answer your research question?

colourspaces, and the 3D Color Inspector program (Barthel 2017) is a useful tool to understand the nuances between various colourspace. The *in situ* measurement of colours uses spectrometry on the actual organism. This has historically been the most common approach to describe colours because it measures the amount of reflected light at specific wavelengths (**Figure 6.6b**). This method is extremely accurate, but it is labour and equipment intensive. For a more comprehensive overview of how to measure colours using spectrophotometry, see (Endler 1990; Johnsen 2016).

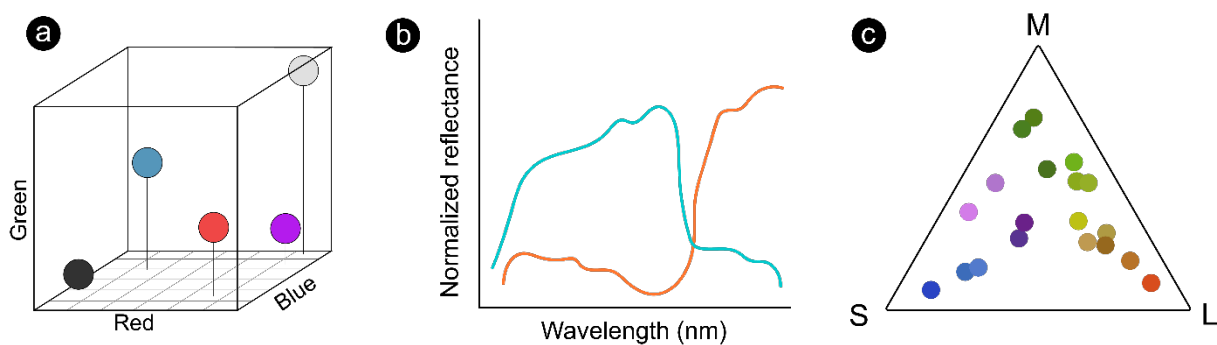


Figure 6.6 Three different ways to represent colours. a) colours represented in the RGB colourspace. This colourspace is most often used to display colour in computer graphics. b) colours represented as a wavelength distribution which displays the relative amount of light at each wavelength. c) colours represented by how strongly they stimulate various photoreceptors. In this example, the viewer has three photoreceptor types that are sensitive to short (S), medium (M), and long (L) wavelengths (identical to human visual systems).

More recent image analysis techniques can assess all colours within an image (although they still disregard the position of each colour within the image). Differences between colours within an image can be visualised using a chromaticity diagram which plot colours in a log transformed opponent colour space (Hempel De Ibarra et al. 2001; Kelber et al. 2003, similar to that shown in **Figure 6.6c**). Quite simply, a colours specific location in this plot reflects how strongly it stimulates different photoreceptors present in a viewer. Every pixel of colour assessed in the image corresponds to a point in the colourspace. If the point clouds created by different colours are distinct, you can conclude that those colours are perceptually different. This approach is particularly useful for comparing similarities and differences between and organism's colouration and its environment. For example, the Killdeer (*Charadrius*

vociferus) is a species of ground-nesting bird found in the Americas which constructs very rudimentary nests (if at all, **Figure 6.7**). Therefore, the eggs rely heavily on camouflage to avoid predation. A chromaticity diagram could be used to assess any perceptive differences between egg colour and substrate colour using known Coyote (*Canis latrans*) spectral sensitivities, a common predator of Killdeer eggs. Indeed, how closely the egg colouration of ground-nesting birds matches the colouration of their nesting habitat is indicative of hatching success (Troscianko et al. 2016).



Figure 6.7 The nest of a Killdeer (*Charadrius vociferus*). This bird lays eggs directly on the ground without constructing a nest. Therefore, the eggs rely heavily on camouflage to protect them from potential predators.

Alternatively, you may want to compare all the colours within an image to all the colours within another image (or multiple other images). *colordistance* is a relatively recent package in R that has utility to measure the similarity between the colours of n images (Weller and Westneat 2019). Although *colordistance* does not incorporate the specific location of where each colour occurs, it does measure a proxy for pattern – the relative abundance of each colour in each image. *colordistance* measures colouration by plotting the pixels of an image within a colourspace specified by the user (RGB, HSL, CIELab). The colourspace is then divided into equal area subsections whose size are determined by the user. The number of pixels that fall within each subsection (which can be thought of as colour categories – e.g. ‘blues’) is recorded and compared between all images using multivariate approaches. This

generates a measure of dissimilarity between the colours found in each image. The intuitive nature of this approach allows for the full colouration of any number of organisms to be compared regardless of morphological differences. Furthermore, the user can specify the: **a)** colourspace used, **b)** how fine the resolution of colours are (i.e. the number of ‘subsections’), and **c)** the method to compare the distribution of colours (e.g. earth movers distance, chi squared distance, etc.).

A further benefit of using multivariate techniques to compare colouration is that differences can be visualised with ordinations. Ordinations are a data plotting technique that aims to reduce dimensionality and display complex, multivariate data in a simplified format (Rabinowitz 1975). Simply put, they seek to display a dataset with many variables into one that can typically be plotted on only 2-3 axes. Thus, an organisms entire colouration (colour + pattern) can be condensed into two values (x and y coordinates in a Cartesian plane; e.g. Alfaro et al. 2019; Hemingson et al. 2019). Various metrics of multivariate space occupation can then be measured (following Mouillot et al. 2013), **Figure 6.8**. This allows for widespread utility in many different applications.

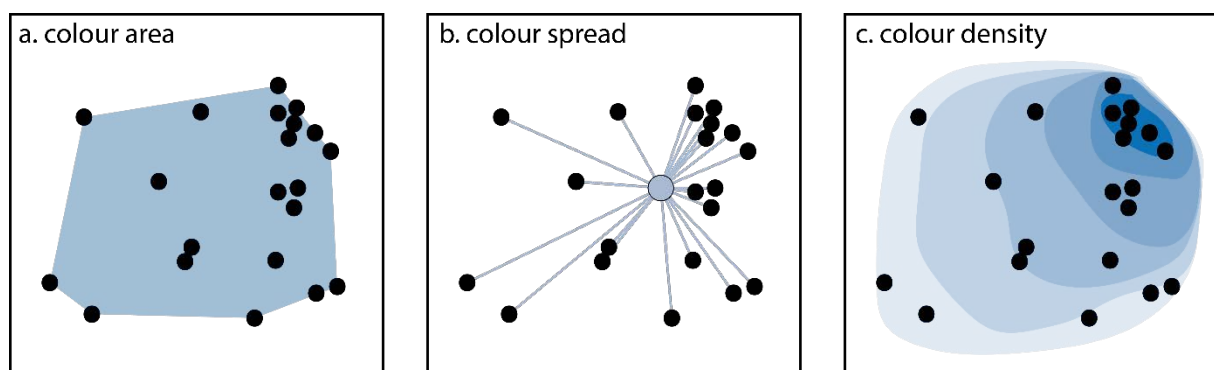


Figure 6.8 Different metrics for characterising the colourations of a group of organisms. *a) colour area: the area of the convex hull. This approach is sensitive to outliers, i.e. very unique coloured organisms. b) colour spread: the average difference between colourations. c) colour density. The metric identifies the most common colourations found within an assemblage.*

C) Comparing the colour patterns within and between images

The most comprehensive techniques analyse the full colourations of an organism or scene. These techniques explicitly incorporate the location of colours (their pattern) into the analyses. However, they are not restricted to only analysing colour patterns at the scale of the individual (e.g. the colouration on

a frog), but can also assess colour differences between elements within an image. For example, some of these techniques could be used to assess how strongly the subject of a photograph (a red flower) stands out against its background (a green, grassy field). In this example, the techniques are not assessing pattern per se, but rather the difference between colours with respect to their location within the image.

When the focus of the research question is assessing aspects of colouration within a single image, the Quantitative Colour Pattern Analysis framework (QCPA; Van Den Berg et al. 2019) using the MICA Toolbox provides numerous resources. Boundary Strength Analysis (Endler et al. 2018) and Local Edge Intensity Analysis (LEIA; Van Den Berg et al. 2019) are useful techniques to explore chromatic contrasts (colour differences) between elements within an image. These approaches work by modelling both the chromatic and luminance differences (ΔS) between various colours. Quite simply, these techniques aim to assess the strength of colour changes from a visual perspective. The strength of these changes will therefore depend on the model visual system. For example, following the previous scenario, let us assume your research question involves how strongly a flower stands out against a grassy background to a Bumble bee (the viewer). You could use either Boundary Strength Analysis or LEIA to determine how significant the perceptual transition is from the flower to the background. Both techniques can be performed using the MICA Toolbox in ImageJ.

If the research question is more concerned with characterising the complexity of a colour pattern at the scale of the individual (i.e. the colour pattern of an Orchid flower – see Van Den Berg et al. 2019), Colour Adjacency Analysis provides a simplified metric. This analysis runs multiple transects across the subject or region of interest in both the x and y dimensions. The colour is recorded at evenly spaced points along the transect. These transects are then summarised and used to create a transition matrix that contains how often one colour changes to another across the entire subject (Van Den Berg et al. 2019). This technique is particularly useful when a single, simple metric is needed to characterise the complexity of an organism's colouration. This Colour Adjacency metric can then be easily used in further statistical analyses. However, if the pattern between two images is the same but the colours are different, the Colour Adjacency metric for both images will be identical. Thus, careful consideration is needed when using and interpreting the output of this technique.

If the focus is on aspects of pattern geometry at the individual scale, the R package *PAT-GEOM* provides the most suited resources for measurement (Chan et al. 2019). These range from assessing the individual markings shape (how round or jagged the patches are), marking size, directionality (how the patches are oriented with respect to the organism's body), randomness, and distribution (where do the patches occur). These methods only work on colour patterns that have distinct differences; that is, the markings clearly stand out against the background colour of the organism. For instance, if you wanted to investigate the direction a certain spotted pattern follows along the body of a lizard, you could use *PAT-GEOM* to determine the pattern's directionality. This technique essentially performs a regression using the colour patches as points to determine a line of best fit along the body of the organism.

Your research question may involve analysing the similarity or difference of colouration among multiple individuals or species. *patternize* is an R package that provides tools to analyse an organism's complete colouration; inclusive of both colours and patterns (Van Belleghem et al. 2018). This resource compares the variation in colours and patterns between every possible pair of images analysed – yielding a unique dissimilarity value for each pair. Importantly, *patternize* can use landmarks identified by the user to align the images which ensures that the colourations can be compared. The algorithms within *patternize* warp and resize each image in certain ways to match up the landmarks. Thus, if the final processed images were stacked on top of each other, a perfectly vertical line could be drawn through all images which would intersect the same landmark in every photo (see **Figure E2** for details). This key functionality allows for the comparison of colour patterns between individuals or species that have different shapes/morphologies or between images in which the orientation of the subject differs. The output of this analysis can be visualised using an ordination, which as discussed previously, allows for further interpretation and unique metrics to be measured.

For example, let's assume our research question is investigating colour pattern variation between two butterfly populations (**Figure 6.9**). One population lives in pristine, old growth forest which has experiences minimal human interference. The second population is found in a highly urbanised area significantly impacted by humans. We are curious if habitat disturbance has selected for butterflies with different colourations. We collect 10 individuals from each habitat (undisturbed vs. disturbed) and

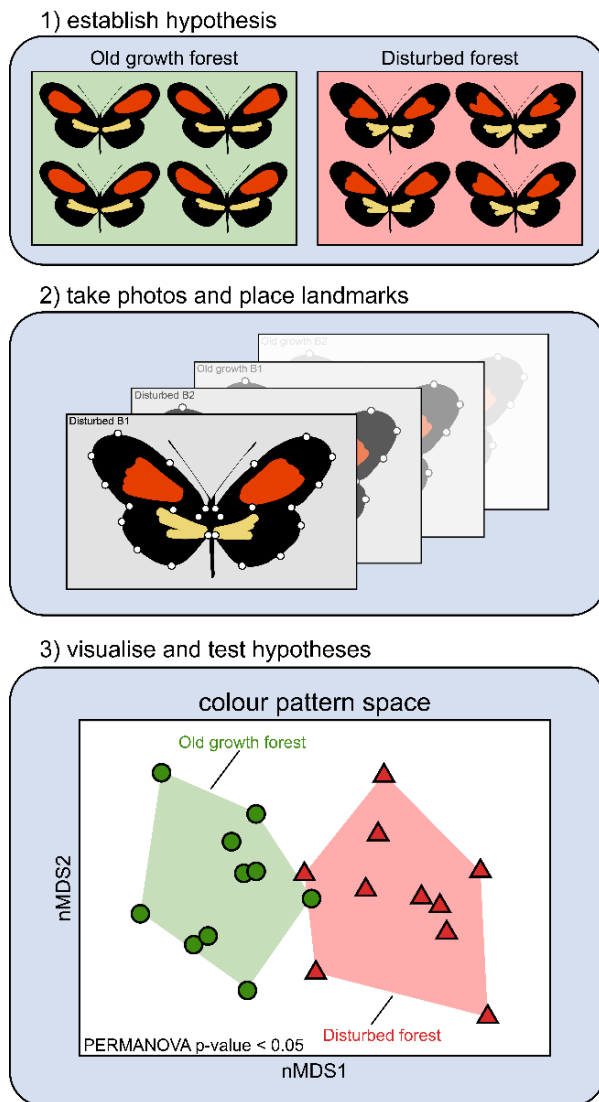


Figure 6.9 An example of how to use *patternize* to test ecological hypotheses. 1) establish a hypothesis to test. In this hypothetical example, anecdotal evidence suggests that populations of butterflies living in more disturbed forests may have different colourations. 2) collect individuals from each location, take photos, and place landmarks. Perform *patternize* analyses to 3) visualise the data and test hypotheses. Colour patterns for all butterflies photographed were visualised using an ordination. Differences between the two groups (old growth forest vs. disturbed) were tested using a PERMANOVA. A significant difference was found ($p\text{-value} < 0.05$) indicating that there are differences in colouration between the two groups.

photograph them individually. Since this species naturally varies in the size and shape of its wing, we manually identify a handful of landmarks across the wing that accurately capture its shape. We then record the x and y coordinates of each landmark on the butterfly in each image. Next, the images (along with their list of coordinates for the landmarks per image) are analysed in *patternize* to assess colour pattern variation. The output of the analysis is a dissimilarity matrix which contains the dissimilarity value for every possible pairwise comparison of images. We visualise the similarity and differences of each butterfly's colouration by using an ordination (specifically a nMDS). Finally, we test for statistical differences in the colouration of the sampled butterflies to determine if forest degradation is possibly causing changes in the colouration of this species. Given the significant finding, we conclude that habitat degradation may be playing a role in causing changes to this species colouration.

6.3 Conclusions and Moving Forward

The multitude of recent advances has made the field of organismal colouration studies exciting. By combining old and new techniques from different fields, we are now capable of asking detailed questions about the appearance of organisms and how they are perceived. This resource provides a solid starting point to help researchers navigate the methodologically dense field of biological colouration. We must be explicit, however, and reiterate that this is a guide; essentially a 'cookbook'. Every good chef makes modifications to the recipe to suit their own taste. Your research questions will almost certainly require modifications to some of these workflows. Furthermore, it is also important to ensure credit is given to the original creators of these various resources. These applications take an immense amount of time to develop and create. Thus, anytime a resource is used, the proper attribution should be given to ensure the creators receive credit for their work.

Future research merging many of these resources will yield new ways of thinking about colouration. Just in the last five years, there have been numerous developments and modifications made to these techniques to answer interesting new questions. By combining new ways to assess colouration and adding in the visual capabilities of a viewer, we are gaining an extremely comprehensive understanding of how colouration functions in the natural world.

Chapter 7: General Discussion

Colouration in coral reef fishes

The processes that shape the evolution of colours and patterns on coral reefs are numerous and complex. Over twenty years ago, when considering colouration on coral reefs, Justin Marshall stated that “it is almost inconceivable for only one evolutionary force to be behind the colours of such a diverse assemblage...” (Marshall 2000a). Since this time, the field has progressed rapidly. However, only in the last decade have new methods allowed us to explore the complexity of this fascinating system. Indeed, using many recently developed analyses, this thesis was able to show some of this complexity, revealing the evolutionary and ecological processes that have influenced the colouration of reef fishes at multiple spatial and temporal scales. At the individual level, there was evidence that a fish’s morphology strongly relates to its colouration, evident in eyespots closely mimicking the size of the real eye, but the pupil being exaggerated. Within clades, speciation processes like reproductive character displacement, shaped the difference in colouration between closely related species. From an ecosystem perspective, certain environmental features clearly shaped the diversity of colours found on fishes, demonstrating real-world implications of current environmental change. And across the entire reef fish tree of life, broad evolutionary processes have had their own consistent impacts dictating the colouration of fishes across large taxonomic groups. So quite simply, yes, numerous evolutionary forces are responsible for the diversity of colours and patterns seen on coral reef fishes.

Future directions and new avenues of research

We are currently experiencing a renaissance in the study of organism colouration. This surge of research interest is largely fuelled by the wide array of newly available image analysis resources, especially image banks and analytical programs, making the future of colour science extremely exciting. Integrating aspects of the full colours and patterns of an organism, the context/environment in which the organism lives, and the visual perception of the viewer allows for an increasingly holistic study of animal colouration. Research is just at the beginning of merging these three aspects. The advancement of new

techniques holds much promise, as each provide their own specific manner in which they assess colours and/or patterns.

In this regard, the study of animal colour patterns is evolving rapidly. Many of these new techniques and approaches are in their infancy and will surely experience significant modifying, tweaking, and perfecting in the coming years. While some of the traditional approaches to analysing colourations will always have their utility (Johnsen 2016; Miyazawa 2020), many of these new methods lend themselves to integrate seamlessly into other fields of study, like ecology and phylogenetics. Crucially, this combination of multiple fields is allowing researchers to ask, and subsequently answer, questions that have not previously been possible.

A prime example of this emergent property of merging fields is characterising the ‘colourfulness’ of a community or assemblage. In recent years, there has been a shift in the field of community ecology to assess an assemblage by the composition of its traits or functions (Tilman et al. 1997; Hemingson and Bellwood 2018; Bellwood et al. 2019b) as opposed to the taxonomic identity of its species (MacArthur and MacArthur 1961; Öhman and Rajasuriya 1998; Anderson and Willis 2003). This shift came with its own construction of new metrics that are used to measure and quantify various aspects of multidimensional trait/function space (Mouillot et al. 2013b). Each metric is selected to provide a distinct insight into the composition, and potentially the functions operating within various assemblages (Legendre et al. 2005). The detailed description of traits and potential functions in trait space is perfectly suited for describing multivariate colour spaces.

These developments offer the potential for new and exciting comparisons to be made in the colouration of organisms between habitats, ecosystems or populations. This community led approach is likely to be particularly important for extremely colourful ecosystems like coral reefs. Previously, trying to simply describe the diversity of different colours and patterns found on coral reefs was nearly impossible. However, within a multivariate framework, the colouration of multiple groups of organisms (be it between habitats, geographic locations, etc.) can be easily compared. In **Chapter 5**, we defined the collective colouration of an entire assemblage of organisms as the ‘assemblage colouration’. We quantified aspects of the assemblage colouration using two of the most fundamental multivariate indices:

convex hulls and multivariate dispersion. These indices were some of the first developed to measure aspects of multivariate space and have a long standing history of use in the literature (DeVantier et al. 1998; Anderson et al. 2006). However, many other measures of multivariate space exist (Mouillot et al. 2013a), with some specifically designed to measure colouration (Gruson 2020).

Current resources also offer an enhanced capability to more accurately model what certain organisms perceive. Applications are available that can both alter the specific colours within an image to recreate what colours a given organism can detect (e.g. Van Den Berg et al. 2019), as well as the level of detail they can perceive those colours and patterns (their visual acuity, e.g. Caves and Johnsen 2018). This allows research questions that directly involve how organisms recognise their world. Thus, there is current capability to: **1)** alter an image based on an organism's spatial and spectral abilities, **2)** analyse the full colouration (both colour and pattern) of the organisms in each image, and **3)** assess the colouration of multiple organisms from an assemblage perspective. Although this thesis did not ask questions related to perception, they can be easily integrated into a similar workflow given these new advances.

Future research will benefit immensely from publicly available images that contain both image metadata and colour standards. Given enough widespread support and participation, researchers will have the ability to assess colour-accurate images for any species without the need to travel, collect, and photograph individuals personally. The current, publicly available image databases (e.g. FishBase, Reef Life Survey, Smithsonian Institute's Division of Fishes Collections, etc.) have been invaluable for science, benefitting researchers around the world, including the research conducted herein. Special thanks must be given to the contributors of these key resources. Maintaining these databases and adding support for image metadata and colour standards will further increase the already immense value these resources currently provided to science.

Concluding remarks

We are only just beginning to understand the functions various colours and patterns serve on coral reefs and how they came to be. Given the incredible methodological advances in recent years, we have

uncovered numerous, complex processes that shape colouration in this highly diverse ecosystem. This thesis contributes to this growing body of work and to our understanding of the factors that may shape colouration in coral reef fishes. However, there is still much to be learned. Given their unique nature, coral reefs offer an unparalleled opportunity to explore the evolutionary origins and ecological maintenance of colouration in one of the most diverse ecosystems found on Earth.

References

- Akaike, H. 1987. Factor analysis and AIC. *Psychometrika* 52:317–332.
- Akkaynak, D. 2019. Sea-thru : A Method For Removing Water From Underwater Images. *Comput. Vis. Found.* 1682–1691.
- Akkaynak, D., T. Treibitz, B. Xiao, U. A. Gürkan, J. J. Allen, U. Demirci, and R. T. Hanlon. 2014. Use of commercial off-the-shelf digital cameras for scientific data acquisition and scene-specific color calibration. *J. Opt. Soc. Am. A* 31:312.
- Alfaro, M. E., E. A. Karan, S. T. Schwartz, and A. J. Shultz. 2019. The Evolution of Color Pattern in Butterflyfishes (Chaetodontidae). *Integr. Comp. Biol.* 59:604–615.
- Alieva, N. O., K. A. Konzen, S. F. Field, E. A. Meleshkevitch, M. E. Hunt, V. Beltran-Ramirez, D. J. Miller, J. Wiedenmann, A. Salih, and M. V Matz. 2008. Diversity and Evolution of Coral Fluorescent Proteins. *PLoS One* 3:e2680.
- Anderson, M. J., K. E. Ellingsen, and B. H. McArdle. 2006. Multivariate dispersion as a measure of beta diversity. *Ecol. Lett.* 9:683–693.
- Anderson, M. J., and T. J. Willis. 2003. Canonical Analysis of Principal Coordinates: A Useful Method of Constrained Ordination for Ecology. *Ecology* 84:511–525.
- Barluenga, M., K. N. Stölting, W. Salzburger, M. Muschick, and A. Meyer. 2006. Sympatric speciation in Nicaraguan crater lake cichlid fish. *Nature* 439:719–723.
- Barracough, T. G., and A. P. Vogler. 2000. Detecting the geographical pattern of speciation from species-level phylogenies. *Am. Nat.* 155:419–434.
- Barthel, K. U. 2017. Color Inspector 3D.
- Bastiaans, E., M. J. Bastiaans, G. Morinaga, J. G. Castañeda Gaytán, J. C. Marshall, B. Bane, F. Méndez De La Cruz, and B. Sinervo. 2014. Female preference for sympatric vs. allopatric male

- throat color morphs in the mesquite lizard (*Sceloporus grammicus*) species complex. *PLoS One* 9:44–48.
- Belant, J. L., P. P. Woronecki, R. A. Dolbeer, and T. W. Seamans. 1998. Ineffectiveness of five commercial deterrents for nesting starlings. *Wildl. Soc. Bull.* 26:264–268.
- Bellwood, D. R., A. H. Baird, M. Depczynski, A. González-Cabello, A. S. Hoey, C. D. Lefèvre, and J. K. Tanner. 2012. Coral recovery may not herald the return of fishes on damaged coral reefs. *Oecologia* 170:567–573.
- Bellwood, D. R., and J. H. Choat. 1990. A functional analysis of grazing in parrotfishes (family Scaridae): the ecological implications. *Environ. Biol. Fishes* 28:189–214.
- Bellwood, D. R., C. H. R. Goatley, and O. Bellwood. 2017. The evolution of fishes and corals on reefs: form, function and interdependence. *Biol. Rev.* 92:878–901.
- Bellwood, D. R., C. R. Hemingson, and S. B. Tebbett. 2020. Subconscious Biases in Coral Reef Fish Studies. *Bioscience* 70:621–627.
- Bellwood, D. R., A. S. Hoey, J. L. Ackerman, and M. Depczynski. 2006. Coral bleaching, reef fish community phase shifts and the resilience of coral reefs. *Glob. Chang. Biol.* 12:1587–1594.
- Bellwood, D. R., T. P. Hughes, C. Folke, and M. Nyström. 2004. Confronting the coral reef crisis. *Nature* 429:827–833.
- Bellwood, D. R., M. S. Pratchett, T. H. Morrison, G. G. Gurney, T. P. Hughes, J. G. Álvarez-Romero, J. C. Day, R. Grantham, A. Grech, A. S. Hoey, G. P. Jones, J. M. Pandolfi, S. B. Tebbett, E. Techera, R. Weeks, and G. S. Cumming. 2019a. Coral reef conservation in the Anthropocene: Confronting spatial mismatches and prioritizing functions.
- Bellwood, D. R., and L. Sorbini. 1996. A review of the fossil record of the Pomacentridae (Teleostei: Labroidei) with a description of a new genus and species from the Eocene of Monte Bolca, Italy.

- Zool. J. Linn. Soc. 117:159–174.
- Bellwood, D. R., R. P. Streit, S. J. Brandl, and S. B. Tebbett. 2019b. The meaning of the term ‘function’ in ecology: A coral reef perspective. *Funct. Ecol.* 33:948–961.
- Bellwood, D. R., and P. C. Wainwright. 2002. The history and biogeography of fishes on coral reefs. Pp. 5–32 *in* *Coral Reef Fishes. Dynamics and diversity in a complex ecosystem.*
- Bergman, T. J., and J. C. Beehner. 2008. A simple method for measuring colour in wild animals: validation and use on chest patch colour in geladas (*Theropithecus gelada*). *Biol. J. Linn. Soc.* 94:231–240.
- Berumen, M. L., M. S. Pratchett, and B. A. Goodman. 2011. Relative gut lengths of coral reef butterflyfishes (Pisces: Chaetodontidae). *Coral Reefs* 30:1005–1010.
- Betancur-R, R., E. O. Wiley, G. Arratia, A. Acero, N. Bailly, M. Miya, G. Lecointre, and G. Ortí. 2017. Phylogenetic classification of bony fishes. *BMC Evol. Biol.* 17:1–40. *BMC Evolutionary Biology.*
- Blest, A. D. 1957. The Function of Eyespot Patterns in the Lepidoptera. *Behaviour* 11:209–256.
- Bollback, J. P. 2006. SIMMAP: Stochastic character mapping of discrete traits on phylogenies. *BMC Bioinformatics* 7:1–7.
- Booth, D. J., and G. A. Beretta. 2002. Changes in a fish assemblage after a coral bleaching event. *Mar. Ecol. Prog. Ser.* 245:205–212.
- Bothwell, E., R. Montgomerie, S. C. Loughheed, and P. R. Martin. 2015. Closely related species of birds differ more in body size when their ranges overlap-in warm, but not cool, climates. *Evolution* (N. Y). 69:1701–1712.
- Bowen, B. W., L. A. Rocha, R. J. Toonen, and S. A. Karl. 2013. The origins of tropical marine biodiversity. *Trends Ecol. Evol.* 28:359–366. Elsevier Ltd.

- Boyle, K. S., and T. C. Tricas. 2014. Discrimination of mates and intruders: visual and olfactory cues for a monogamous territorial coral reef butterflyfish. *Anim. Behav.* 92:33–43. Elsevier Ltd.
- Brandl, S. J., C. H. R. Goatley, D. R. Bellwood, and L. Tornabene. 2018. The hidden half: ecology and evolution of cryptobenthic fishes on coral reefs. *Biol. Rev.* 93:1846–1873.
- Brandl, S. J., L. Tornabene, C. H. R. Goatley, J. M. Casey, R. A. Morais, I. M. Côté, C. C. Baldwin, V. Parravicini, N. M. D. Schiettekatte, and D. R. Bellwood. 2019. Demographic dynamics of the smallest marine vertebrates fuel coral reef ecosystem functioning. *Science* (80-.). 364:1189–1192.
- Brewin, R. J. W., S. J. Lavender, and N. J. Hardman-Mountford. 2010. Mapping size-specific phytoplankton primary production on a global scale. *J. Maps* 6:448–462.
- Bruno, J. F., and E. R. Selig. 2007. Regional decline of coral cover in the Indo-Pacific: Timing, extent, and subregional comparisons. *PLoS One* 2:e711.
- Camacho, C., A. Sanabria-fernández, and A. Baños-villalba. 2020. Experimental evidence that matching habitat choice drives local adaptation in a wild population. *Proc. R. Soc. B* 287:1–8.
- Cantalice, K. M., J. Alvarado-Ortega, and D. R. Bellwood. 2020. †*Chaychanus gonzalezorum* gen. et sp. nov.: A damselfish fossil (Percomorphaceae; Pomacentridae), from the Early Paleocene outcrop of Chiapas, Southeastern Mexico. *J. South Am. Earth Sci.* 98:102322. Elsevier.
- Caro, T. 2005. The adaptive significance of coloration in mammals. *Bioscience* 55:125.
- Caro, T. 2017. Wallace on Coloration: Contemporary Perspective and Unresolved Insights. *Trends Ecol. Evol.* 32:23–30. Elsevier Ltd.
- Caro, T., and W. L. Allen. 2017. Interspecific visual signalling in animals and plants: a functional classification. *Philos. Trans. R. Soc. B Biol. Sci.* 372:20160344.
- Caro, T., and R. Mallarino. 2020. Coloration in Mammals. *Trends Ecol. Evol.* 35:357–366. Elsevier

Ltd.

Caro, T., and G. Ruxton. 2019. Aposematism: Unpacking the Defences. *Trends Ecol. Evol.* 34:595–604. Elsevier Ltd.

Caves, E. M., N. C. Brandley, and S. Johnsen. 2018. Visual Acuity and the Evolution of Signals. *Trends Ecol. Evol.* 33:358–372. Elsevier Ltd.

Caves, E. M., T. M. Frank, and S. Johnsen. 2016. Spectral sensitivity, spatial resolution and temporal resolution and their implications for conspecific signalling in cleaner shrimp. *J. Exp. Biol.* 219:597–608.

Caves, E. M., and S. Johnsen. 2018. AcuityView: An R package for portraying the effects of visual acuity on scenes observed by an animal. *Methods Ecol. Evol.* 9:793–797.

Caves, E. M., S. Nowicki, and S. Johnsen. 2019. Von Uexküll Revisited: Addressing Human Biases in the Study of Animal Perception. *Integr. Comp. Biol.* 1–12.

Chan, I. Z. W., M. Stevens, and P. A. Todd. 2019. pat-geom: A software package for the analysis of animal patterns. *Methods Ecol. Evol.* 10:591–600.

Cheney, K. L., A. S. Grutter, S. P. Blomberg, and N. J. Marshall. 2009. Blue and Yellow Signal Cleaning Behavior in Coral Reef Fishes. *Curr. Biol.* 19:1283–1287. Elsevier Ltd.

Choat, J. H., O. S. Klanten, L. Van Herwerden, D. R. Robertson, and K. D. Clements. 2012. Patterns and processes in the evolutionary history of parrotfishes (Family Labridae). *Biol. J. Linn. Soc.* 107:529–557.

Cooney, C. R., J. A. Tobias, J. T. Weir, C. A. Botero, and N. Seddon. 2017. Sexual selection, speciation and constraints on geographical range overlap in birds. *Ecol. Lett.* 20:863–871.

Cortesi, F., W. E. Feeney, M. C. O. Ferrari, P. A. Waldie, G. A. C. Phillips, E. C. McClure, H. N. Sköld, W. Salzburger, N. J. Marshall, and K. L. Cheney. 2015. Phenotypic plasticity confers

- multiple fitness benefits to a mimic. *Curr. Biol.* 25:949–954.
- Cortesi, F., Z. Musilová, S. M. Stieb, N. S. Hart, U. E. Siebeck, K. L. Cheney, W. Salzburger, and N. J. Marshall. 2016. From crypsis to mimicry: changes in colour and the configuration of the visual system during ontogenetic habitat transitions in a coral reef fish. *J. Exp. Biol.* 219:2545–2558.
- Costanza, R., R. D'Arge, R. de Groot, S. Farber, M. Grasso, B. Hannon, K. Limburg, S. Naeem, R. V. O'Neill, J. Paruelo, R. G. Raskin, P. Sutton, and M. van den Belt. 1997. The value of the world's ecosystem services and natural capital. *Nature* 387:253–260.
- Costanza, R., R. de Groot, P. Sutton, S. van der Ploeg, S. J. Anderson, I. Kubiszewski, S. Farber, and R. K. Turner. 2014. Changes in the global value of ecosystem services. *Glob. Environ. Chang.* 26:152–158. Elsevier Ltd.
- Cowman, P. F., and D. R. Bellwood. 2011. Coral reefs as drivers of cladogenesis: Expanding coral reefs, cryptic extinction events, and the development of biodiversity hotspots. *J. Evol. Biol.* 24:2543–2562.
- Cowman, P. F., V. Parravicini, M. Kulbicki, and S. R. Floeter. 2017. The biogeography of tropical reef fishes: endemism and provinciality through time. *Biol. Rev.* 92:2112–2130.
- Cribari-Neto, F., and A. Zeileis. 2010. Beta Regression in R. *J. Stat. Softw.* 34:1–24.
- Curnock, M. I., N. A. Marshall, L. Thiault, S. F. Heron, J. Hoey, G. Williams, B. Taylor, P. L. Pert, and J. Goldberg. 2019. Shifts in tourists' sentiments and climate risk perceptions following mass coral bleaching of the Great Barrier Reef. *Nat. Clim. Chang.* 9:535–541. Springer US.
- Cuthill, I. C., W. L. Allen, K. Arbuckle, B. Caspers, G. Chaplin, M. E. Hauber, G. E. Hill, N. G. Jablonski, C. D. Jiggins, A. Kelber, J. Mappes, N. J. Marshall, R. Merrill, D. Osorio, R. Prum, N. W. Roberts, A. Roulin, H. M. Rowland, T. N. Sherratt, J. Skelhorn, M. P. Speed, M. Stevens, M. C. Stoddard, D. Stuart-Fox, L. Talas, E. Tibbetts, and T. Caro. 2017. The biology of color. *Science* (80-.). 357:1–7.

- Dalrymple, R. L., F. K. C. Hui, H. Flores-Moreno, D. J. Kemp, and A. T. Moles. 2015a. Roses are red, violets are blue - so how much replication should you do? An assessment of variation in the colour of flowers and birds. *Biol. J. Linn. Soc.* 114:69–81.
- Dalrymple, R. L., D. J. Kemp, H. Flores-Moreno, S. W. Laffan, T. E. White, F. A. Hemmings, M. L. Tindall, and A. T. Moles. 2015b. Birds, butterflies and flowers in the tropics are not more colourful than those at higher latitudes. *Glob. Ecol. Biogeogr.* 24:1424–1432.
- Darwin, C. 1859. *On the origin of species by means of natural selection, or, the preservation of favoured races in the struggle for life.* London: J. Murray.
- De Bona, S., J. K. Valkonen, A. López-Sepulcre, and J. Mappes. 2015. Predator mimicry, not conspicuousness, explains the efficacy of butterfly eyespots. *Proc. R. Soc. B Biol. Sci.* 282.
- Deppe, C., D. Holt, J. Tewksbury, L. Broberg, J. Petersen, and K. Wood. 2003. Effect of Northern Pygmy-Owl (*Glaucidium gnoma*) eyespots on avian mobbing. *Auk* 120:765–771.
- DeVantier, L. M., G. De'ath, T. J. Done, and E. Turak. 1998. Ecological assessment of a complex natural system: A case study from the Great Barrier Reef. *Ecol. Appl.* 8:480–496.
- DiBattista, J. D., E. Waldrop, B. W. Bowen, J. K. Schultz, M. R. Gaither, R. L. Pyle, and L. A. Rocha. 2012. Twisted sister species of pygmy angelfishes: Discordance between taxonomy, coloration, and phylogenetics. *Coral Reefs* 31:839–851.
- Dominici-Arosemena, A., and M. Wolff. 2006. Reef fish community structure in the Tropical Eastern Pacific (Panamá): Living on a relatively stable rocky reef environment. *Helgol. Mar. Res.* 60:287–305.
- Doutrelant, C., M. Paquet, J. P. Renoult, A. Grégoire, P. A. Crochet, and R. Covas. 2016. Worldwide patterns of bird colouration on islands. *Ecol. Lett.* 19:537–545.
- Eakley, A. L., and A. E. Houde. 2004. Possible role of female discrimination against “redundant”

- males in the evolution of colour pattern polymorphism in guppies. *Proc. R. Soc. B Biol. Sci.* 271:299–301.
- Eaton, R. C., and D. S. Emberley. 1991. How stimulus direction determines the trajectory of the Mauthner-initiated escape response in a teleost fish. *J. Exp. Biol.* 161:469–487.
- Egger, B., Y. Klaefiger, A. Theis, and W. Salzburger. 2011. A sensory bias has triggered the evolution of egg-spots in cichlid fishes. *PLoS One* 6.
- Endler, J. A. 1978. A Predator's View of Animal Color Patterns. Pp. 319–364 *in* *Evolutionary Biology*.
- Endler, J. A. 1980. Natural Selection on Color Patterns in *Poecilia reticulata*. *Evolution* (N. Y.) 34:76–91.
- Endler, J. A. 1990. On the measurement and classification of color in studies of animal color patterns. *Biol. J. Linn. Soc.* 41:315–352.
- Endler, J. A. 1992. Signals, Signal Conditions, and the Direction of Evolution. *Evolution* (N. Y.) 139:S125-153.
- Endler, J. A., G. L. Cole, and A. M. Kranz. 2018. Boundary strength analysis: Combining colour pattern geometry and coloured patch visual properties for use in predicting behaviour and fitness. *Methods Ecol. Evol.* 9:2334–2348.
- Eschmeyer, W. N., R. Fricke, and R. van der Laans. 2018. *Catalog of fishes: genera, species, references*.
- Felsenstein, J. 2012. A comparative method for both discrete and continuous characters using the threshold model. *Am. Nat.* 179:145–156.
- Felsenstein, J. 1985. Phylogenies and the comparative method. *Am. Nat.* 125:1–15.

- Figuerola, J., and A. J. Green. 2000. The evolution of sexual dimorphism in relation to mating patterns, cavity nesting, insularity and sympatry in the Anseriformes. *Funct. Ecol.* 14:701–710.
- Floeter, S. R., M. G. Bender, A. C. Siqueira, and P. F. Cowman. 2017. Phylogenetic perspectives on reef fish functional traits. *Biol. Rev.* 93:131–151.
- Froese R., and Pauly D. 2019. FishBase.
- Fuller, R. C. 2002. Lighting environment predicts the relative abundance of male colour morphs in bluefin killifish (*Lucania goodei*) populations. *Proc. R. Soc. B Biol. Sci.* 269:1457–1465.
- Gagliano, M. 2008. On the spot: The absence of predators reveals eyespot plasticity in a marine fish. *Behav. Ecol.* 19:733–739.
- Gagliano, M., and M. Depczynski. 2013. Spot the Difference: Mimicry in a Coral Reef Fish. *PLoS One* 8:1–7.
- Gaither, M. R., M. A. Bernal, R. R. Coleman, B. W. Bowen, S. A. Jones, W. B. Simison, and L. A. Rocha. 2015. Genomic signatures of geographic isolation and natural selection in coral reef fishes. *Mol. Ecol.* 24:1543–1557.
- Gaither, M. R., J. K. Schultz, D. R. Bellwood, R. L. Pyle, J. D. DiBattista, L. A. Rocha, and B. W. Bowen. 2014. Evolution of pygmy angelfishes: Recent divergences, introgression, and the usefulness of color in taxonomy. *Mol. Phylogenet. Evol.* 74:38–47.
- Goatley, C. H. R., and D. R. Bellwood. 2016. Body size and mortality rates in coral reef fishes : a three-phase relationship. *Proc. R. Soc. B Biol. Sci.* 283:20161858.
- Goatley, C. H. R., and D. R. Bellwood. 2009. Morphological structure in a reef fish assemblage. *Coral Reefs* 28:449–457.
- Gower, J. C. 1971. A general coefficient of similarity and some of its properties. *Biometrics* 27:857–871.

- Graham, N. A. J., S. Jennings, M. A. MacNeil, D. Mouillot, and S. K. Wilson. 2015. Predicting climate-driven regime shifts versus rebound potential in coral reefs. *Nature* 518:94–97. Nature Publishing Group.
- Gray, S. M., and J. S. McKinnon. 2007. Linking color polymorphism maintenance and speciation. *Trends Ecol. Evol.* 22:71–79.
- Green, S. D., R. C. Duarte, E. Kellett, N. Alagaratnam, and M. Stevens. 2019. Colour change and behavioural choice facilitate chameleon prawn camouflage against different seaweed backgrounds. *Commun. Biol.* 1–10. Springer US.
- Grether, G. F., J. P. Drury, E. Berlin, and C. N. Anderson. 2015. The role of wing coloration in sex recognition and competitor recognition in Rubyspot Damselflies (*Hetaerina* spp.). *Ethology* 121:674–685.
- Gruson, H. 2020. Estimation of colour volumes as concave hypervolumes using α -shapes. *Methods Ecol. Evol.* 2020:1–9.
- Halali, D., A. Krishna, U. Kodandaramaiah, and F. Molleman. 2019. Lizards as Predators of Butterflies: Shape of Wing Damage and Effects of Eyespots. *J. Lepid. Soc.* 73:78–86.
- Hamilton III, W. J., and R. M. Peterman. 1971. Countershading in the colourful reef fish *Chaetodon lunula*: concealment, communication or both? *Anim. Behav.* 19:357–364.
- Hemingson, C. R., and D. R. Bellwood. 2018. Biogeographic patterns in major marine realms: function not taxonomy unites fish assemblages in reef, seagrass and mangrove systems. *Ecography (Cop.)*. 41:174–182.
- Hemingson, C. R., and D. R. Bellwood. 2020. Greater multihabitat use in Caribbean fishes when compared to their Great Barrier Reef counterparts. *Estuar. Coast. Shelf Sci.* 239:106748. Elsevier Ltd.

- Hemingson, C. R., P. F. Cowman, and D. R. Bellwood. 2020. Body size determines eyespot size and presence in coral reef fishes. *Ecol. Evol.* 10:8144–8152.
- Hemingson, C. R., P. F. Cowman, J. R. Hodge, and D. R. Bellwood. 2019. Colour pattern divergence in reef fish species is rapid and driven by both range overlap and symmetry. *Ecol. Lett.* 22:190–199.
- Hempel De Ibarra, N., M. Giurfa, and M. Vorobyev. 2001. Detection of coloured patterns by honeybees through chromatic and achromatic cues. *J. Comp. Physiol. - A Sensory, Neural, Behav. Physiol.* 187:215–224.
- Hench, K., M. Vargas, M. P. Höppner, W. O. McMillan, and O. Puebla. 2019. Inter-chromosomal coupling between vision and pigmentation genes during genomic divergence. *Nat. Ecol. Evol.* 3:657–667. Springer US.
- Hill, G. E. 1990. Female house finches prefer colourful males: sexual selection for a condition-dependent trait. *Anim. Behav.* 40:563–572.
- Hill, G. E., C. Y. Inouye, and R. Montgomerie. 2002. Dietary carotenoids predict plumage coloration in wild house finches. *Proc. R. Soc. B Biol. Sci.* 269:1119–1124.
- Ho, S., S. R. Schachat, W. H. Piel, and A. Monteiro. 2016. Attack risk for butterflies changes with eyespot number and size. *R. Soc. Open Sci.* 3.
- Höbel, G., and H. C. Gerhardt. 2003. Reproductive character displacement in the acoustic communication system of Green Tree Frogs. *Evolution (N. Y.)* 57:894–904.
- Hodge, J. R., C. Alim, N. G. Bertrand, W. Lee, S. A. Price, B. Tran, and P. C. Wainwright. 2018. Ecology shapes the evolutionary trade-off between predator avoidance and defence in coral reef butterflyfishes. *Ecol. Lett.* 21:1033–1042.
- Hodge, J. R., C. I. Read, L. van Herwerden, and D. R. Bellwood. 2012. The role of peripheral

- endemism in species diversification: Evidence from the coral reef fish genus *Anampses* (Family: Labridae). *Mol. Phylogenet. Evol.* 62:653–663. Elsevier Inc.
- Hossie, T. J., and T. N. Sherratt. 2013. Defensive posture and eyespots deter avian predators from attacking caterpillar models. *Anim. Behav.* 86:383–389. Elsevier Ltd.
- Hossie, T. J., and T. N. Sherratt. 2012. Eyespots interact with body colour to protect caterpillar-like prey from avian predators. *Anim. Behav.* 84:167–173. Elsevier Ltd.
- Hossie, T. J., J. Skelhorn, J. W. Breinholt, A. Y. Kawahara, and T. N. Sherratt. 2015. Body size affects the evolution of eyespots in caterpillars. *Proc. Natl. Acad. Sci.* 112:6664–6669.
- Howland, H. C., S. Merola, and J. R. Basarab. 2004. The allometry and scaling of the size of vertebrate eyes. *Vision Res.* 44:2043–2065.
- Hughes, T. P., J. T. Kerry, M. Álvarez-Noriega, J. G. Álvarez-Romero, K. D. Anderson, A. H. Baird, R. C. Babcock, M. Beger, D. R. Bellwood, R. Berkelmans, T. C. Bridge, I. R. Butler, M. Byrne, N. E. Cantin, S. Comeau, S. R. Connolly, G. S. Cumming, S. J. Dalton, G. Diaz-Pulido, C. M. Eakin, W. F. Figueira, J. P. Gilmour, H. B. Harrison, S. F. Heron, A. S. Hoey, J. P. A. Hobbs, M. O. Hoogenboom, E. V. Kennedy, C. Y. Kuo, J. M. Lough, R. J. Lowe, G. Liu, M. T. McCulloch, H. A. Malcolm, M. J. McWilliam, J. M. Pandolfi, R. J. Pears, M. S. Pratchett, V. Schoepf, T. Simpson, W. J. Skirving, B. Sommer, G. Torda, D. R. Wachenfeld, B. L. Willis, and S. K. Wilson. 2017. Global warming and recurrent mass bleaching of corals. *Nature* 543:373–377.
- Hulse, S. V., J. P. Renoult, and T. C. Mendelson. 2020. Sexual signalling pattern correlates with habitat pattern in visually ornamented fishes. *Nat. Commun.* 2561. Springer US.
- Hulsey, C. D., and P. C. Wainwright. 2002. Projecting mechanics into morphospace: Disparity in the feeding system of labrid fishes. *Proc. R. Soc. B Biol. Sci.* 269:317–326.
- Johnsen, S. 2016. How to measure color using spectrometers and calibrated photographs. *J. Exp. Biol.* 219:772–778.

- Karplus, I., and D. Algom. 1981. Visual Cues for Predator Face Recognition by Reef Fishes. *Z. Tierpsychol.* 55:343–364.
- Kelber, A., M. Vorobyev, and D. Osorio. 2003. Animal colour vision – behavioural tests and physiological concepts. *Biol. Rev.* 78:S1464793102005985.
- Kelley, J. L., J. L. Fitzpatrick, and S. Merilaita. 2013. Spots and stripes: ecology and colour pattern evolution in butterflyfishes. *Proc. R. Soc. B* 280:20122730.
- Kelley, J. L., B. Phillips, G. H. Cummins, and J. Shand. 2012. Changes in the visual environment affect colour signal brightness and shoaling behaviour in a freshwater fish. *Anim. Behav.* 83:783–791. Elsevier Ltd.
- Kelley, J. L., G. M. Rodgers, and L. J. Morrell. 2016. Conflict between background matching and social signalling in a colour-changing freshwater fish. *R. Soc. Open Sci.* 3.
- Kelley, J. L., N. J. Tataric, G. E. Schröder-Turk, J. A. Endler, and B. D. Wilts. 2019. A Dynamic Optical Signal in a Nocturnal Moth. *Curr. Biol.* 29:2919-2925.e2.
- Kelley, J. L., I. Taylor, N. S. Hart, and J. C. Partridge. 2017. Aquatic prey use countershading camouflage to match the visual background. *Behav. Ecol.* 28:1314–1322.
- Kjernsmo, K., M. Grönholm, and S. Merilaita. 2016. Adaptive constellations of protective marks: Eyespots, eye stripes and diversion of attacks by fish. *Anim. Behav.* 111:189–195.
- Kjernsmo, K., M. Grönholm, and S. Merilaita. 2018. Size and contrast increase the divertive effect of eyespots. *Behav. Ecol.* 1–7.
- Kjernsmo, K., and S. Merilaita. 2013. Eyespots divert attacks by fish. *Proc. R. Soc. B* 280:1–7.
- Kjernsmo, K., and S. Merilaita. 2017. Resemblance to the Enemy’s Eyes Underlies the Intimidating Effect of Eyespots. *Am. Nat.* 190:594–600.

- Kocher, T. D. 2004. Adaptive evolution and explosive speciation: the cichlid fish model. *Nat. Rev. Genet.* 5:288–298.
- Kodandaramaiah, U. 2011. The evolutionary significance of butterfly eyespots. *Behav. Ecol.* 22:1264–1271.
- Kodandaramaiah, U., P. Lindenfors, and B. S. Tullberg. 2013. Deflective and intimidating eyespots: A comparative study of eyespot size and position in *Junonia* butterflies. *Ecol. Evol.* 3:4518–4524.
- Kodric-Brown, A. 1985. Female Preference and Sexual Selection for Male Coloration in the Guppy (*Poecilia reticulata*). *Behav. Ecol. Sociobiol.* 17:199–205.
- Kondrashov, A. S., and F. A. Kondrashov. 1999. Interactions among quantitative traits in the course of sympatric speciation. *Nature* 400:351–354.
- Kondrashov, A. S., and M. V. Mina. 1986. Sympatric speciation: when is it possible? *Biol. J. Linn. Soc.* 27:201–223.
- Koslow, J. A. 1996. Energetic and life-history patterns of deep-sea benthic, benthopelagic and seamount-associated fish. *J. Fish Biol.* 49:54–74.
- Kulbicki, M., V. Parravicini, D. R. Bellwood, E. Arias-González, P. Chabanet, S. R. Floeter, A. Friedlander, J. McPherson, R. E. Myers, L. Vigliola, and D. Mouillot. 2013. Global biogeography of reef fishes: A hierarchical quantitative delineation of regions. *PLoS One* 8.
- Lambers, H., F. S. Chapin, and T. L. Pons. 2008. Photosynthesis. Pp. 11–99 *in* *Plant Physiological Ecology*. Springer New York, New York, NY.
- Lapshin, G., A. Salih, P. Kolosov, M. Golovkina, Y. Zavorotnyi, T. Ivashina, and L. Vinokurov. 2015. Fluorescence color diversity of great barrier reef corals. *J. Innov. Opt. Health Sci.* 8:1–11.
- Legendre, P., D. Borcard, and P. R. Peres-Neto. 2005. Analyzing beta diversity: partitioning the spatial variation of community composition data. *Ecol. Monogr.* 75:435–450.

- Lemmon, E. M. 2009. Diversification of conspecific signals in sympatry: Geographic overlap drives multidimensional reproductive character displacement in frogs. *Evolution* (N. Y). 63:1155–1170.
- Lenth, R. 2020. emmeans: Estimated Marginal Means, aka Least-Squares Means.
- Lester, E. K., T. J. Langlois, S. D. Simpson, M. I. McCormick, and M. G. Meekan. 2020. The hemisphere of fear: the presence of sharks influences the three dimensional behaviour of large mesopredators in a coral reef ecosystem. *Oikos* 1–9.
- Levine, J. S., and E. F. MacNichol. 1982. Color vision in fishes. *Sci. Am.* 246:140–149.
- Lewis, M. R., N. Kuring, and C. Yentsch. 1988. Global patterns of ocean transparency: Implications for the new production of the open ocean. *J. Geophys. Res.* 93:6847–6856.
- Longley, W. H. 1917. Studies upon the biological significance of animal coloration. I. The colors and color changes of West Indian reef-fishes. *J. Exp. Zool.* 23:533–601.
- Losey, G. S., T. Cronin, T. Goldsmith, D. Hydes, N. J. Marshall, and W. McFarland. 1999. The UV visual world of fishes: A review. *J. Fish Biol.* 54:921–943.
- Losey, G. S., W. N. McFarland, E. R. Loew, J. P. Zamzow, P. A. Nelson, and N. J. Marshall. 2003. Visual biology of Hawaiian coral reef fishes. I. Ocular transmission and visual pigments. *Copeia* 2003:433–454.
- Lyytinen, A., P. M. Brakefield, L. Lindström, and J. Mappes. 2004. Does predation maintain eyespot plasticity in *Bicyclus anynana*? *Proc. R. Soc. B Biol. Sci.* 271:279–283.
- Lyytinen, A., P. M. Brakefield, and J. Mappes. 2003. Significance of butterfly eyespots as an anti-predator device in ground-based and aerial attacks. *Oikos* 100:373–379.
- Maan, M. E., and M. E. Cummings. 2012. Poison frog colors are honest signals of toxicity, particularly for bird predators. *Am. Nat.* 179.

- MacArthur, R. H., and J. W. MacArthur. 1961. On Bird Species Diversity. *Ecology* 42:594–598.
- Malay, M. C. D., and G. Paulay. 2010. Peripatric speciation drives diversification and distributional pattern of reef hermit crabs (Decapoda: Diogenidae: Calcinus). *Evolution* (N. Y). 64:634–662.
- Marshall, J. 2000a. The Visual Ecology of Reef Fish Colours. Pp. 83–120 *in* *Animal Signals: Signalling and Signal Design in Animal Communication*. Tapir Academic Press, Torndheim, Norway.
- Marshall, J. L., M. L. Arnold, and D. J. Howard. 2002. Reinforcement: The road not taken. *Trends Ecol. Evol.* 17:558–563.
- Marshall, N., M. L. Barnes, A. Birtles, K. Brown, J. Cinner, M. Curnock, H. Eakin, J. Goldberg, M. Gooch, J. Kittinger, P. Marshall, D. Manuel-Navarrete, M. Pelling, P. L. Pert, B. Smit, and R. Tobin. 2018a. Measuring what matters in the Great Barrier Reef. *Front. Ecol. Environ.* 16:271–277.
- Marshall, N. J. 2000b. Communication and camouflage with the same “bright” colours in reef fishes. *Philos. Trans. R. Soc. Lond. B. Biol. Sci.* 355:1243–1248.
- Marshall, N. J. 2017. Vision and lack of vision in the ocean. *Curr. Biol.* 27:R494–R502. Elsevier.
- Marshall, N. J., F. Cortesi, F. de Busserolles, U. E. Siebeck, and K. L. Cheney. 2018b. Colours and colour vision in reef fishes: Past, present and future research directions. *J. Fish Biol.* 95:5–38.
- Marshall, N. J., K. Jennings, W. N. McFarland, E. R. Loew, and G. S. Losey. 2003. Visual biology of Hawaiian coral reef fishes. II. colors of Hawaiian coral reef fish. *Copeia* 2003:455–466.
- Marshall, N., P. Marshall, M. Curnock, P. Pert, A. Smith, and B. Visperas. 2019. Identifying indicators of aesthetics in the Great Barrier Reef for the purposes of management. *PLoS One* 14.
- Martin, P. R., R. Montgomerie, and S. C. Loughheed. 2010. Rapid sympatry explains greater color pattern divergence in high latitude birds. *Evolution* (N. Y). 64:336–347.

- Mason, N. A., and R. C. K. Bowie. 2020. Plumage patterns: Ecological functions, evolutionary origins, and advances in quantification. *Auk* 137:1–29.
- Mavárez, J., C. A. Salazar, E. Bermingham, C. Salcedo, C. D. Jiggins, and M. Linares. 2006. Speciation by hybridization in *Heliconius* butterflies. *Nature* 441:868–871.
- McClure, E. C., L. E. Richardson, A. Graba-Landry, Z. Loffler, G. R. Russ, and A. S. Hoey. 2019. Cross-shelf differences in the response of herbivorous fish assemblages to severe environmental disturbances. *Diversity* 11.
- McGraw, K. J., G. E. Hill, R. Stradi, and R. S. Parker. 2002. The effect of dietary carotenoid access on sexual dichromatism and plumage pigment composition in the American goldfinch. *Comp. Biochem. Physiol. - B Biochem. Mol. Biol.* 131:261–269.
- Mcmillan, W. O., L. A. Weigt, and S. R. Palumbi. 1999. Color pattern evolution, assortative mating, and genetic differentiation in brightly colored Butterflyfishes. *Evolution (N. Y.)* 53:247–260.
- McWilliam, M., M. O. Hoogenboom, A. H. Baird, C. Kuo, J. S. Madin, and T. P. Hughes. 2018. Biogeographical disparity in the functional diversity and redundancy of corals. *Proc. Natl. Acad. Sci.* 115:3084–3089.
- Meade, A., and M. Pagel. 2019. BayesTraits: a computer package for analyses of trait evolution.
- Merilaita, S., N. E. Scott-Samuel, and I. C. Cuthill. 2017. How camouflage works. *Philos. Trans. R. Soc. B Biol. Sci.* 372.
- Merilaita, S., A. Vallin, U. Kodandaramaiah, M. Dimitrova, S. Ruuskanen, and T. Laaksonen. 2011. Number of eyespots and their intimidating effect on naïve predators in the peacock butterfly. *Behav. Ecol.* 22:1326–1331.
- Mihalitsis, M., and D. R. Bellwood. 2017. A morphological and functional basis for maximum prey size in piscivorous fishes. *PLoS One* 12:1–19.

- Mihalitsis, M., and D. R. Bellwood. 2019. Morphological and functional diversity of piscivorous fishes on coral reefs. *Coral Reefs* 38:945–954. Springer Berlin Heidelberg.
- Mittelbach, G. 1986. Predator-mediated habitat use: some consequences for species interactions. *Environ. Biol. Fishes* 16:159–169.
- Miyazawa, S. 2020. Pattern blending enriches the diversity of animal colorations. *Sci. Adv.* (in press).
- Molina-Venegas, R., and M. Rodríguez. 2017. Revisiting phylogenetic signal; strong or negligible impacts of polytomies and branch length information? *BMC Evol. Biol.* 17:1–10. BMC Evolutionary Biology.
- Morais, R. A., M. Depczynski, C. J. Fulton, M. J. Mamane, P. Narvaez, V. Huertas, S. J. Brandl, and D. R. Bellwood. 2020. Severe coral loss shifts energetic dynamics on a coral reef. *Funct. Ecol.* 1–12.
- Morgan, M. J., and J. J. Godin. 1985. Antipredator Benefits of Schooling Behaviour in a Cyprinodontid Fish, the Banded Killifish (*Fundulus diaphanus*). *Z. Tierpsychol.* 70:236–246.
- Motro, R., I. Ayalon, and A. Genin. 2005. Near-bottom depletion of zooplankton over coral reefs: III: Vertical gradient of predation pressure. *Coral Reefs* 24:95–98.
- Mouillot, D., N. A. J. Graham, S. Villéger, N. W. H. Mason, and D. R. Bellwood. 2013a. A functional approach reveals community responses to disturbances. *Trends Ecol. Evol.* 28:167–177.
- Mouillot, D., N. A. J. Graham, S. Villéger, N. W. H. Mason, and D. R. Bellwood. 2013b. A functional approach reveals community responses to disturbances. *Trends Ecol. Evol.* 28:167–177.
- Münkemüller, T., S. Lavergne, B. Bzeznik, S. Dray, T. Jombart, K. Schiffers, and W. Thuiller. 2012. How to measure and test phylogenetic signal. *Methods Ecol. Evol.* 3:743–756.
- Nakatani, Y., A. Kawakami, and A. Kudo. 2007. Cellular and molecular processes of regeneration, with special emphasis on fish fins. *Dev. Growth Differ.* 49:145–154.

- Nash, K. L., J. Q. Welsh, N. A. J. Graham, and D. R. Bellwood. 2015. Home-range allometry in coral reef fishes: comparison to other vertebrates, methodological issues and management implications. *Oecologia* 177:73–83.
- Nyström, M., C. Folke, and F. Moberg. 2000. Coral reef disturbance and resilience in a human-dominated environment. *Trends Ecol. Evol.* 15:413–417.
- Öhman, M. C., and A. Rajasuriya. 1998. Relationships between habitat structure and fish communities on coral and sandstone reefs.
- Öhman, M. C., A. Rajasuriya, and E. Ólafsson. 1997. Reef fish assemblages in north-western Sri Lanka : distribution patterns and influences of fishing practices. *Environ. Biol. Fishes* 49:45–61.
- Oksanen, J., F. G. Blanchet, M. Friendly, R. Kindt, P. Legendre, D. McGlenn, P. R. Minchin, R. B. O'Hara, G. L. Simpson, P. Solymos, M. H. H. Stevens, E. Szoecs, and H. Wagner. 2019. *vegan: Community Ecology Package*.
- Olofsson, M., A. Vallin, S. Jakobsson, and C. Wiklund. 2010. Marginal eyespots on butterfly wings deflect bird attacks under low light intensities with UV wavelengths. *PLoS One* 5.
- Olofsson, M., C. Wiklund, and A. Favati. 2015. On the deterring effect of a butterfly's eyespot in juvenile and sub-adult chickens. *Curr. Zool.* 61:749–757.
- Ortolani, A. 1999. Spots, stripes, tail tips and dark eyes: Predicting the function of carnivore colour patterns using the comparative method. *Biol. J. Linn. Soc.* 67:433–476.
- Osorio, D., and M. Vorobyev. 2008. A review of the evolution of animal colour vision and visual communication signals. *Vision Res.* 48:2042–2051.
- Osorio, D., and M. Vorobyev. 2005. Photoreceptor spectral sensitivities in terrestrial animals: Adaptations for luminance and colour vision. *Proc. R. Soc. B Biol. Sci.* 272:1745–1752.
- Pagel, M. 1994. Detecting correlated evolution on phylogenies: A general method for the comparative

- analysis of discrete characters. *Proc. R. Soc. B Biol. Sci.* 255:37–45.
- Pagel, M. 1999. Inferring the historical patterns of biological evolution. *Nature* 401:877–884.
- Panhuis, T. M., R. Butlin, M. Zuk, and T. Tregenza. 2001. Sexual Selection and Speciation. *Annu. Rev. Ecol. Evol. Syst.* 16:364–371.
- Paradis, E., and K. Schliep. 2019. Ape 5.0: An environment for modern phylogenetics and evolutionary analyses in R. *Bioinformatics* 35:526–528.
- Parravicini, V., M. Kulbicki, D. R. Bellwood, A. M. Friedlander, J. E. Arias-Gonzalez, P. Chabanet, S. R. Floeter, R. Myers, L. Vigliola, S. D’Agata, and D. Mouillot. 2013. Global patterns and predictors of tropical reef fish species richness. *Ecography (Cop.)*. 36:1254–1262.
- Pert, P. L., L. Thiault, M. I. Curnock, S. Becken, and J. Claudet. 2020. Beauty and the reef: Evaluating the use of non-expert ratings for monitoring aesthetic values of coral reefs. *Sci. Total Environ.* 730:139156. Elsevier B.V.
- Phillips, G. A. C., M. J. How, J. E. Lange, N. J. Marshall, and K. L. Cheney. 2017. Disruptive colouration in reef fish: does matching the background reduce predation risk? *J. Exp. Biol.* 220:1962–1974.
- Pinheiro, J., D. DebRoy, S. Sarkar, and . R Core Team. 2019. nlme: Linear and nonlinear mixed effects models. R package version 3.1-140.
- Poulton, E. B. 1890. *The colours of animals, their meaning and use, especially considered in the case of insects.* D. Appleton and Company, New York.
- Prudic, K. L., A. M. Stoehr, B. R. Wasik, and A. Monteiro. 2014. Eyespots deflect predator attack increasing fitness and promoting the evolution of phenotypic plasticity. *Proc. R. Soc. B Biol. Sci.* 282.
- Puebla, O., E. Bermingham, F. Guichard, and E. Whiteman. 2007. Colour pattern as a single trait

- driving speciation in *Hypoplectrus* coral reef fishes? *Proc. Biol. Sci.* 274:1265–1271.
- R Core Team. 2020. R: A language and environment for statistical computing. Vienna, Austria.
- Rabinowitz, G. B. 1975. An Introduction to Nonmetric Multidimensional Scaling. *Am. J. Pol. Sci.* 19:343–390.
- Rabosky, D. L. 2015. No substitute for real data: A cautionary note on the use of phylogenies from birth-death polytomy resolvers for downstream comparative analyses. *Evolution* (N. Y). 69:3207–3216.
- Rabosky, D. L., J. Chang, P. O. Title, P. F. Cowman, L. Sallan, M. Friedman, K. Kaschner, C. Garilao, T. J. Near, M. Coll, and M. E. Alfaro. 2018. An inverse latitudinal gradient in speciation rate for marine fishes. *Nature* 559:392–395. Springer US.
- Revell, L. J. 2012. phytools: An R package for phylogenetic comparative biology (and other things). *Methods Ecol. Evol.* 3:217–223.
- Reynolds, G. R., and B. M. Fitzpatrick. 2007. Assortative mating in poison-dart frogs based on an ecologically important trait. *Evolution* (N. Y). 21:1215–1221.
- Richardson, L. E., N. A. J. Graham, M. S. Pratchett, J. G. Eurich, and A. S. Hoey. 2018. Mass coral bleaching causes biotic homogenization of reef fish assemblages. *Glob. Chang. Biol.* 24:3117–3129.
- Righton, D., and C. Mills. 2006. Application of GIS to investigate the use of space in coral reef fish: A comparison of territorial behaviour in two Red Sea butterflyfishes. *Int. J. Geogr. Inf. Sci.* 20:215–232.
- Roberts, C. M., and R. F. Y. Ormond. 1992. Butterfly fish social behavior, with special reference to the incidence of territoriality - a review. *Environ. Biol. Fishes* 34:79–93.
- Robertson, K. A., and A. Monteiro. 2005. Female *Bicyclus anynana* butterflies choose males on the

- basis of their dorsal UV-reflective eyespot pupils. *Proc. R. Soc. B Biol. Sci.* 272:1541–1546.
- Rocha, L. A., J. D. DiBattista, T. H. Sinclair-Taylor, and M. L. Berumen. 2020. Wolves in sheep's clothing: three new cases of aggressive mimicry in Red Sea coral reef fishes. *J. Nat. Hist.* 54:1019–1023. Taylor & Francis.
- Rocha, L. A., K. C. Lindeman, C. R. Rocha, and H. A. Lessios. 2008. Historical biogeography and speciation in the reef fish genus *Haemulon* (Teleostei: Haemulidae). *Mol. Phylogenet. Evol.* 48:918–928.
- Rodgers, G. M., N. W. Gladman, H. F. Corless, and L. J. Morrell. 2013. Costs of colour change in fish: Food intake and behavioural decisions. *J. Exp. Biol.* 216:2760–2767.
- Rogers, A. D., P. A. Tyler, D. P. Connelly, J. T. Copley, R. James, R. D. Larter, K. Linse, R. A. Mills, A. N. Garabato, R. D. Pancost, D. A. Pearce, N. V. C. Polunin, C. R. German, T. Shank, P. H. Boersch-Supan, B. J. Alker, A. Aquilina, S. A. Bennett, A. Clarke, R. J. J. Dinley, A. G. C. Graham, D. R. H. Green, J. A. Hawkes, L. Hepburn, A. Hilario, V. A. I. Huvenne, L. Marsh, E. Ramirez-Llodra, W. D. K. Reid, C. N. Roterman, C. J. Sweeting, S. Thatje, and K. Zwirgmaier. 2012. The discovery of new deep-sea hydrothermal vent communities in the Southern ocean and implications for biogeography. *PLoS Biol.* 10.
- Romero, A., and S. M. Green. 2005. The end of regressive evolution and cave fishes.pdf. *J. Fish Biol.* 67:3–32.
- Ryan, M. J., and S. A. Rand. 1993. Species recognition and sexual selection as a unitary problem in animal communication. *Evolution* (N. Y). 47:647–657.
- Salis, P., N. Roux, O. Soulat, D. Lecchini, V. Laudet, and B. Frédérick. 2018. Ontogenetic and phylogenetic simplification during white stripe evolution in clownfishes. *BMC Biol.* 16:1–13. BMC Biology.
- Schmitz, L., and P. C. Wainwright. 2011a. Ecomorphology of the eyes and skull in zooplanktivorous

- labrid fishes. *Coral Reefs* 30:415–428.
- Schmitz, L., and P. C. Wainwright. 2011b. Nocturnality constrains morphological and functional diversity in the eyes of reef fishes. *BMC Evol. Biol.* 11:338.
- Schneider, C. A., W. S. Rasband, and K. W. Eliceiri. 2012. NIH Image to ImageJ: 25 years of image analysis. *Nat. Methods* 9:671–675. Nature Publishing Group.
- Seddon, N. 2005. Ecological adaptation and species recognition drives vocal evolution in neotropical suboscine birds. *Evolution (N. Y.)* 59:200–215.
- Seddon, N., and J. A. Tobias. 2007. Song divergence at the edge of Amazonia: An empirical test of the peripatric speciation model. *Biol. J. Linn. Soc.* 90:173–188.
- Seehausen, O. 1997. Distribution of and reproductive isolation among color morphs of a rock-dwelling Lake Victoria cichlid. *Ecol. Freshw. Fish* 6:59–66.
- Seehausen, O., P. J. Mayhew, and J. J. M. Van Alphen. 1999. Evolution of colour patterns in East African cichlid fish. *J. Evol. Biol.* 12:514–534.
- Seehausen, O., and D. Schluter. 2004. Male-male competition and nuptial-colour displacement as a diversifying force in Lake Victoria cichlid fishes. *Proc. R. Soc. B Biol. Sci.* 271:1345–1353.
- Seehausen, O., J. J. M. van Alphen, and F. Witte. 1997. Cichlid fish diversity threatened by eutrophication that curbs sexual selection. *Science (80-.)*. 277:1808–1812.
- Siebeck, U. E. 2004. Communication in coral reef fish: The role of ultraviolet colour patterns in damselfish territorial behaviour. *Anim. Behav.* 68:273–282.
- Siqueira, A. C., R. A. Morais, D. R. Bellwood, and P. F. Cowman. 2020. Trophic innovations fuel reef fish diversification. *Nat. Commun.* 11:1–11.
- Smith, P. F., and I. Kornfield. 2002. Phylogeography of Lake Malawi cichlids of the genus

- Pseudotropheus: significance of allopatric colour variation. *Proc. R. Soc. B Biol. Sci.* 269:2495–2502.
- Soares, D., and M. L. Niemiller. 2020. Extreme Adaptation in Caves. *Anat. Rec.* 303:15–23.
- Stevens, M. 2005. The role of eyespots as anti-predator mechanisms, principally demonstrated in the Lepidoptera. *Biol. Rev. Camb. Philos. Soc.* 80:573–588.
- Stevens, M., and S. Merilaita. 2011. *Animal camouflage: mechanisms and function*. Cambridge University Press.
- Stevens, M., C. A. Parraga, I. C. Cuthill, J. C. Partridge, and T. S. Troscianko. 2007. Using digital photography to study animal coloration. *Biol. J. Linn. Soc.* 90:211–237.
- Stevens, M., and G. D. Ruxton. 2014. Do animal eyespots really mimic eyes? *Curr. Zool.* 60:26–36.
- Stevens, M., and G. D. Ruxton. 2019. The key role of behaviour in animal camouflage. *Biol. Rev.* 94:116–134.
- Stevens, M., C. L. Stubbins, and C. J. Hardman. 2008. The anti-predator function of “eyespot” on camouflaged and conspicuous prey. *Behav. Ecol. Sociobiol.* 62:1787–1793.
- Su, G., S. Villéger, and S. Brosse. 2019. Morphological diversity of freshwater fishes differs between realms, but morphologically extreme species are widespread. *Glob. Ecol. Biogeogr.* 28:211–221.
- Summers, K., and M. E. Clough. 2001. The evolution of coloration and toxicity in the poison frog family (Dendrobatidae). *Proc. Natl. Acad. Sci. U. S. A.* 98:6227–6232.
- Templeton, A. R. 1981. Mechanisms of speciation - A population genetic approach. *Annu. Rev. Ecol. Syst.* 12:23–48.
- Theis, A., W. Salzburger, and B. Egger. 2012. The function of anal fin egg-spots in the cichlid fish *Astatotilapia burtoni*. *PLoS One* 7.

- Tilman, D., J. Knops, D. Wedin, P. Reich, M. Ritchie, and E. Siemann. 1997. The influence of functional diversity and composition on ecosystem processes. *Science* (80-.). 277:1300–1302.
- Tribot, A., Q. Carabeux, J. Deter, T. Claverie, S. Villéger, and N. Mouquet. 2018. Confronting species aesthetics with ecological functions in coral reef fish. *Sci. Rep.* 8:1–7.
- Tribot, A., J. Deter, T. Claverie, F. Guillhaumon, S. Villéger, and N. Mouquet. 2019. Species diversity and composition drive the aesthetic value of coral reef fish assemblages. *Biol. Lett.*
- Tribot, A. S., N. Mouquet, S. Villéger, M. Raymond, F. Hoff, P. Boissery, F. Holon, and J. Deter. 2016. Taxonomic and functional diversity increase the aesthetic value of coralligenous reefs. *Sci. Rep.* 6:1–12. Nature Publishing Group.
- Tricas, T. C., and K. S. Boyle. 2014. Acoustic behaviors in Hawaiian coral reef fish communities. *Mar. Ecol. Prog. Ser.* 511:1–16.
- Troscianko, J., and M. Stevens. 2015. Image calibration and analysis toolbox - a free software suite for objectively measuring reflectance, colour and pattern. *Methods Ecol. Evol.* 6:1320–1331.
- Troscianko, J., J. Wilson-Aggarwal, M. Stevens, and C. N. Spottiswoode. 2016. Camouflage predicts survival in ground-nesting birds. *Sci. Rep.* 6:1–8. Nature Publishing Group.
- Turner, A. M., and G. G. Mittelbach. 1990. Predator Avoidance and Community Structure: Interactions among Piscivores, Planktivores, and Plankton. *Ecology* 71:2241–2254.
- Tyrie, E. K., R. T. Hanlon, L. A. Siemann, and M. C. Uyarra. 2015. Coral reef flounders, *Bothus lunatus*, choose substrates on which they can achieve camouflage with their limited body pattern repertoire. *Biol. J. Linn. Soc.* 114:629–638.
- Umeton, D., G. Tarawneh, E. Fezza, J. C. A. Read, and C. Rowe. 2019. Pattern and Speed Interact to Hide Moving Prey. *Curr. Biol.* 1–5. Elsevier Ltd.
- Vallin, A., M. Dimitrova, U. Kodandaramaiah, and S. Merilaita. 2011. Deflective effect and the effect

- of prey detectability on anti-predator function of eyespots. *Behav. Ecol. Sociobiol.* 65:1629–1636.
- Vallin, A., S. Jakobsson, and C. Wiklund. 2007. “An eye for an eye?” - On the generality of the intimidating quality of eyespots in a butterfly and a hawkmoth. *Behav. Ecol. Sociobiol.* 61:1419–1424.
- Van Belleghem, S. M., R. Papa, H. Ortiz-Zuazaga, F. Hendrickx, C. D. Jiggins, W. O. Mcmillan, and B. A. Counterman. 2018. *patternize*: An R package for quantifying colour pattern variation. *Methods Ecol. Evol.* 390–398.
- Van Den Berg, C. P., J. Troscianko, J. A. Endler, N. J. Marshall, and K. L. Cheney. 2019. Quantitative Colour Pattern Analysis (QCPA): A Comprehensive Framework for the Analysis of Colour Patterns in Nature. *Methods Ecol. Evol.* 2019:1–17.
- Venditti, C., A. Meade, and M. Pagel. 2011. Multiple routes to mammalian diversity. *Nature* 479:393–396. Nature Publishing Group.
- Vernerey, F. J., and F. Barthelat. 2014. Skin and scales of teleost fish: Simple structure but high performance and multiple functions. *J. Mech. Phys. Solids* 68:66–76. Elsevier.
- Villéger, S., N. W. H. Mason, and D. Mouillot. 2008. New multidimensional functional diversity indices for a multifaceted framework in functional ecology. *Ecology* 89:2290–2301.
- Vliieger, L., and P. M. Brakefield. 2007. The deflection hypothesis: Eyespots on the margins of butterfly wings do not influence predation by lizards. *Biol. J. Linn. Soc.* 92:661–667.
- Wagenmakers, E. J., and S. Farrell. 2004. AIC model selection using Akaike weights AIC model selection using Akaike weights. *Psychon. Bull. Rev.* 11:192–196.
- Wainwright, P. C., M. E. Alfaro, D. I. Bolnick, and C. D. Hulsey. 2005. Many-to-one mapping of form to function: A general principle in organismal design? *Integr. Comp. Biol.* 45:256–262.

- Wallace, A. R. 1877. The colour of animals and plants. I. - the colours of animals. *Am. Nat.* 11:348–408.
- Warwick, R. M., and K. R. Clarke. 1991. A comparison of some methods for analysing changes in benthic community structure. *J. Mar. Biol. Assoc. United Kingdom* 71:225–244.
- Weller, H. I., and M. W. Westneat. 2019. Quantitative color profiling of digital images with earth mover's distance using the R package *colordistance*. *PeerJ* 1–31.
- Werner, E. E., J. F. Gilliam, D. J. Hall, and G. G. Mittelbach. 2012. An experimental test of the effects of predation risk on habitat use in fish. *Ecology* 64:1540–1548.
- Westley, P. A. H., R. Stanley, and I. A. Fleming. 2013. Experimental tests for heritable morphological color plasticity in non-native brown trout (*Salmo trutta*) populations. *PLoS One* 8.
- White, T. E., R. L. Dalrymple, D. W. A. Noble, J. C. O'Hanlon, D. B. Zurek, and K. D. L. Umbers. 2015. Reproducible research in the study of biological coloration. *Anim. Behav.* 106:51–57. Elsevier Ltd.
- Whitney, J. L., B. W. Bowen, and S. A. Karl. 2018. Flickers of speciation: sympatric colour morphs of the arc-eye hawkfish, *Paracirrhites arcatus*, reveal key elements of divergence with gene flow. *Mol. Ecol.*, doi: 10.1111/mec.14527.
- Wickham, H. 2016. *ggplot2: Elegant Graphics for Data Analysis*. Springer-Verlag New York.
- Wickham, H., R. Francois, L. Henry, and K. Muller. 2020. *dplyr: a Grammar of Data Manipulation*.
- Williams, J. T., K. E. Carpenter, J. L. van Tassell, P. Hoetjes, W. Toller, P. Etnoyer, and M. Smith. 2010. Biodiversity assessment of the fishes of Saba Bank atoll, Netherlands antilles. *PLoS One* 5:1–37.
- Winemiller, K. O. 1990. Caudal Eyespots as Deterrents against Fin Predation in the Neotropical Cichlid *Astronotus ocellatus*. *Copeia* 1990:665–673.

- Wisocki, P. A., P. Kennelly, I. R. Rivera, P. Cassey, M. L. Burkey, and D. Hanley. 2019. The global distribution of avian eggshell colours suggest a thermoregulatory benefit of darker pigmentation. *Nat. Ecol. Evol.*, doi: 10.1038/s41559-019-1003-2. Springer US.
- Wood, S. N. 2011. Fast stable restricted maximum likelihood and marginal likelihood estimation of semiparametric generalized linear models. *J. R. Stat. Soc.* 73:3–36.
- Xie, W., P. O. Lewis, Y. Fan, L. Kuo, and M. H. Chen. 2011. Improving marginal likelihood estimation for bayesian phylogenetic model selection. *Syst. Biol.* 60:150–160.
- Yaakub, S. M., D. R. Bellwood, L. van Herwerden, and F. M. Walsh. 2006. Hybridization in coral reef fishes: introgression and bi-directional gene exchange in *Thalassoma* (family Labridae). *Mol. Phylogenet. Evol.* 40:84–100.
- Zaret, T. M. 1977. Inhibition of Cannibalism in *Cichla ocellaris* and Hypothesis of Predator Mimicry Among South American Fishes. *Evolution* (N. Y). 31:421–437.
- Zeuss, D., R. Brandl, M. Brändle, C. Rahbek, and S. Brunzel. 2014. Global warming favours light-coloured insects in Europe. *Nat. Commun.* 5.

Appendix A

Eyespot Definition:

We defined an eyespot based on the following three criteria. 1) The entire eyespot needs to be approximately circular or elliptic in shape. 2) it has a (typically) black interior circle or ellipse that is surrounded by no less than 75% of its circumference by a contrasted concentric ring of differing, much lighter colour. 3) there could be no more than 10 eyespots present on an individual. These criteria were chosen to ensure that the pattern was clearly an eyespot that functions as a distinct marking that is visually conspicuous against rest of the fish's colouration. These criteria were necessary since there is a broad spectrum of markings present on coral reef. Establishing strict criteria allow us to focus on the species with a consistent eyespot form to explore their subsequent function.

Table A1. Parameters estimates and selection criteria for each model of discrete character evolution. 10 different models of evolution were generated and the most parsimonious was selected using AICc. ER = equal rates, ARD = all rates different, lnL = log likelihood. Each model was run for 1000 iterations and fit using the 'fitDiscrete' function in the geiger library. Models are ranked in descending order from best to worst.

Model	Extra Parameter	Parameter Estimate	AICc	Δ AICc	lnL
ARD	Lambda (λ)	$\lambda = 0.9309$	922.49	0	-458.24
ARD	Kappa (κ)	$\kappa = 0.3068$	947.20	24.71	-470.59
ARD	Alpha (α)	$\alpha = 0.0203$	953.21	30.72	-473.59
ARD	Delta (δ)	$\delta = 2.9999$	956.19	33.7	-475.09
ARD	n/a	n/a	967.41	44.92	-481.70
ER	Lambda (λ)	$\lambda = 0.8536$	1009.99	87.5	-502.99
ER	Kappa (κ)	$\kappa = 0.1827$	1012.84	90.35	-504.41
ER	Alpha (α)	$\alpha = 0.0796$	1020.33	97.84	-508.16
ER	Delta (δ)	$\delta = 2.9999$	1058.52	136.03	-527.26
ER	n/a	n/a	1083.98	161.49	-540.99

Table A2. List of species used in the heatmap analysis.

NO.	SPECIES	CATEGORY
1	Acanthurus bariene	active
2	Acanthurus tennentii	active
3	Anampses femininus	active
4	Anampses geographicus	active
5	Anampses meleagrides	active
6	Anampses neoguinaicus	active
7	Anampses twistii	active
8	Apolemichthys trimaculatus	active
9	Arothron hispidus	active
10	Belonoperca chabanaudi	active
11	Bodianus bimaculatus	active
12	Bodianus diana	active
13	Bodianus neilli	active
14	Canthigaster bennetti	active
15	Canthigaster papua	active
16	Canthigaster rostrata	active
17	Canthigaster solandri	active
18	Centropyge flavissima	active
19	Centropyge multispinis	active
20	Cephalopholis leopardus	active
21	Cetoscarus bicolor	active
22	Chaetodon bennetti	active
23	Chaetodon capistratus	active
24	Chaetodon lunula	active
25	Chaetodon madagaskariensis	active
26	Chaetodon melannotus	active
27	Chaetodon ocellicaudus	active
28	Chaetodon octofasciatus	active
29	Chaetodon plebeius	active
30	Chaetodon striatus	active
31	Chaetodon unimaculatus	active
32	Chaetodon xanthurus	active
33	Cheilinus oxycephalus	active
34	Chelmon marginalis	active
35	Chelmon muelleri	active
36	Chelmon rostratus	active
37	Choerodon fasciatus	active
38	Chrysiptera biocellata	active
39	Chrysiptera brownriggii	active
40	Chrysiptera talboti	active
41	Chrysiptera unimaculata	active
42	Cirrhilabrus cyanopleura	active
43	Cirrhilabrus exquisitus	active
44	Coradion altivelis	active
45	Coradion chrysozonus	active
46	Coradion melanopus	active
47	Coris aygula	active
48	Coris batuensis	active
49	Coris dorsomacula	active
50	Coris formosa	active
51	Coris variegata	active
52	Cymolutes praetextatus	active
53	Diodon liturosus	active
54	Dischistodus melanotus	active
55	Dischistodus perspicillatus	active
56	Dischistodus prosopotaenia	active
57	Halichoeres biocellatus	active
58	Halichoeres bivittatus	active
59	Halichoeres chrysus	active
60	Halichoeres cosmetus	active
61	Halichoeres hortulanus	active
62	Halichoeres leucoxanthus	active
63	Halichoeres margaritaceus	active
64	Halichoeres marginatus	active
65	Halichoeres melanurus	active
66	Halichoeres melasmopomus	active
67	Halichoeres miniatus	active
68	Halichoeres nebulosus	active
69	Halichoeres nigrescens	active
70	Halichoeres ornatissimus	active
71	Halichoeres prosopeion	active
72	Halichoeres radiatus	active
73	Halichoeres trispilus	active
74	Heniochus chrysostomus	active
75	Holacanthus ciliaris	active
76	Holacanthus tricolor	active
77	Iniistius aneitensis	active
78	Iniistius pavo	active
79	Macropharyngodon kuiteri	active
80	Macropharyngodon meleagris	active
81	Neoglyphidodon polyacanthus	active
82	Oxycheilinus arenatus	active
83	Oxycheilinus digramma	active
84	Oxycheilinus unifasciatus	active
85	Paracentropyge multifasciata	active
86	Parachaetodon ocellatus	active
87	Parma polylepis	active
88	Plectroglyphidodon leucozonus	active
89	Plectroglyphidodon phoenixensis	active

90	<i>Pomacanthus chrysurus</i>	active	137	<i>Fowleria variegata</i>	crypto
91	<i>Pomacanthus imperator</i>	active	138	<i>Grammistops ocellatus</i>	crypto
92	<i>Pomacentrus amboinensis</i>	active	139	<i>Iracundus signifer</i>	crypto
93	<i>Pomacentrus bankanensis</i>	active	140	<i>Koumansetta hectori</i>	crypto
94	<i>Pomacentrus chrysurus</i>	active	141	<i>Koumansetta rainfordi</i>	crypto
95	<i>Pomacentrus indicus</i>	active	142	<i>Labrisomus nigricinctus</i>	crypto
96	<i>Pomacentrus nagasakiensis</i>	active	143	<i>Labrisomus nuchipinnis</i>	crypto
97	<i>Pomacentrus sulfureus</i>	active	144	<i>Liopropoma carmabi</i>	crypto
98	<i>Pomacentrus vaiuli</i>	active	145	<i>Lipogramma evides</i>	crypto
99	<i>Pseudocheilinus hexataenia</i>	active	146	<i>Lotilia graciliosa</i>	crypto
100	<i>Pseudocheilinus ocellatus</i>	active	147	<i>Lucayablennius zingaro</i>	crypto
101	<i>Pteragogus cryptus</i>	active	148	<i>Neosynchiropus ocellatus</i>	crypto
102	<i>Pteragogus enneacanthus</i>	active	149	<i>Ostorhinchus cookii</i>	crypto
103	<i>Pygoplites diacanthus</i>	active	150	<i>Paraclinus nigripinnis</i>	crypto
104	<i>Roa excelsa</i>	active	151	<i>Parapercis clathrata</i>	crypto
105	<i>Stegastes diencaeus</i>	active	152	<i>Parapercis hexophtalma</i>	crypto
106	<i>Stegastes variabilis</i>	active	153	<i>Pseudogramma polyacantha</i>	crypto
107	<i>Stethojulis albovittata</i>	active	154	<i>Pseudorhombus duplici-cellatus</i>	crypto
108	<i>Stethojulis bandanensis</i>	active	155	<i>Rainfordia opercularis</i>	crypto
109	<i>Stethojulis strigiventer</i>	active	156	<i>Signigobius biocellatus</i>	crypto
110	<i>Symphoricthys spilurus</i>	active	157	<i>Valenciennea helsdingenii</i>	crypto
111	<i>Thalassoma janseni</i>	active	158	<i>Valenciennea wardii</i>	crypto
112	<i>Thalassoma quinquevittatum</i>	active	159	<i>Wetmorella albofasciata</i>	crypto
113	<i>Xyrichtys splendens</i>	active	160	<i>Wetmorella nigropinnata</i>	crypto
114	<i>Acanthemblemaria aspera</i>	crypto	161	<i>Xiphasia setifer</i>	crypto
115	<i>Amblycirrhitus bimacula</i>	crypto			
116	<i>Amblyeleotris randalli</i>	crypto			
117	<i>Amblygobius decussatus</i>	crypto			
118	<i>Amblygobius phalaena</i>	crypto			
119	<i>Amblygobius semicinctus</i>	crypto			
120	<i>Antennatus nummifer</i>	crypto			
121	<i>Apogonichthys ocellatus</i>	crypto			
122	<i>Belonepterygion fasciolatum</i>	crypto			
123	<i>Calloplelesops altivelis</i>	crypto			
124	<i>Chaenopsis limbaughi</i>	crypto			
125	<i>Cheilodipterus artus</i>	crypto			
126	<i>Cheilodipterus quinquelineatus</i>	crypto			
127	<i>Cirrhichthys aprinus</i>	crypto			
128	<i>Cirripectes quagga</i>	crypto			
129	<i>Crossosalarias macrospilus</i>	crypto			
130	<i>Cryptocentrus caeruleopunctatus</i>	crypto			
131	<i>Cryptocentrus strigiliceps</i>	crypto			
132	<i>Cypho purpurascens</i>	crypto			
133	<i>Dactylopus kuiteri</i>	crypto			
134	<i>Dendrochirus biocellatus</i>	crypto			
135	<i>Fowleria aurita</i>	crypto			
136	<i>Fowleria marmorata</i>	crypto			

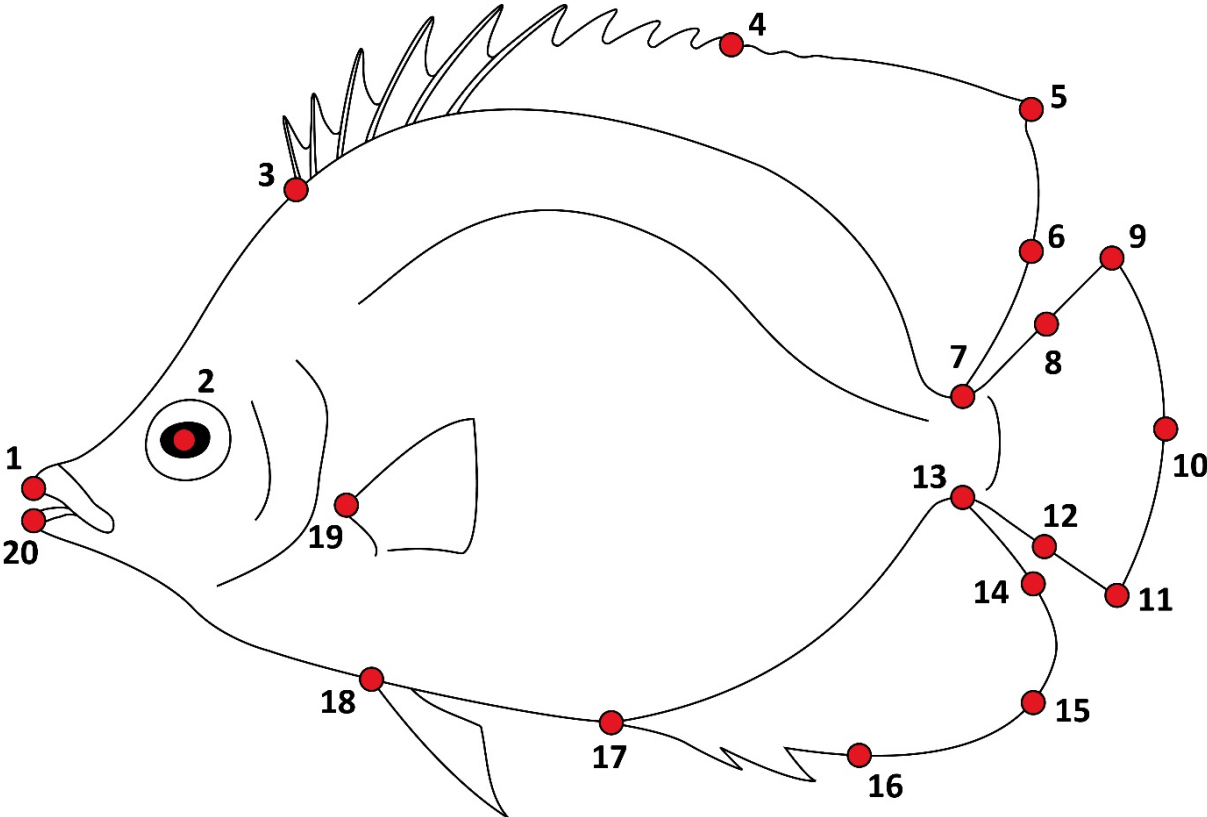


Figure A1. The 20 morphological landmarks used for image alignment in 'patternize'.

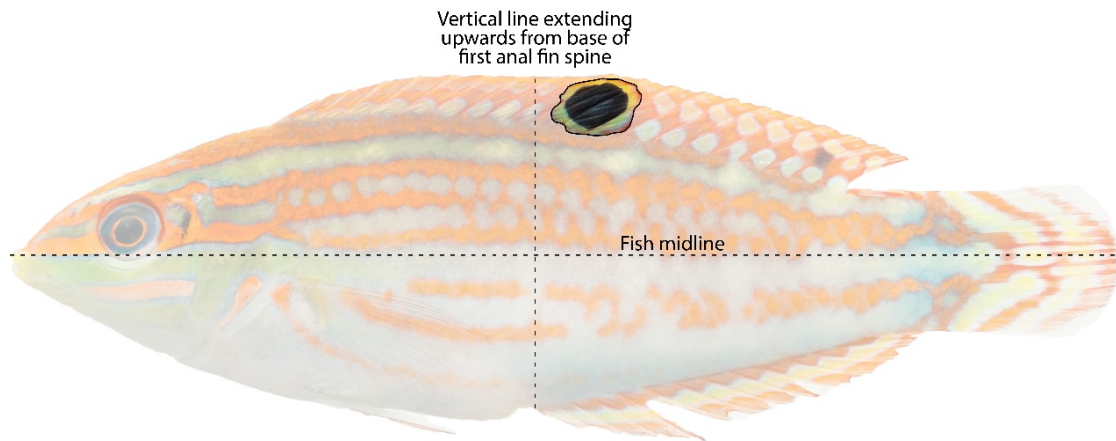


Figure A2. Guidelines used to classify eyespot location in active and cryptobenthic fishes.

Table A3. *P-values of 'prop.test' (stats library R) pairwise comparisons between locations of the proportion of species with and without eyespots. Significant differences in proportions are denoted in bold. Only the tropical eastern pacific was significantly different from the Great Barrier Reef and Indian Ocean.*

	Atlantic	GBR	Indian	TEP
Atlantic	-			
GBR	0.6898	-		
Indian	0.6268	0.9463	-	
TEP	0.0842	0.0055	0.0045	-

Table A4. *Models of independent and dependent trait evolution.*

Model	Dependent Trait	Independent Trait	AIC	ΔAIC	Log-Lik	Significantly different from Ind. Model?
ARD	Location	Activity	223.843	-	-105.9215	p-value = 0.0148
ARD	Location & Activity	-	226.0975	2.1725	-105.0487	p-value = 0.0376
ARD	Activity	Location	227.8384	0.4316	-107.9192	p-value = 0.1091
ARD	-	Location & Activity	228.2700	4.427	-110.135	n/a

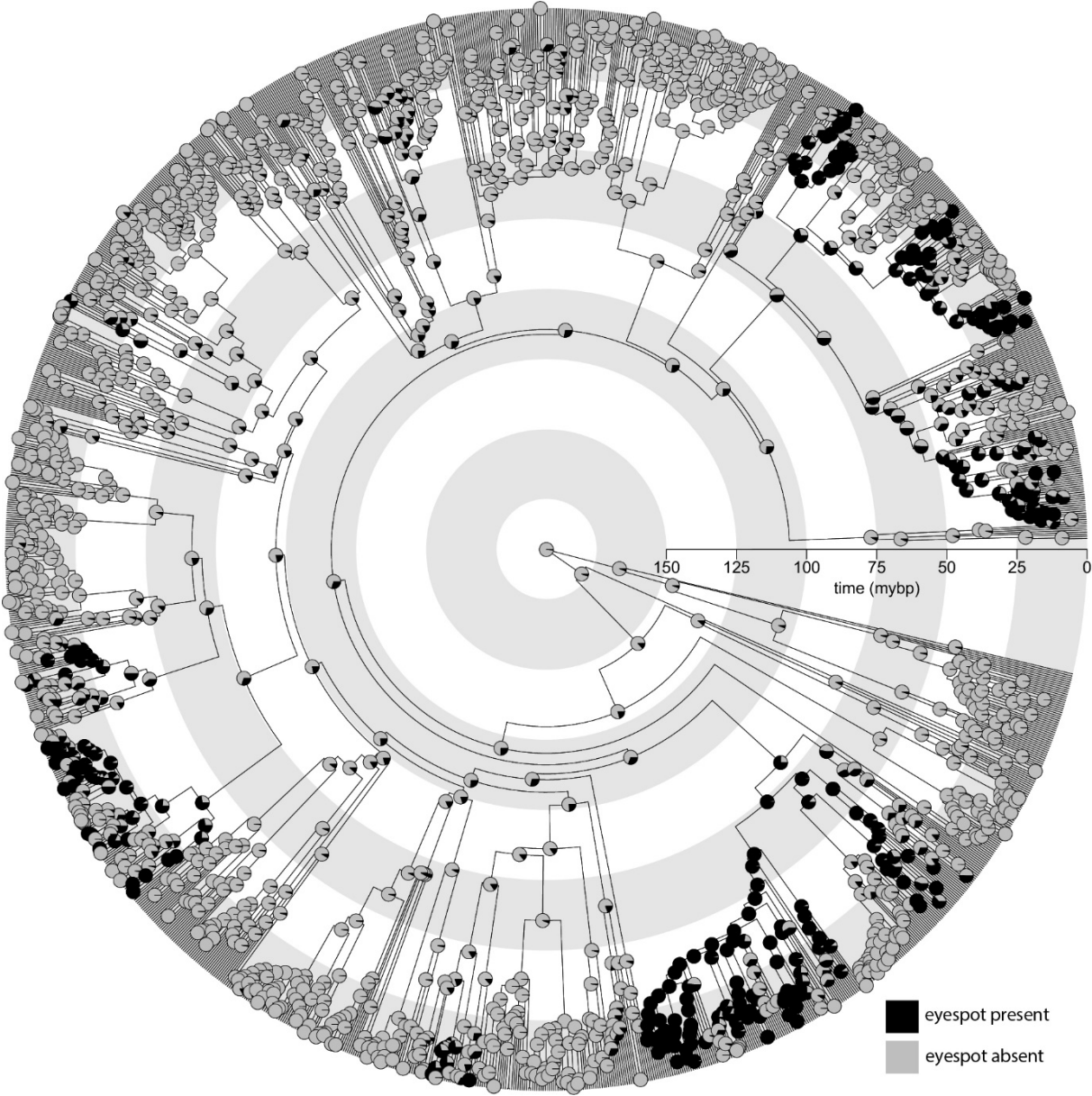


Figure A3. 1000 averaged stochastic character maps of eyespot evolution. The node values represent the averaged probabilities calculated across all 1000 SIMMAP iterations.

Appendix B

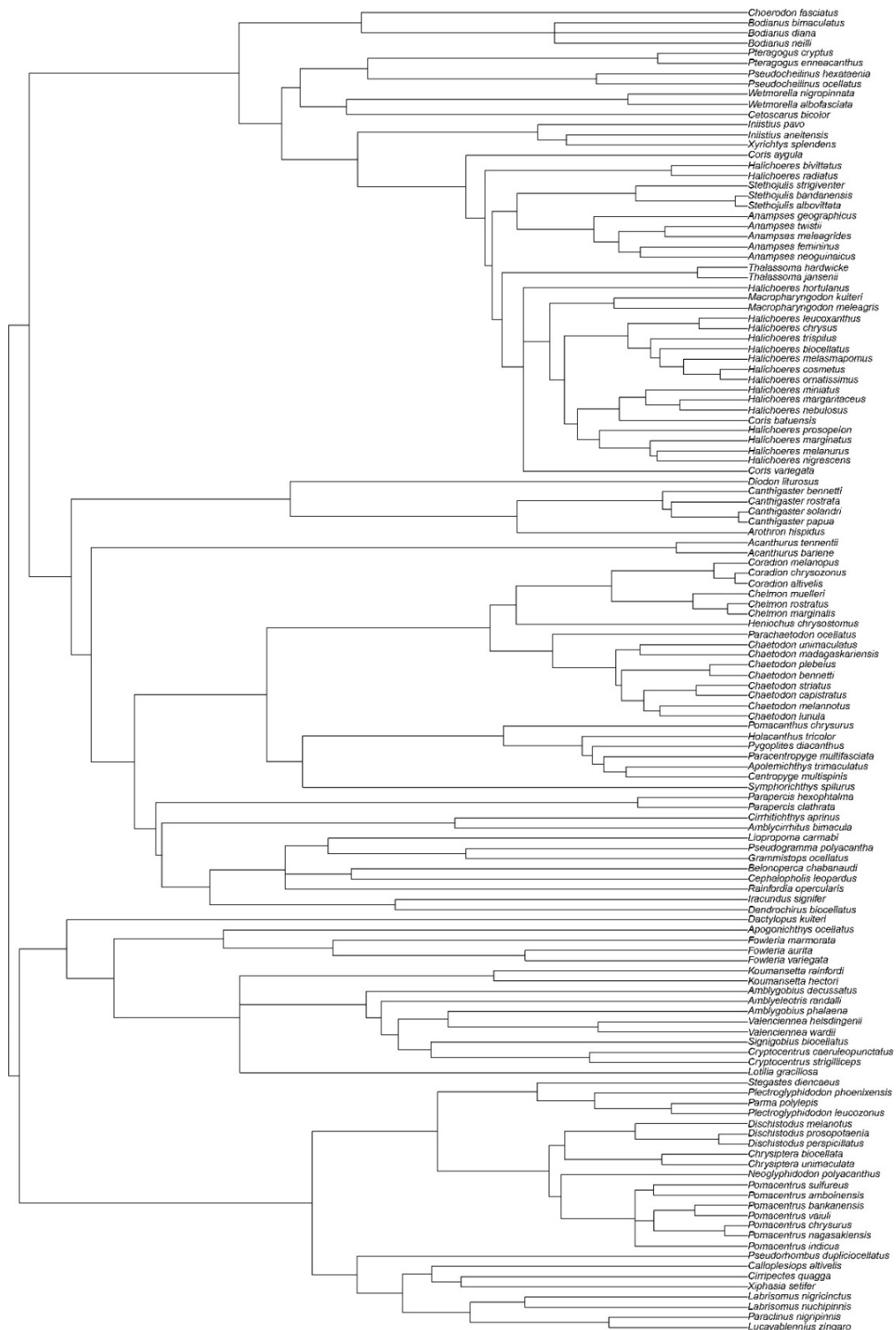


Figure B1. Phylogenetic tree of all species measured herein to account for non-independence in the regression analysis.

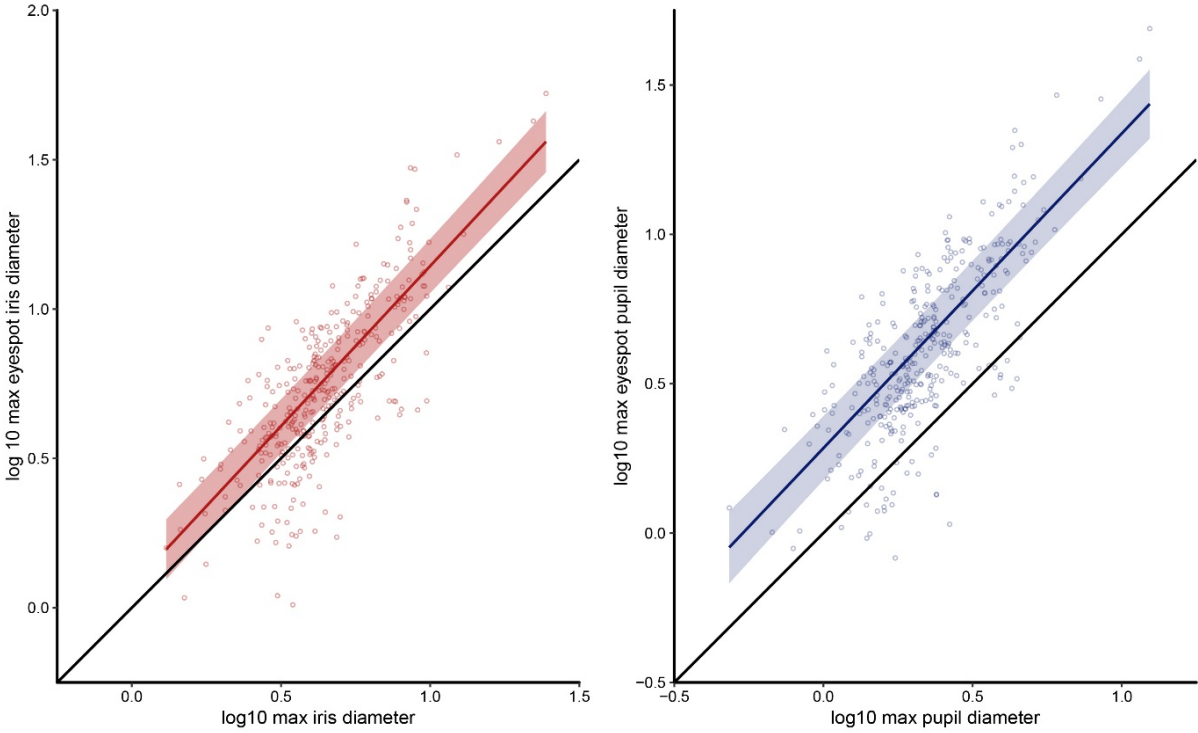


Figure B2. Morphological regressions using linear measurements of eye/eyespot (left) and pupil/eyespot pupil (right) features.

Table B1. Summary statistics from phylogenetic generalised least squares regression analysis of eye/eyespot diameter and pupil/eyespot 'pupil' diameter.

<i>Predictors</i>	<i>Estimate</i>	<i>Confidence Interval</i>	<i>t - value</i>	<i>p - value</i>	<i>R²</i>
Intercept	0.07	-0.03 – 0.18	1.35	0.178	0.57
log ₁₀ (Eye Diameter)	1.07	0.99 – 1.15	26.56	<0.001	
Intercept	0.28	0.18 – 0.39	5.23	<0.001	0.54
log ₁₀ (Pupil Diameter)	1.05	0.96 – 1.14	23.36	<0.001	

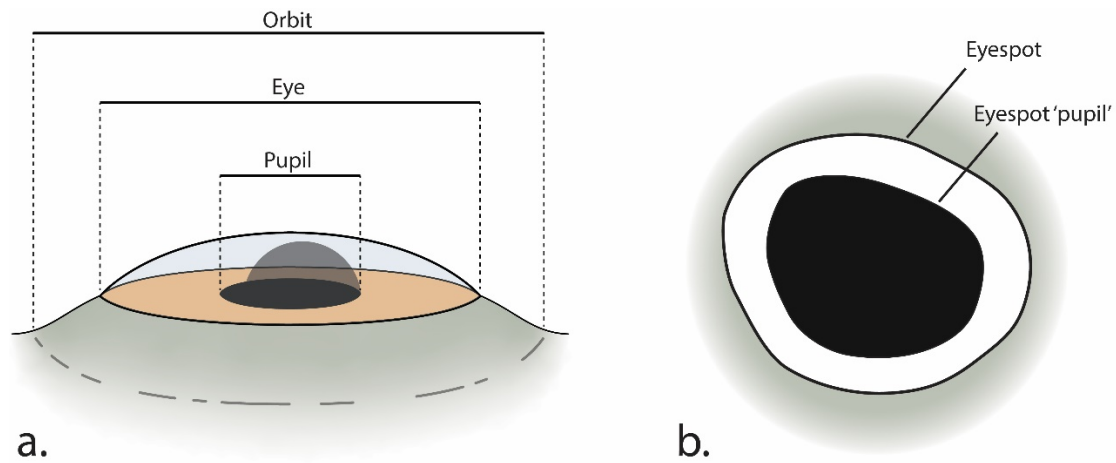


Figure B3. *a) Lateral view of the eye's external components. Herein, 'eye area' is defined to be the approximately flat disc that equivalates the iris in many other vertebrates (the orange disc in this figure). This feature is the outermost portion of the internal bones that form the sclerotic ring. b) The eyespot components. The eyespot's area is the full area of the entire feature whereas the eyespot's 'pupil' area is only that of the dark interior.*

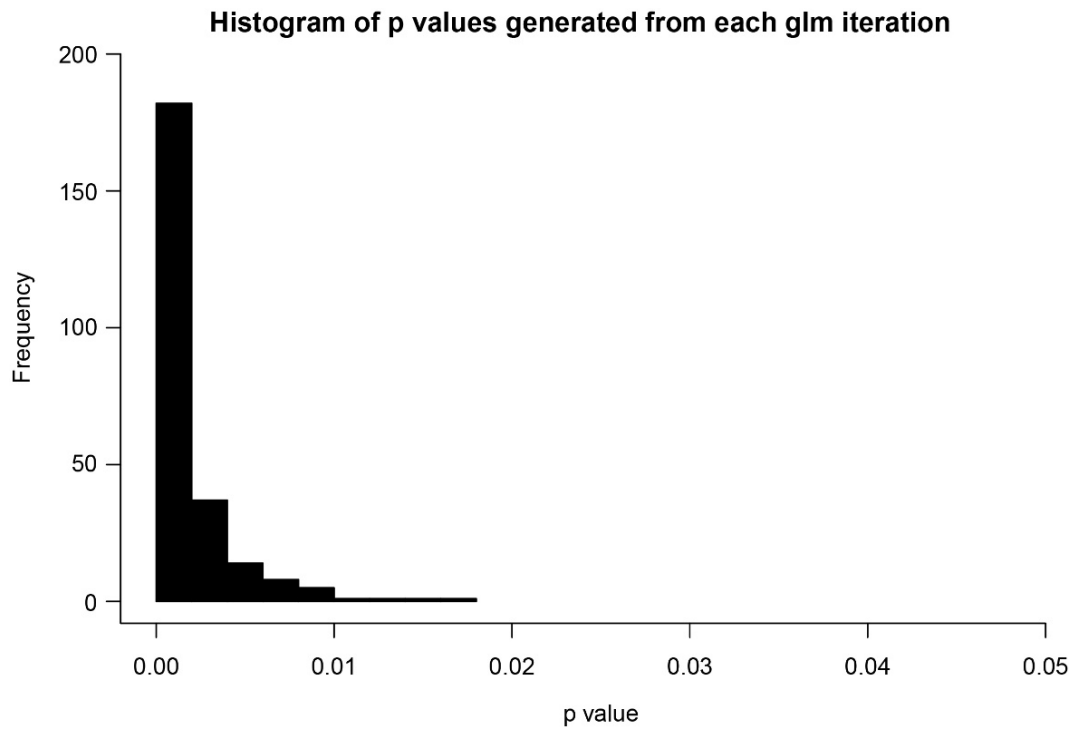


Figure B4. Distribution of p -values from the generalised linear model using a gamma distribution. This analysis was used to test for differences between the size distribution of fishes with and fishes that no longer/are yet to have an eyespot.

Table B2. Summary statistics from phylogenetic generalised least squares regression analysis of eye/eyespot area and pupil/eyespot 'pupil' area.

<i>Predictors</i>	<i>Estimate</i>	<i>Confidence Interval</i>	<i>t - value</i>	<i>p - value</i>	<i>R²</i>
Intercept	0.06	-0.13 – 0.24	0.58	0.565	0.61
log ₁₀ (Eye Area)	1.11	1.03 – 1.18	29.14	<0.001	
Intercept	0.48	0.28 – 0.67	4.70	<0.001	0.55
log ₁₀ (Pupil Area)	1.06	0.97 – 1.14	24.53	<0.001	

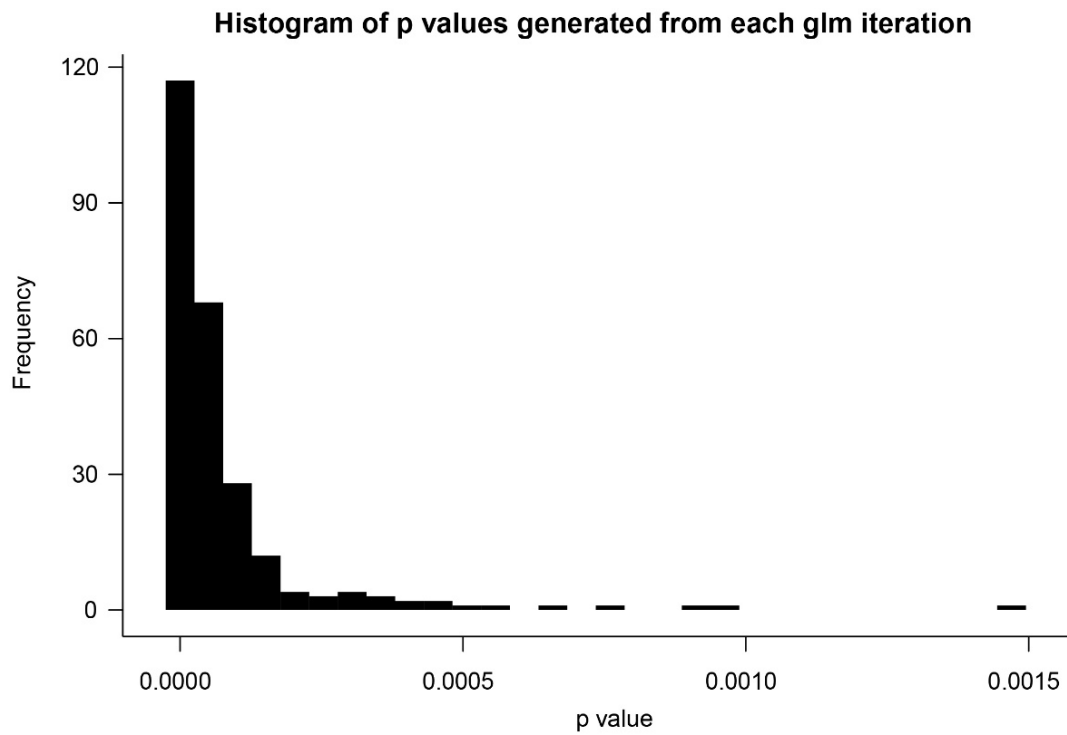


Figure B5. Distribution of p -values from the generalised linear model using a binomial distribution. This analysis was used to test for the relationship between standard length and the probability of having an eyespot. All 250 iterations were significant.

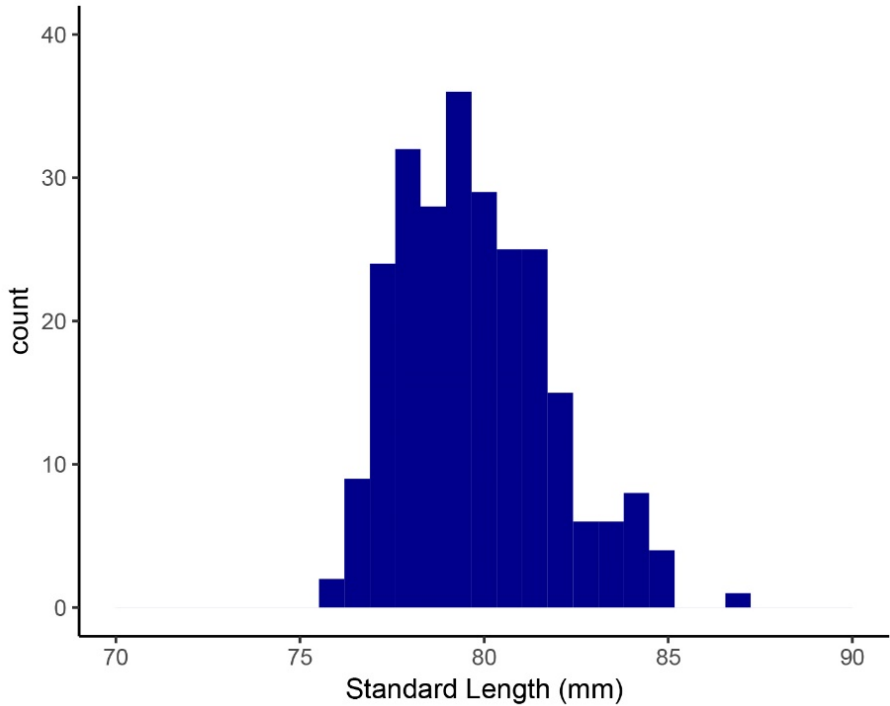


Figure B6. The distribution of 50-50 probability points for each of the 250 iterations of the binomial glm.

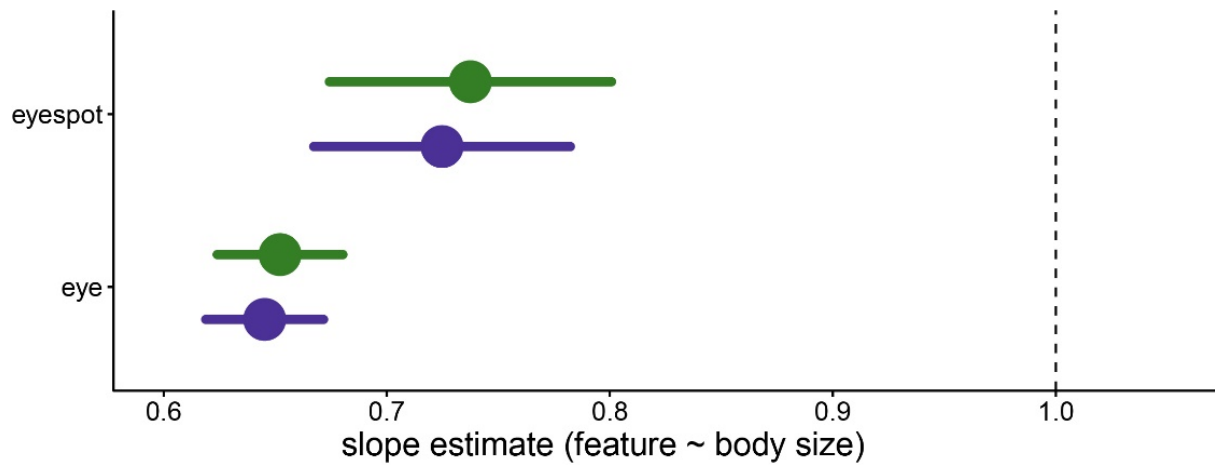


Figure B7. Slope estimates between body size and eye/eyespot size. Both body size and eye/eyespot diameters were \log_{10} transformed to yield these slope estimates. Green indicates the max diameter of the full eye/eyespot; purple indicates the max diameter of the pupil/eyespot pupil. All slope estimates are <1 indicating negative allometry.

Table B3. Summary statistics from phylogenetic generalised least squares regression analysis of eye diameter, eyespot diameter, pupil diameter, and eyespot 'pupil' diameter. The explanatory variable in all models was the standard length (mm).

<i>Response</i>	<i>Estimate</i>	<i>Confidence Interval</i>	<i>t - value</i>	<i>p - value</i>	<i>R²</i>
Intercept	-0.52	-0.59 – -0.45	-15.45	<0.001	0.75
log ₁₀ (Eye diam)	0.65	0.62 – 0.67	48.09	<0.001	
Intercept	-0.55	-0.69 – -0.41	-7.49	<0.001	0.45
log ₁₀ (Eyespot diam)	0.72	0.67 – 0.78	24.79	<0.001	
Intercept	-0.83	-0.90 – -0.76	-22.99	<0.001	0.69
log ₁₀ (Pupil diam)	0.65	0.62 – 0.68	45.54	<0.001	
Intercept	-0.68	-0.84 – -0.53	-8.48	<0.001	0.42
log ₁₀ (Eyespot pupil diam)	0.74	0.67 – 0.80	22.94	<0.001	

Appendix C

Table C1: Colour centre point RGB values and offsets used in colour pattern detection performed by patternize.

Colour	Red	Green	Blue	Offset
Yellow	220	220	20	0.35
Black	0	0	0	0.30
White	255	255	255	0.45

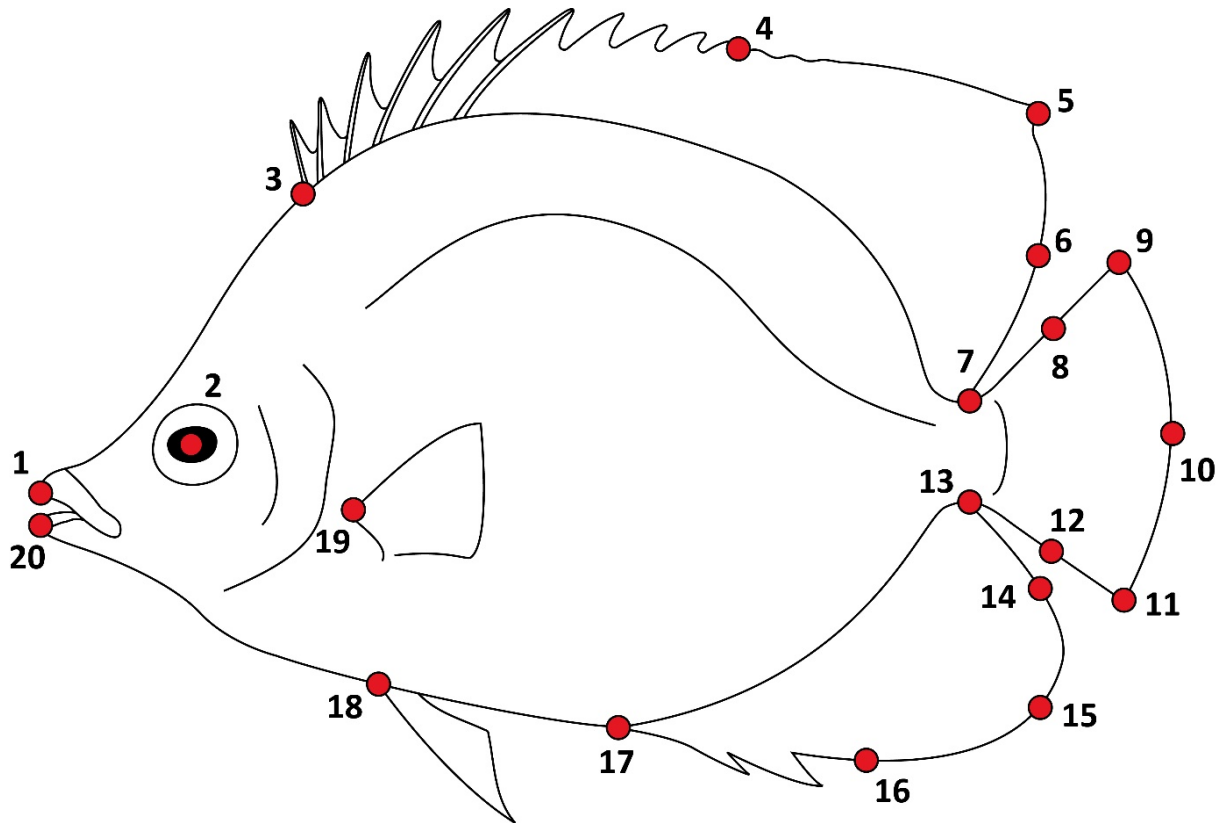


Figure C1: Graphic displaying the location of the 20 morphological landmarks used to align each image. 1) anterior most point of premaxilla, 2) centre of pupil, 3) anterior attachment of the dorsal fin, 4) midpoint between landmarks 3 and 5, 5) point on dorsal fin in which the direction of the fin changes from running primarily horizontal to primarily, 6) midpoint between landmarks 5 and 7, 7) posterior attachment of the dorsal fin, 8) midpoint between landmarks 7 and 9, 9) dorsal tip of the caudal fin, 10) midpoint between landmarks 9 and 11, 11) ventral tip of the caudal fin, 12) midpoint between landmarks 11 and 13, 13) posterior attachment of the anal fin, 14) midpoint between landmarks 13 and 15, 15) point on anal fin in which the direction of the fin changes from running primarily vertical to primarily horizontal, 16) midpoint between landmarks 15 and 17, 17) anterior attachment of anal fin, 18) anterior attachment of pelvic fin, 19) dorsal attachment of pectoral fin, 20) anterior most point of dentary.

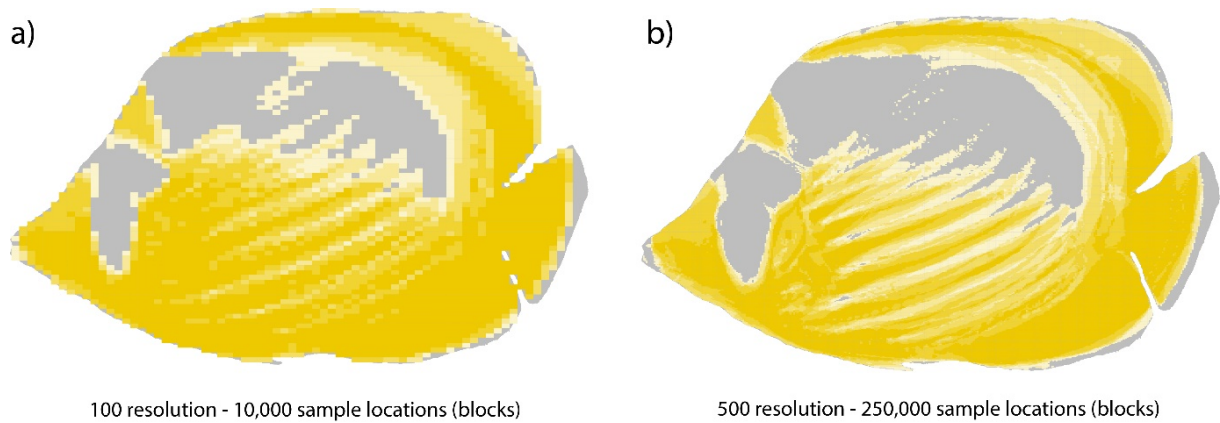


Figure C2: Alternative outputs of *patternize*'s *plotHeat* function showing two analyses of the same five images using different resolutions. Plots represent heatmaps: the darker the yellow the greater the number of images were found to have yellow in that location. a) output using 100 resolution yielding 10,000 sample locations (blocks) that were analysed for the presence of yellow. Note that this resolution is low enough to see the individual blocks. b) same analysis but using 500 resolution which generates 25x the number of sample locations (250,000 blocks). The higher the resolution used, the finer the amount of small-scale pattern captured. Note: resolution ("res") is an argument within the *patternize* functions – the actual resolution of the original images analysed remains unchanged between these two outputs.

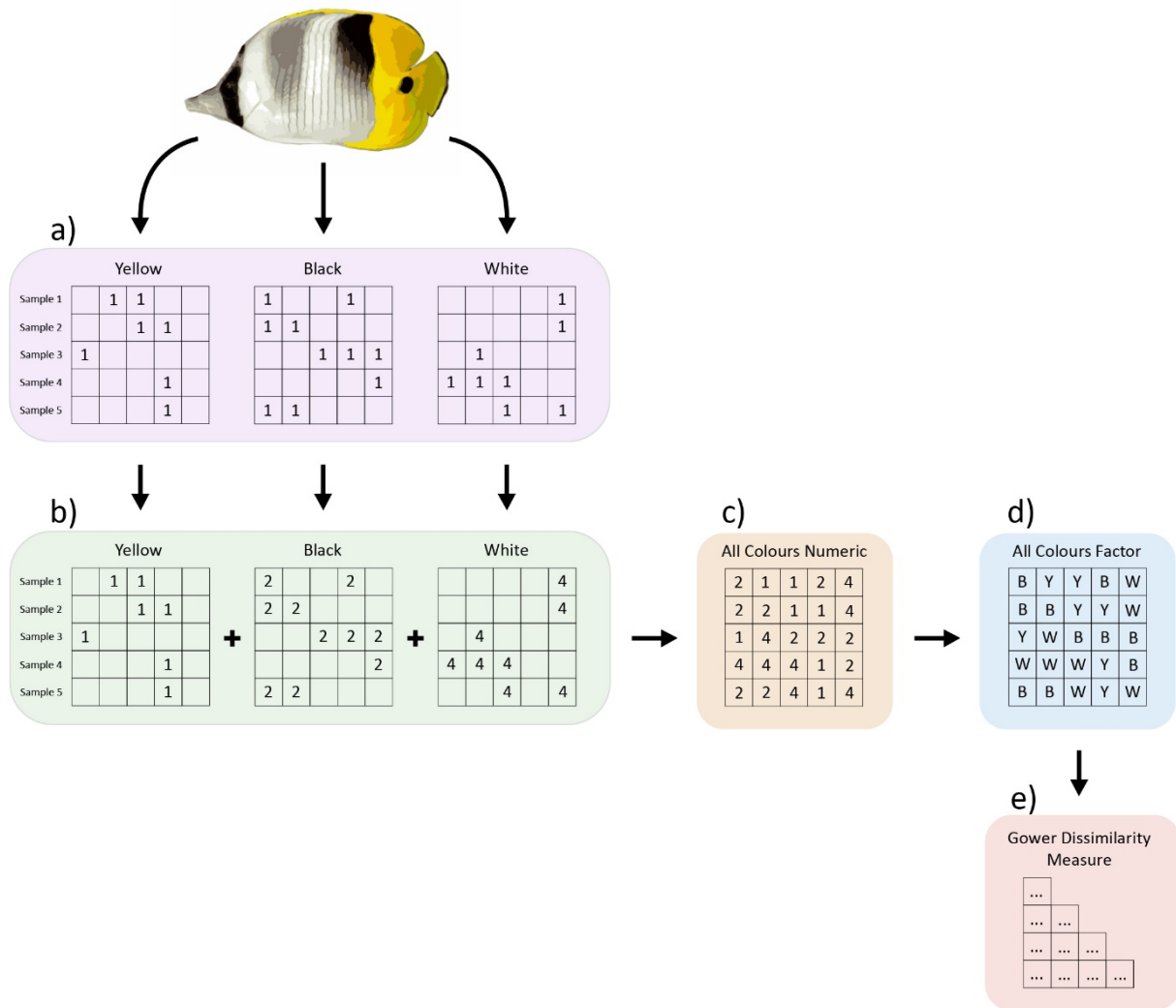


Figure C3: Workflow of numeric individual colour detection to full colour pattern analysis. **a.)** run colour detection for each colour of interest. In our study and for this example, the colours detected are yellow, black and white. patternize’s colour detection protocol works by creating a presence/absence data matrix in which each column (variable) is a block associated to a specific location on the image and the rows (samples) are each image analysed. If the colour analysed is found within the block according the RGB values we tell patternize to detect, the that cell in the data matrix is recorded as a 1 for presence. If it is lacking that colour, as 0. We have left 0’s out for visualization purposes. **b.)** convert each colour to a unique numeric identifier. This follows a binary logic; calculated for each number by the following equation: 2^{n-1} . Each colour represents an integer in the series 0 to n, where n is the total number of individual colours being analysed. In this example, yellow is the first colour of interest, so $2^{1-1} = 1$. Therefore, we code all presences for yellow in the yellow data matrix to “1” (for the first colour, it always remains 1). For black, our second colour of interest, we code to $2^{2-1} = 2$, so we recode all presences in the black data matrix to “2”. White is our third

and final colour of interest, so we recode it to $2^{3-1} = 4$. Now, each data matrix has a unique numeric identifier that represents each colour. **c.)** add together all the colour pattern matrices, yielding a full numeric colour pattern matrix. **d.)** convert our numeric colour pattern matrix into a character colour pattern matrix. This is done by changing all values of our converted series into a character that represents them. In our example, yellow (which is 1) is converted to a "Y". Black, which is 2 in the numeric matrix, is converted to "B". Lastly, white which is 4 in the numeric matrix, is converted to "W". A binary series is used because it provides flexibility with overlapping colour categories. If our colour categories had overlapping values (let's say a specific RGB value fell within two of our colour ranges for two separate colours we are analysing), when we add our matrices together in the previous step c.), we would know exactly which colours created that value. For example, if colour detection was positive for both yellow which is numerically coded as "1", and also white, which is numerically coded as "4", we would know for sure that a 5 in our combined colour matrix meant that the specific colour in that location was categorised as both "yellow" and "white". This logic is useful when analysing many colours that may have overlapping RGB ranges. **e.)** Lastly, we analyse the full, character colour pattern matrix using Gower's dissimilarity measure. The result is a diagonal dissimilarity matrix containing the dissimilarity values between every possible pair of images analysed.

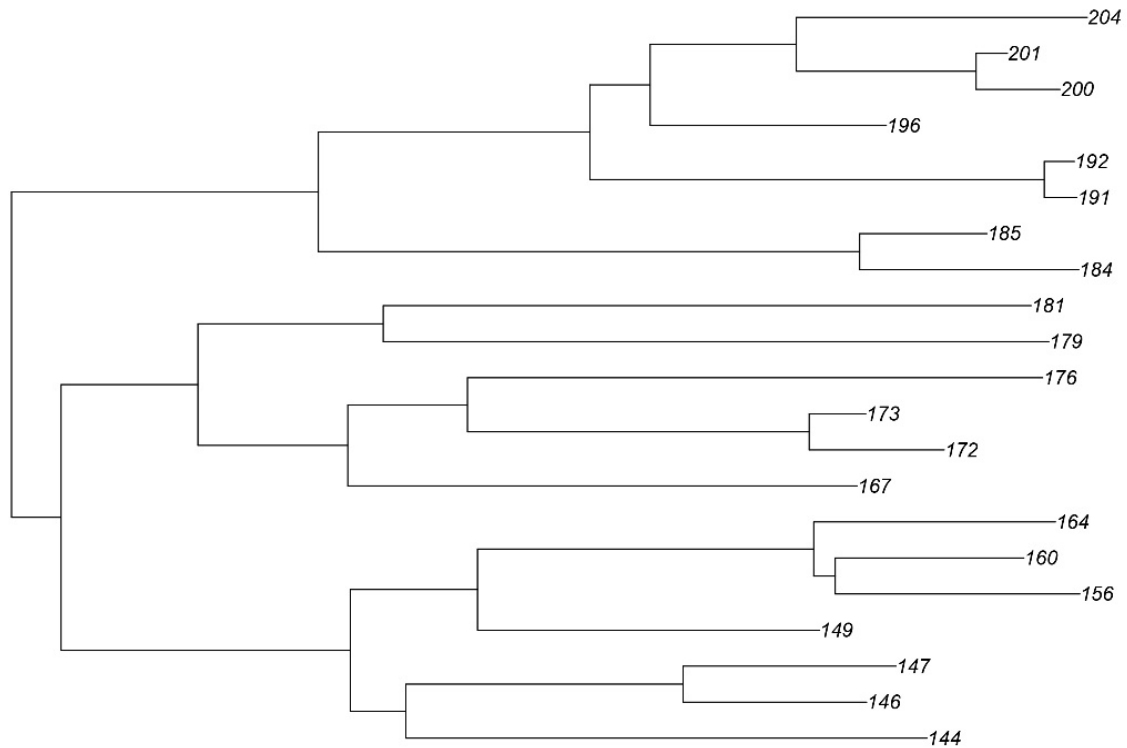


Figure C4: Phylogeny adapted from Cowman and Bellwood (2011) that contains only reciprocally monophyletic species pairs (from species in which molecular data exists). The species-pairs have been collapsed to the nodes that represent the estimated time of divergence for each respective pair. This yields a tree with non-contemporaneous tips (i.e. a non-ultrametric tree). Since the residual variance may differ, we altered the weights of the model (gls) to represent the diagonal of the phylogenetic variance-covariance matrix. The number at each tip are the node numbers from the original phylogeny. Each number represents a species pair; for the pair that each number specifically represents, see the column in raw data called 'pairID'.

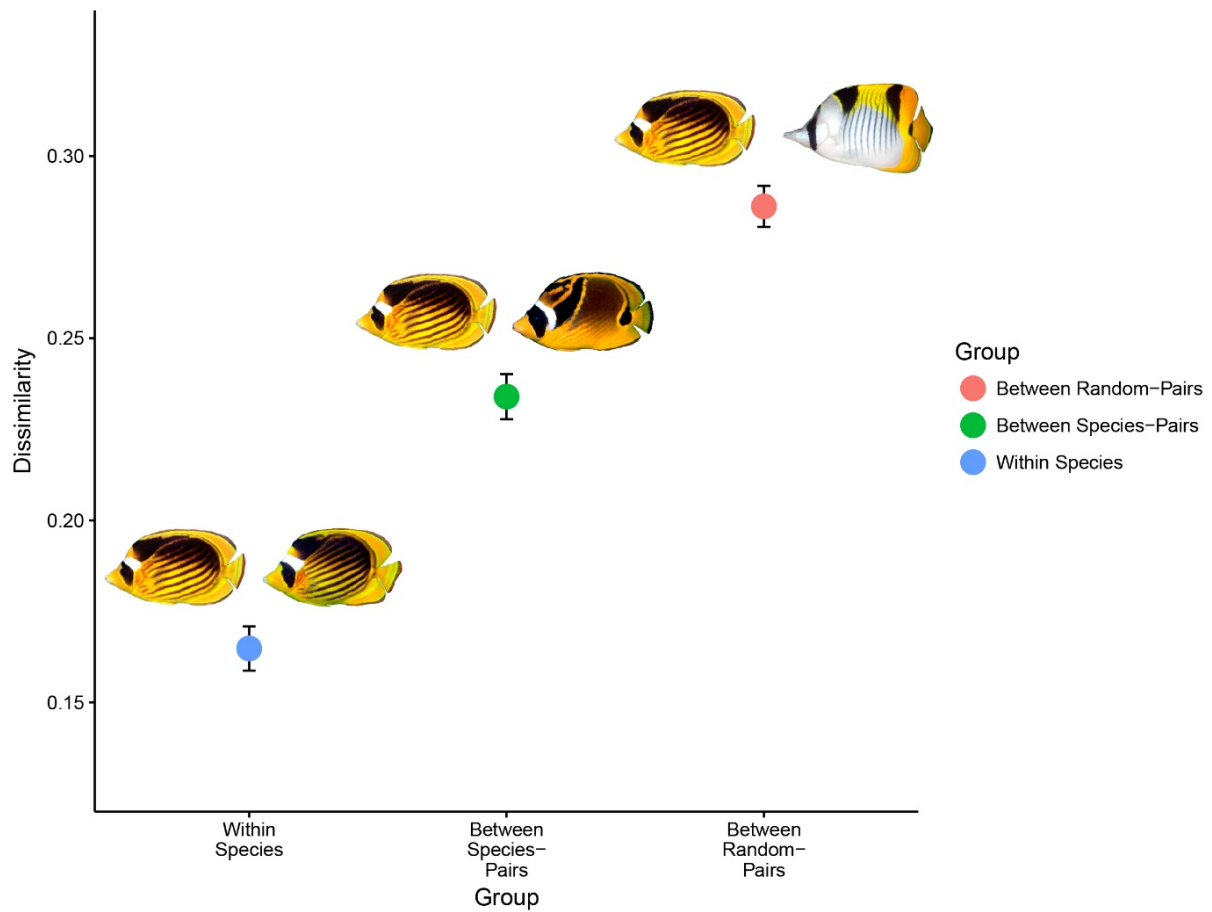


Figure C5: Plot displaying the mean within-species ($n = 420$), between species-pairs ($n = 420$), and between random-pair ($n = 420$) dissimilarity values with 95% confidence intervals. Between-species pairs and random-pair values analysed were randomly sub-sampled to allow for an even comparison with ANOVA and Tukey's HSD post hoc test.

Table C2: Mean and 95% confidence intervals for within-species, between species-pairs and random-pair dissimilarity values. Asterisks denote significant differences from pairwise Tukey's HSD post-hoc test. All groups were significantly different from each other group. A subset of random pair values were randomly sampled from all possible random pair values to allow for a balanced statistical comparison.

Group	Mean	Lower 95% CI	Upper 95% CI	Significance
Within Species	0.1648	0.1587	0.1709	***
Between Species Pairs	0.2340	0.2278	0.2401	***
Random Pairs	0.2862	0.2806	0.2918	***

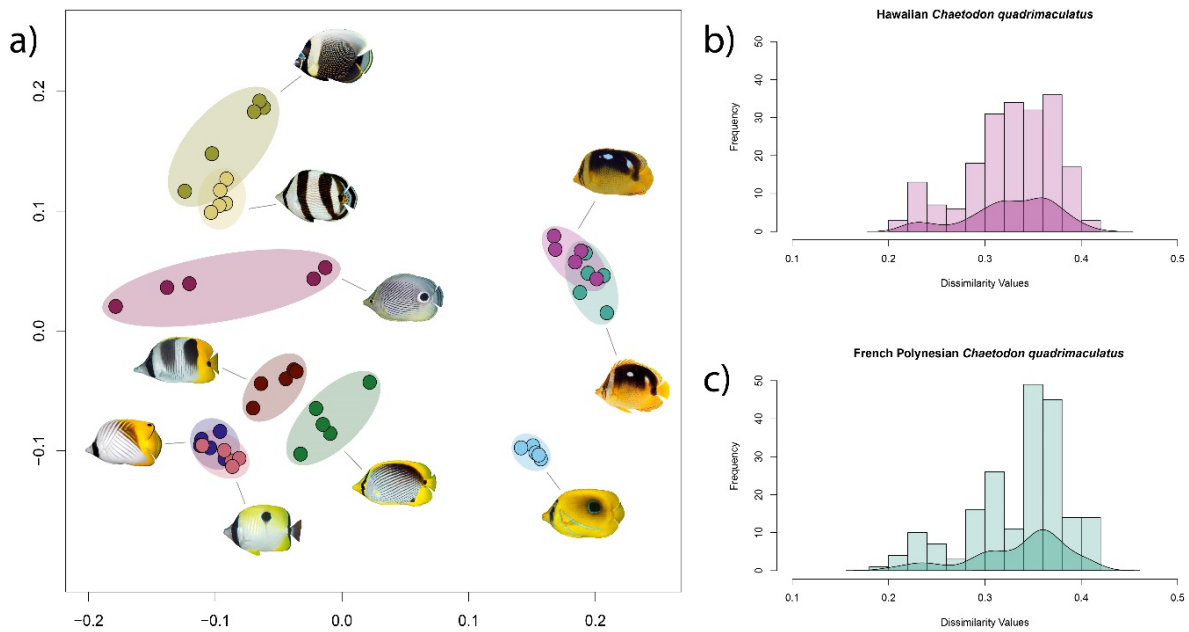


Figure C6: Comparison of colour patterns between sample species, one of which (*Chaetodon quadrimaculatus*) possesses images two different geographic provinces. a) PCoA of colour patterns of nine sample species with five images per species except for *Chaetodon quadrimaculatus* which had five from French Polynesia (turquoise) and five from Hawaii (purple). Clear congruence is observed when using images from either location. Histogram and density estimates of dissimilarity values to all other species for b) Hawaiian individuals and c) French Polynesian individuals. To ensure that these sets of images from different locations had no effect on colour pattern dissimilarity calculations, we compared images of *C. quadrimaculatus* from both locations to 8 other test species. These 200 pairwise comparisons (5 images of *C. quadrimaculatus* x 5 images of each 8 other species = 200 total) were compared using a Welch's two sample *t*-test. There was no significant difference between the mean colour pattern dissimilarity of fishes from French Polynesia or Hawaii when compared to the other fishes. This shows there is no geographic variation in butterflyfish colour patterns.

Table C3: Test statistics of a Welch's Two Sample *t*-test comparing colour pattern dissimilarity from French Polynesia or Hawaii to all other samples.

	Df	t value	p - value
FPoly ~ Hawaii	395.45	1.8809	0.0607

Table C4: Model selection diagnostics. Models are ranked in descending order from best to worst based on AICc weights. All variables were mean-centred.

Model Variables	K	AICc	Delta AICc	AICc Weight	Cumulative Weight	Log Likelihood
Overlap * Symmetry	6	-80.41	0.00	0.76	0.76	49.20
ToD * Overlap	6	-78.05	2.36	0.23	1.00	48.02
ToD * Symmetry	6	-68.14	12.26	0.00	1.00	43.07
ToD	4	-61.27	19.14	0.00	1.00	35.89
Overlap * ToD * Symmetry	10	-59.58	20.83	0.00	1.00	50.79
Overlap	4	-59.05	21.36	0.00	1.00	34.77
Symmetry	4	-59.02	21.39	0.00	1.00	34.76

Table C5: Test statistics for phylogenetic generalized least squares of time of divergence on species-pair colour pattern dissimilarity.

	Value	Standard Error	t - value	p - value
Intercept	0.2421	0.0325	7.4472	< 0.0001
Time of Divergence	0.0143	0.0091	1.5608	0.1351

Table C6: Test statistics for phylogenetic generalized least squares of geographic range aspects on species-pair colour pattern dissimilarity.

	Value	Standard Error	t - value	p - value
Intercept	0.2275	0.0297	7.6486	< 0.0001
% Overlap	0.0001	0.0002	0.3909	0.7007
Symmetry	0.0460	0.0548	0.78390	0.4131
% Overlap : Symmetry	0.0038	0.0014	2.7783	0.0129

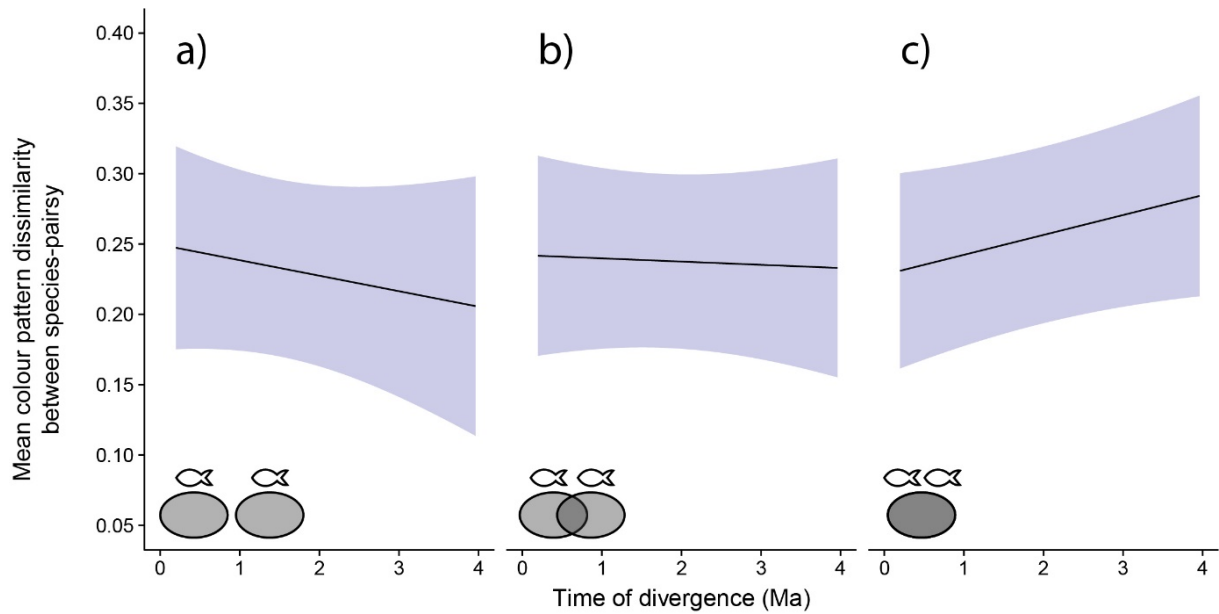


Figure C7: Phylogenetic generalised least squares regressions of time of divergence and range overlap (a – c). This model was the only other model that received support, however it was substantially worse than the best fit model. The x-axis represents increasingly greater time since the hypothesized divergence of each species-pair. We see a mirrored relationship as to the one observed when comparing range overlap and range symmetry in the main text. a – c) reversal of colour pattern dissimilarity related to varying levels of range overlap. a) 0% range overlap between species-pairs, b) mean overlap % = 34.66, c) 100% range overlap. When species have a high amount of range overlap which would equate to high levels of interaction, we see the colour pattern dissimilarity increasing through time. Essentially, the older a species pair gets, the more different looking the two species become. The negative relationship displayed in a) is likely a product of high range asymmetry, which is not captured in this model. Test statistics for the phylogenetic regression are given in the following **Table C6**.

Table C7: Test statistics for phylogenetic generalized least squares of range overlap and time of divergence on species-pair colour pattern dissimilarity (**Figure C7**). Both variables were mean-centred.

	Value	Standard Error	t - value	p - value
Intercept	0.2384	0.0291	8.2035	< 0.0001
Time of Divergence	-0.0023	0.0103	-0.2234	0.8259
Overlap %	0.0002	0.0001	1.7193	0.1037
ToD : Overlap %	0.0003	0.0001	2.4706	0.0244

Appendix D

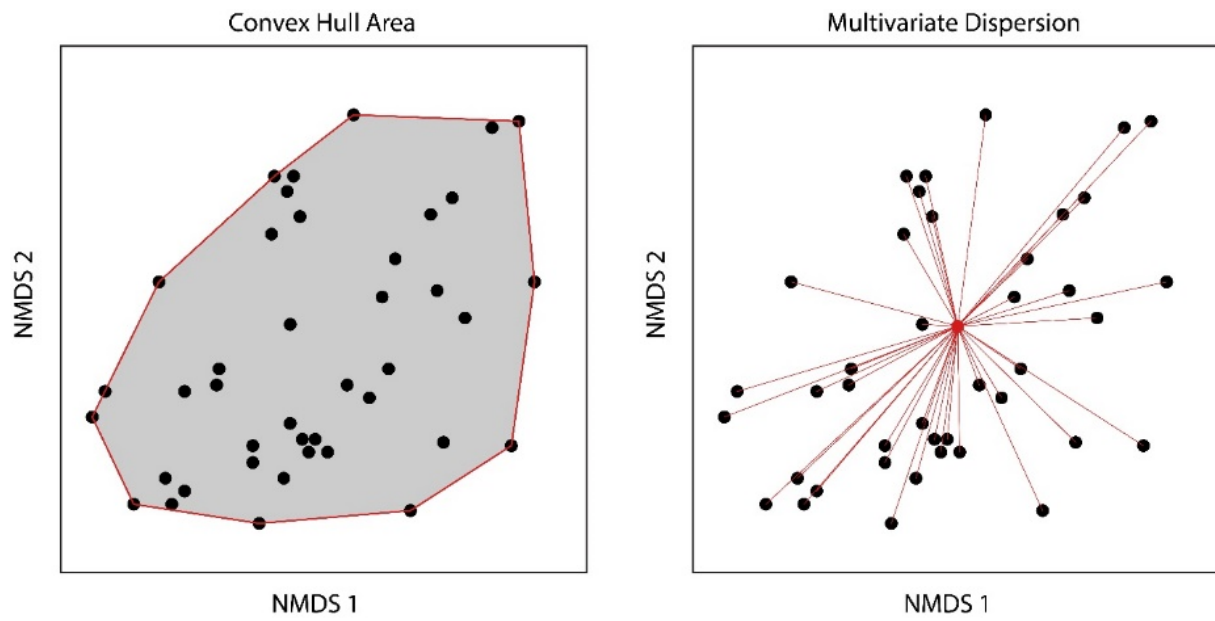


Figure D1. The difference between convex hull area (left) and multivariate dispersion (right). The convex hull is the area created by the smallest possible polygon that encompasses all points. Multivariate dispersion is the average distance from all points to their geometric median (the red dot).

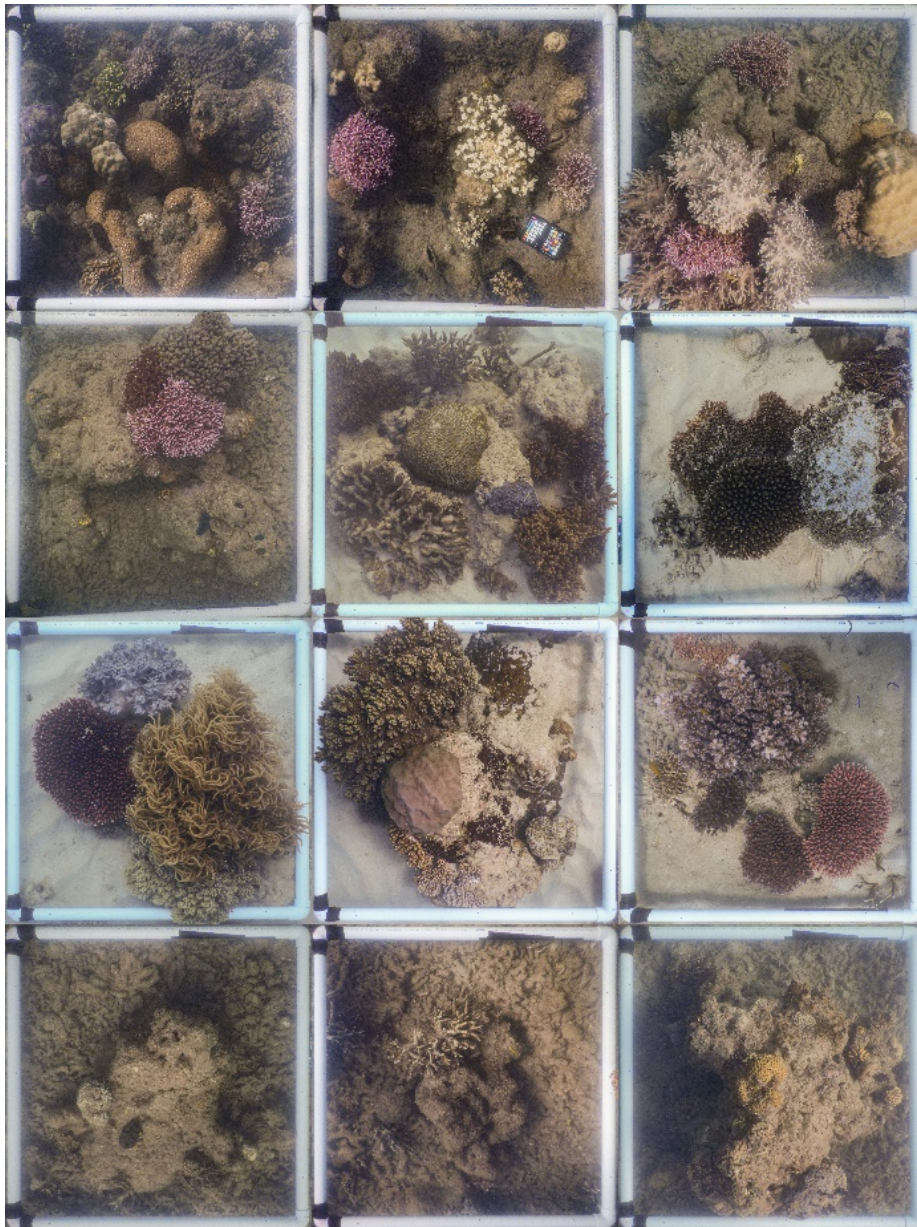


Figure D2. Photographs of the 12 quadrats sampled herein. As displayed, a wide diversity of substrate configurations were surveyed.

Table D1. Model parameters from PERMANOVA tests using different dissimilarity indices. Regardless of the indices chosen, the results are identical.

<i>Terms</i>	<i>Dissimilarity measure</i>	<i>Permutations</i>	<i>d.f.</i>	<i>F model</i>	<i>p - value</i>	<i>R²</i>
Sampling site	Euclidean	10,000	2	6.2021	0.0011	0.58
Residuals	-	-	9	-	-	0.42
Sampling site	Bray-Curtis	10,000	2	6.5730	<0.0001	0.59
Residuals	-	-	9	-	-	0.41
Sampling site	Gower	10,000	2	5.6217	0.0011	0.56
Residuals	-	-	9	-	-	0.44



Figure D3. The typical procedure for sampling a fish community using an enclosed clove oil station. C.R.H. is applying diluted clove oil solution which can be seen as the white haze filtering out of the upper section of the net. The floats help keep the net suspended in an upright position. Following a soak time of approximately 5 minutes, both divers then systematically survey portions of the quadrat to collect any fishes that have been euthanized by the clove oil.

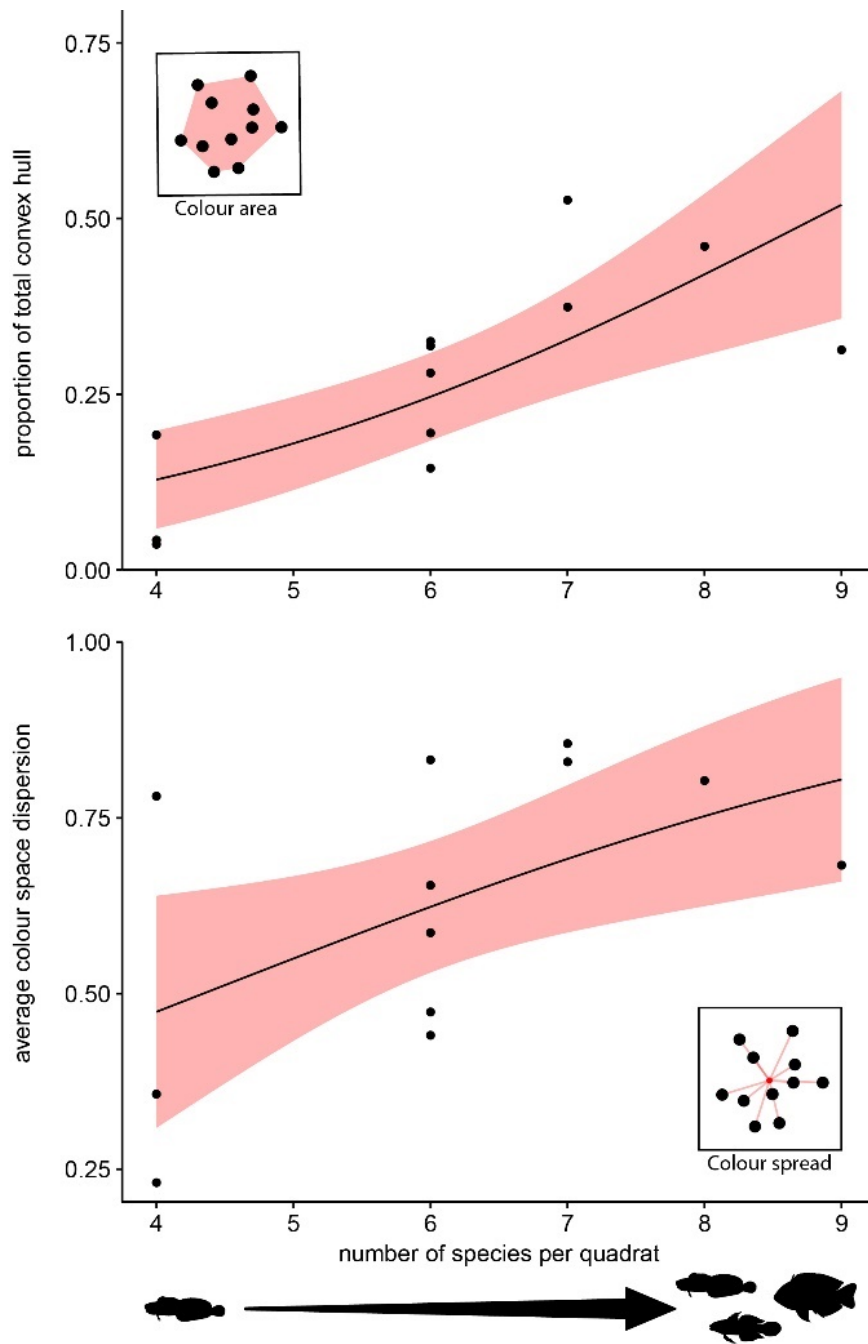


Figure D4. Beta regressions of species richness relating to colour area (above) and colour spread (below).

Both are significantly related to species richness.

Table D2. Model parameters from the abundance and richness beta regressions.

<i>Predictor</i>	<i>Response</i>	<i>Estimate</i>	<i>Confidence Interval</i>	<i>z - value</i>	<i>p - value</i>	<i>pseudo R²</i>
Abundance	Colour-area	0.0527	-0.05 – 0.16	1.01	0.315	0.07
Richness	Colour-area	0.3998	0.18 – 0.62	3.57	< 0.001	0.58
Abundance	Colour-spread	0.0274	-0.08 – 0.13	0.50	0.617	0.02
Richness	Colour-spread	0.3040	0.03 – 0.58	2.19	0.029	0.28

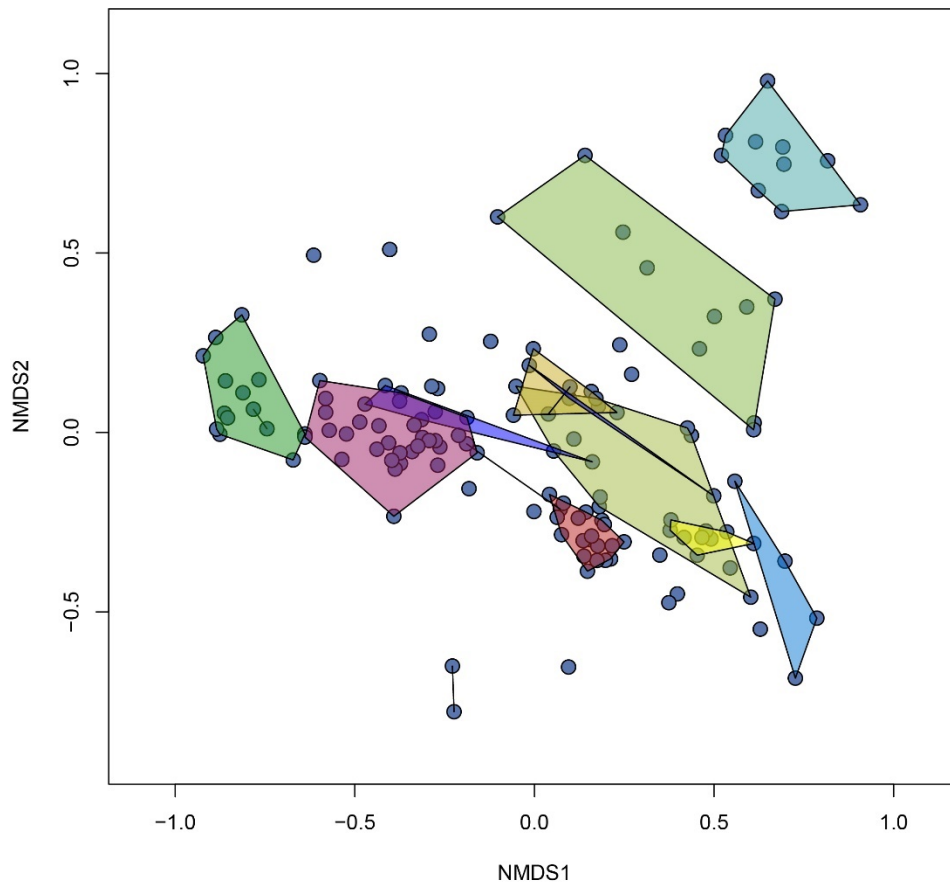


Figure D5. Convex hulls for all species surveyed herein. Points connected by a line are species with only 2 individuals collected. Lone points are species in which only 1 individual was collected.

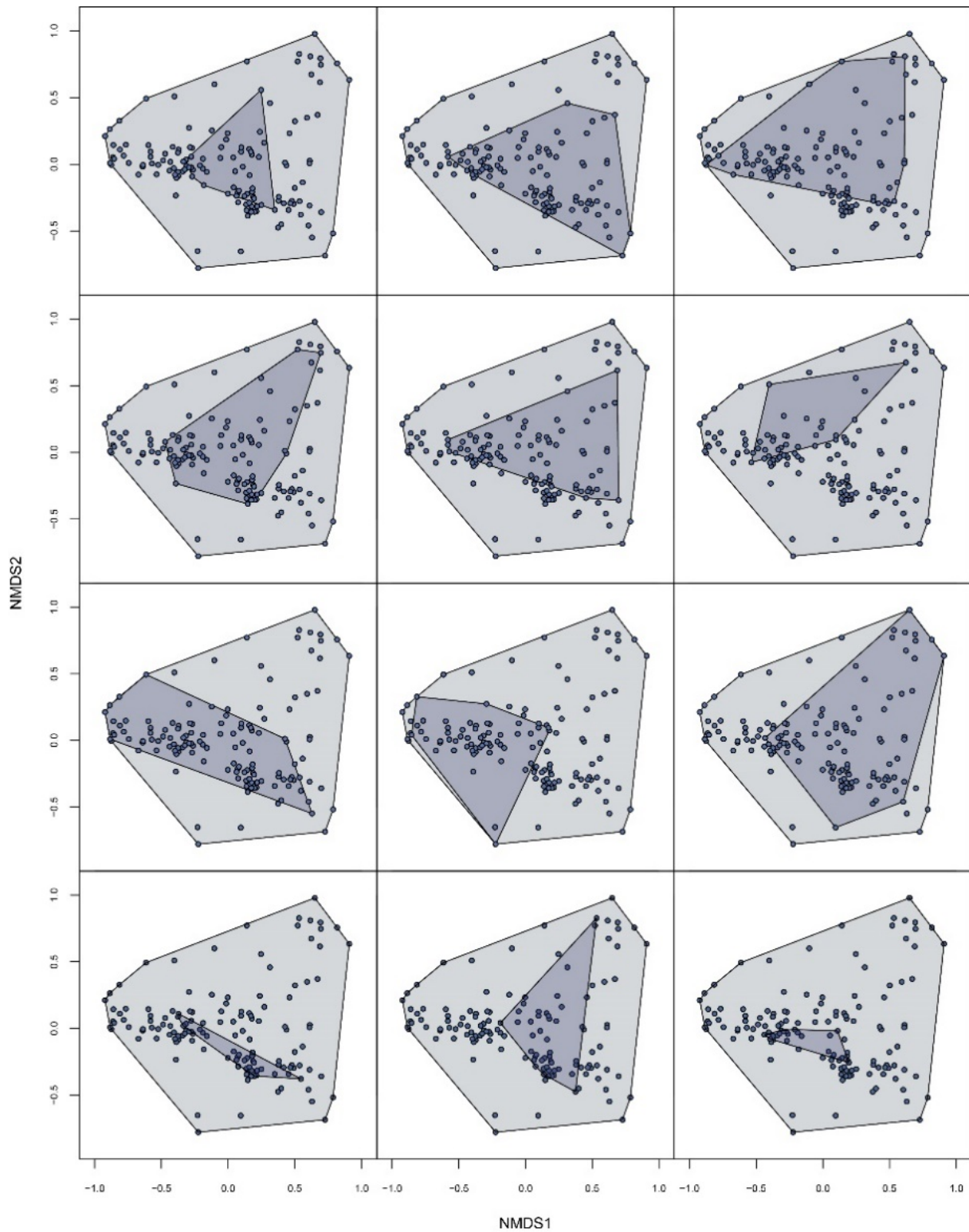


Figure D6. Colour areas (convex hulls) for each quadrat's fish community. As a guide, the full colour area has been highlighted for all fishes sampled. Each plot corresponds to the quadrat in the same position as displayed in **Figure D2**.

Temporal assemblage colouration reconstruction

Since the number of individuals per species varied from year to year in the long-term sampling dataset, we needed to create a procedure that could simulate new individuals within our pre-constructed colourspace. While a basic approach would be to simply use the centroid of each convex hull created by each species to describe what the ‘average’ colouration is for a species, by doing this we lose variation that is clearly present in the colouration between individuals. We therefore created a procedure that would simulate individuals within a pre-established colourspace. This gives us more representative colour-areas per year that reflect differences in the colourations of individuals of the same species.

To aid understanding this process, the figure below has been made to help interpretation. First, we needed to define the colouration of each species in colourspace. To do this, we utilised the photographs of fishes that were collected herein. The colourspace MDS displayed in **Figure 6.2** was used as our ‘key’ (**Figure D7a** in the example). We generated the convex hull for each species in our dataset that contained ≥ 3 individuals per species (since a minimum of three points are needed to create a polygon; **Figure D7b**). The convex hull for a given species represent the most ‘extreme’ or ‘unique’ colourations for that species. Therefore, we can assume the area within the convex hull, or the polygon created by the convex hull, represents a conservative estimate of possible colourations for that species (**Figure D7c**). Although it is distinctly possible that new individuals make occupy locations outside of our defined polygon, we cannot know how far outside the polygon they may be. Thus, we rely only on the distinct possibilities defined from our data.

Points were then generated for each species within their respective polygons according to the number present in the long-term monitoring dataset (**Figure D7d**). For example, if 13 *Eviota zebrina* were collected in 2008, 13 points were generated with random coordinates that fall within the convex hull for that species. This procedure was used to reconstruct the colour-area for each year (**Figure D7e & D7f**). Some species only had two or one individual present within the colourspace key. If two individuals were present, one of the two coordinates were randomly selected with equal. If a species only had one individual, the coordinates for this point were generated as many times as there were individuals.

Since this procedure is simulating the hypothetical appearance of individuals, there is inherent variation in the size of the colour-area per year since the colour-area is directly a product of where the points

fall in colour-space. Although most species colourations are often quite similar and have small convex hulls, they can lead to differences in colour-area depending on exact location of where a simulated individual is placed. Therefore, we ran the simulation procedure five times for every year to capture the inherent variability of individual colouration. These five different estimates are represented in **Figure 5.3a** as the lines extending from the point (which is the mean) for each year. Almost all years had relatively little variation in the different simulated colour-areas leading us to conclude that this procedure is effective and accurate.

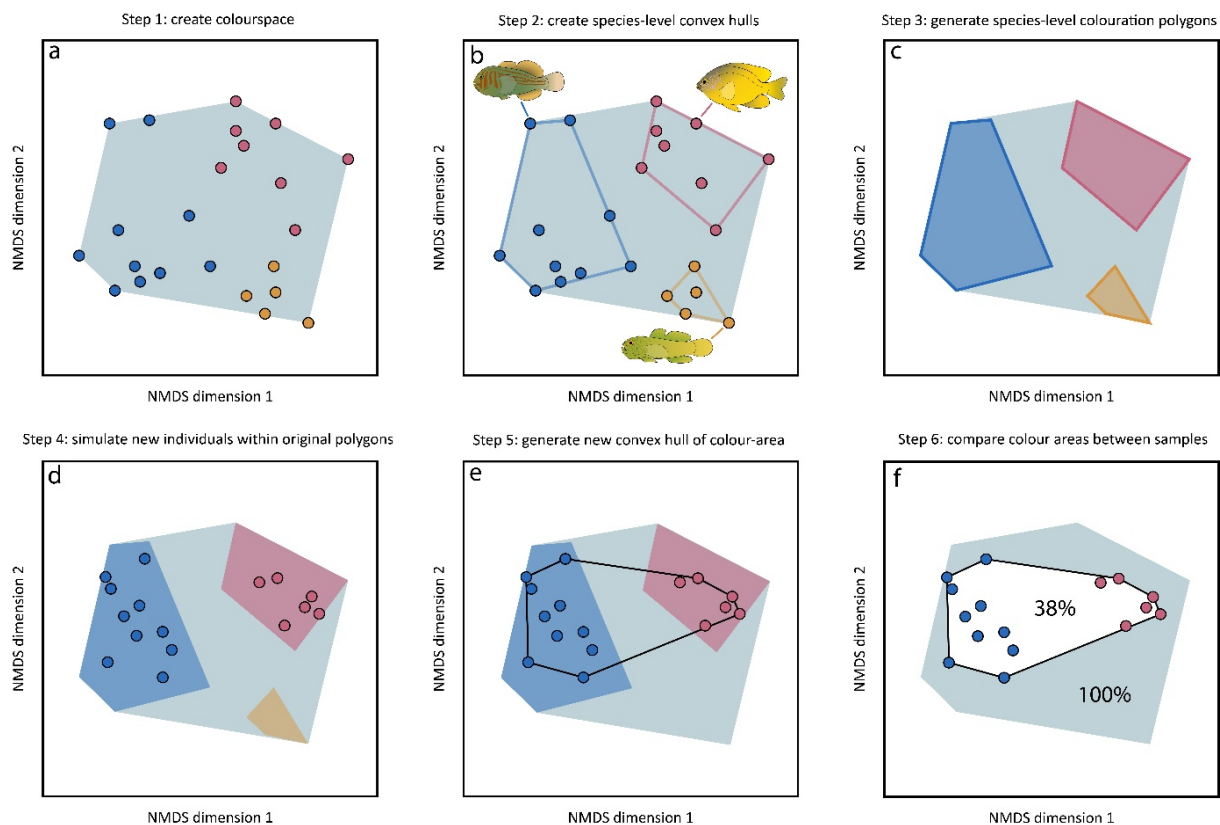


Figure D7. How to simulate new individuals within a pre-made colour-space.

Colour-spread between quadrats

The spread of the least colourful quadrat (station 12, 0.23) was close to 1/4th the spread of the most colourful quadrat (station 9, 0.86). The average colour spread (distance to the median) was 0.63 ± 0.06 .

Table D3. Model comparison for colour-area (convex hull).

<i>Predictor</i>	<i>K</i>	<i>AICc</i>	$\Delta AICc$	<i>AICc weight</i>	<i>Cum. weight</i>	<i>Log Lik.</i>
Complex corals	3	31.83	0.00	0.50	0.50	-11.42
Matrix & Rubble	3	32.67	0.83	0.33	0.84	-11.83
Live coral	3	35.54	3.70	0.08	0.91	-13.27
Sand	3	36.02	4.19	0.06	0.98	-13.51
Rubble	3	40.12	8.29	0.01	0.98	-15.56
Branching corals	3	40.35	8.51	0.01	0.99	-15.67
Turf covered matrix	3	42.09	10.26	0.00	0.99	-16.55
Hard corals	3	42.24	10.41	0.00	1.00	-16.62
Soft corals	3	43.00	11.17	0.00	1.00	-17.00
Massive corals	3	45.71	13.87	0.00	1.00	-18.35

Table D4. Model comparison for colour-spread (multivariate dispersion).

<i>Predictor</i>	<i>K</i>	<i>AICc</i>	Δ <i>AICc</i>	<i>AICc</i> <i>weight</i>	<i>Cum.</i> <i>weight</i>	<i>Log Lik.</i>
Matrix & Rubble	3	37.37	0.00	0.22	0.22	-14.19
Complex corals	3	37.50	0.12	0.21	0.43	-14.25
Branching corals	3	37.84	0.47	0.18	0.61	-14.42
Sand	3	37.98	0.61	0.17	0.78	-14.49
Live corals	3	39.55	2.18	0.08	0.85	-15.28
Rubble	3	39.61	2.23	0.07	0.93	-15.30
Hard Corals	3	40.24	2.87	0.05	0.98	-15.62
Turf covered matrix	3	43.84	6.46	0.01	0.99	-17.42
Soft corals	3	44.48	7.11	0.01	0.99	-17.74
Massive corals	3	44.93	7.56	0.01	1.00	-17.97

Table D5. Model parameters from the top two most parsimonious models for colour-area and spread.

<i>Predictor</i>	<i>Response</i>	<i>Estimate</i>	<i>Confidence Interval</i>	<i>t - value</i>	<i>p - value</i>	<i>adj. R²</i>
Complex corals	Colour-area	4.6774	2.50 – 6.86	4.780	<0.001	0.67
Matrix & Rubble	Colour-area	-2.7858	-4.15 – -1.42	-4.545	0.001	0.64
Complex corals	Colour-spread	3.7686	1.01 – 6.53	3.042	0.012	0.43
Matrix & Rubble	Colour-spread	-2.2933	-3.96 – -0.63	-3.075	0.012	0.43

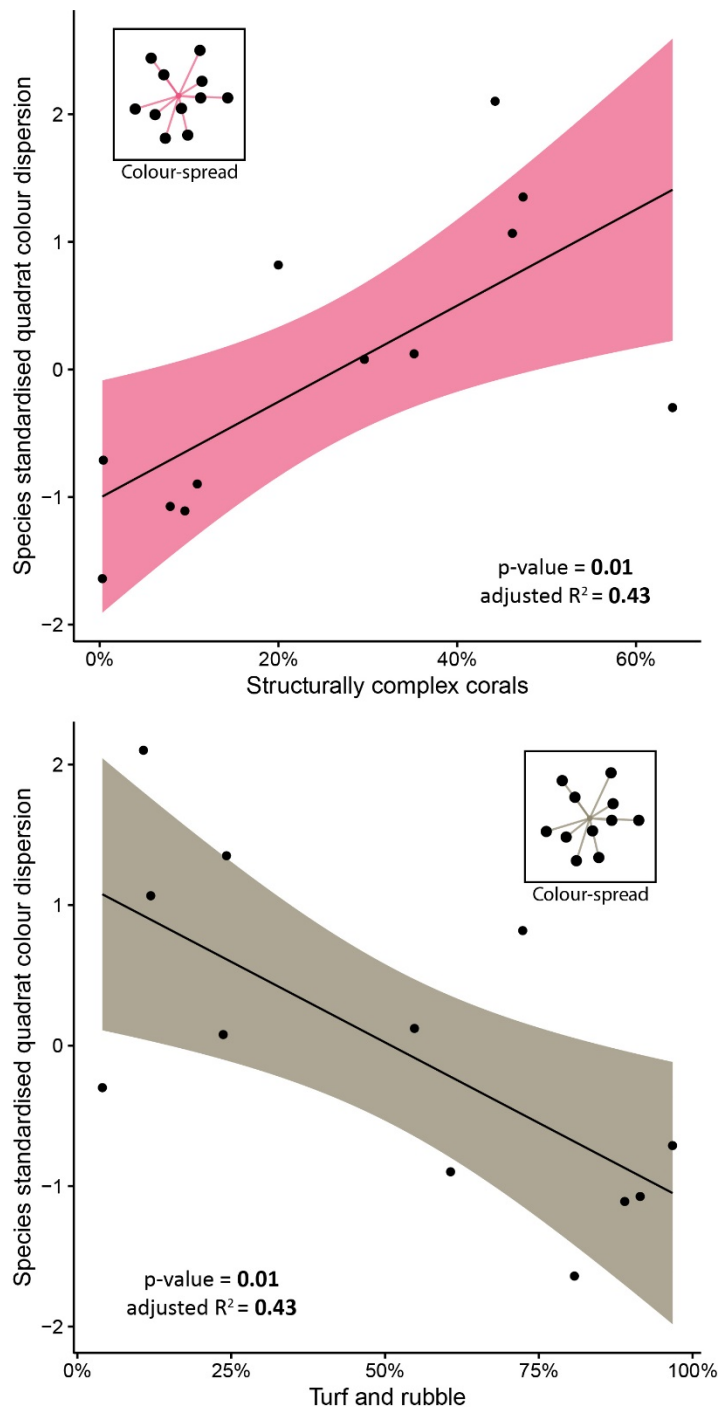


Figure D8. The linear regression \pm 95% confidence intervals display the relationship between colour-spread and the cover of structurally complex corals (top) and turf and rubble (bottom) per quadrat.

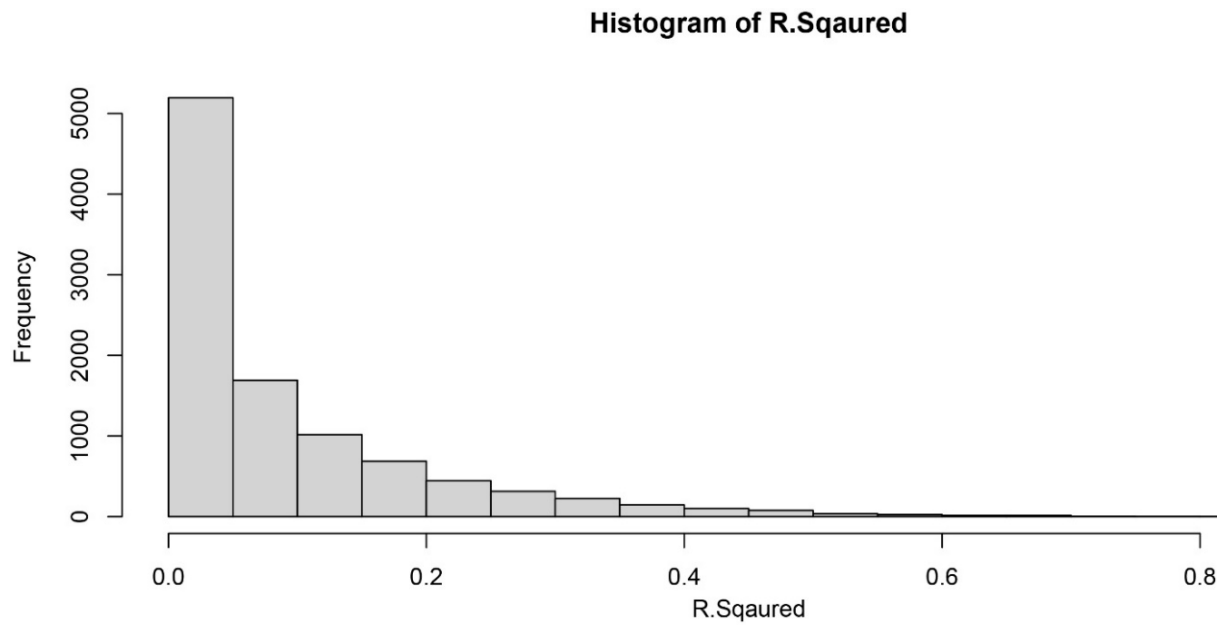


Figure D9. The distribution of R^2 values from 10,000 random linear regression permutations. In each permutation, a random y -value (colour area) was selected within our observed range of y -values and regressed against the known x -value (complex coral cover per quadrat). Our studied yielded an R^2 value of 0.67. The chance of observing a similar relationship with identical strength ($R^2 > 0.65$) by chance is 0.0026, or approximately 1 in 386. Our results are therefore highly improbable if only due to chance.

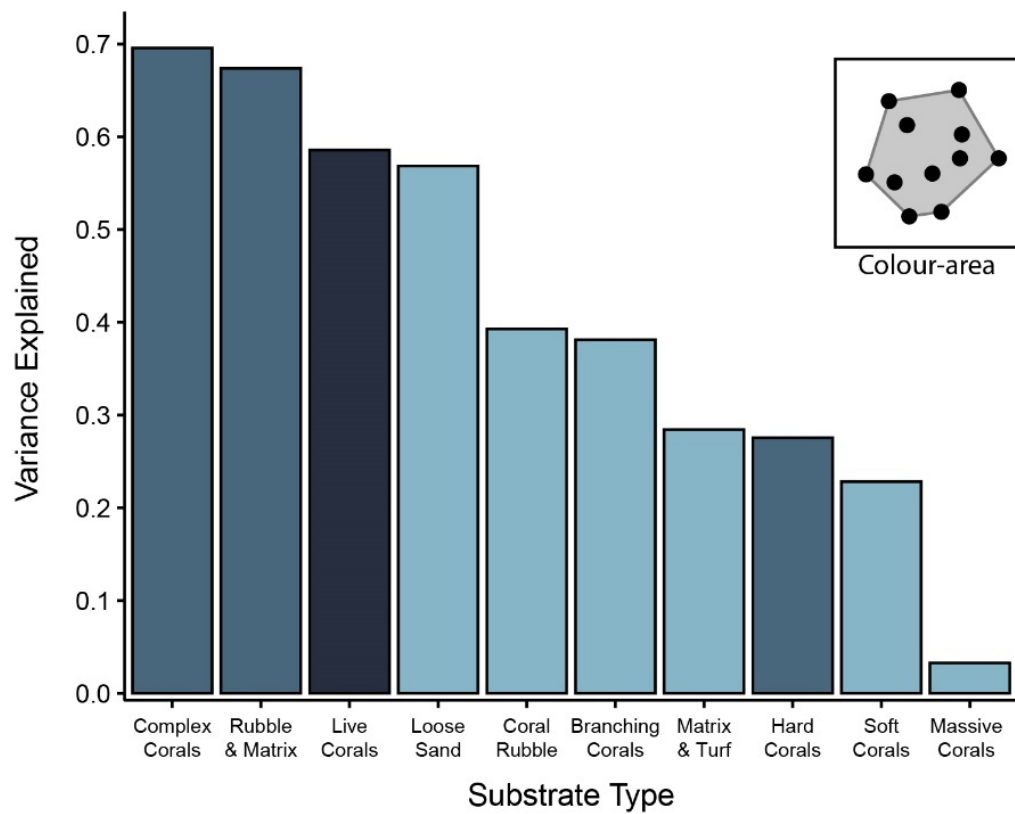


Figure D10. The variance in colour-area explained (R^2 values) by each substratum type. Single substratum variables are coloured in light blue, combinations of two variables (e.g. rubble & matrix) are displayed in middle-tone blue, and combinations of three variables (i.e. all live corals) are displayed in dark blue.

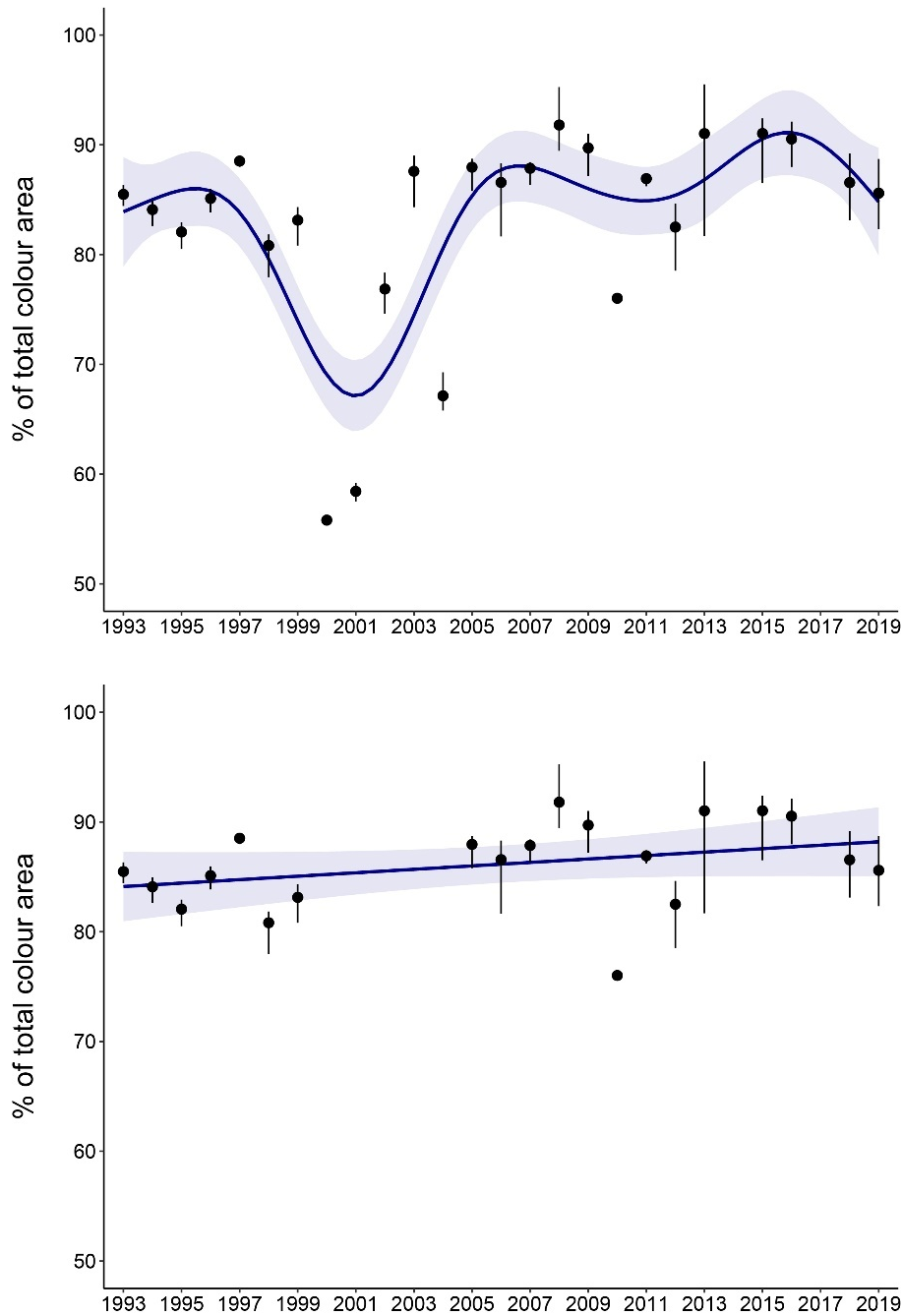


Figure D11. The relationship between year surveyed and the colour area with (top) and without (bottom) the 5 years following the recovery from bleaching. If these five years are removed (bottom) the generalised additive model (gam) actually determined the line of best fit is linear, even though it was given the freedom to add splines (wiggleness) if necessary. A linear regression (the model output table following) displayed no significant relationship between year and colour-area. Therefore, without major disturbance, there is a 'base-line' level of colour-area characteristic to the reefs surrounding Orpheus Island.

Table D6. Model parameters for the linear regression removing the five recovery years.

<i>Predictor</i>	<i>Response</i>	<i>Estimate</i>	<i>Confidence Interval</i>	<i>t - value</i>	<i>p - value</i>	<i>R²</i>
Year (sampled)	Colour-area	0.1569	-0.06 – 0.38	1.505	0.150	0.06

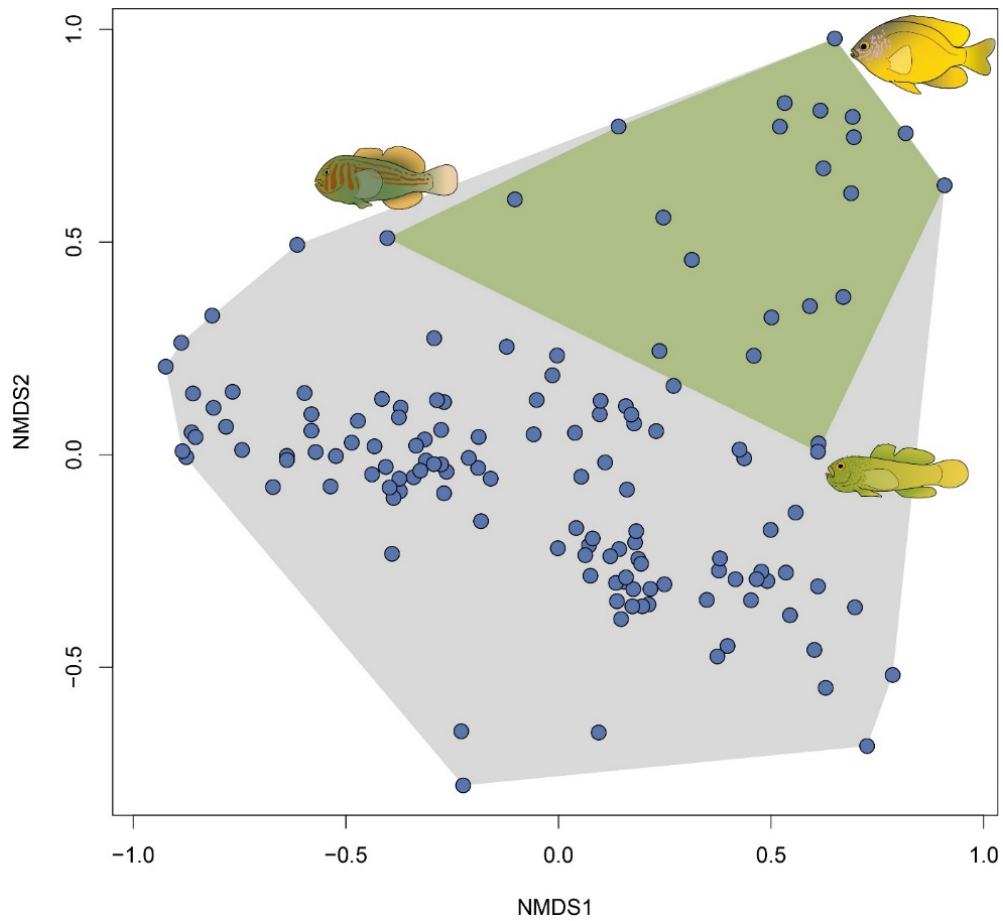


Figure D12. The colourspace occupied by yellow and green species. The green polygon represents approximately 29% of the total colourspace and is created from just three species: *Pomacentrus moluccensis*, *Gobiodon histrio*, and *Paragobiodon xanthosoma*.

Table D7. Model parameters from the negative binomial abundance regression.

<i>Predictor</i>	<i>Response</i>	<i>Estimate</i>	<i>Confidence Interval</i>	<i>z - value</i>	<i>p - value</i>	<i>adj. R²</i>
Year sampled	Abundance	-0.066	-0.11 – -0.02	-2.847	0.004	0.39

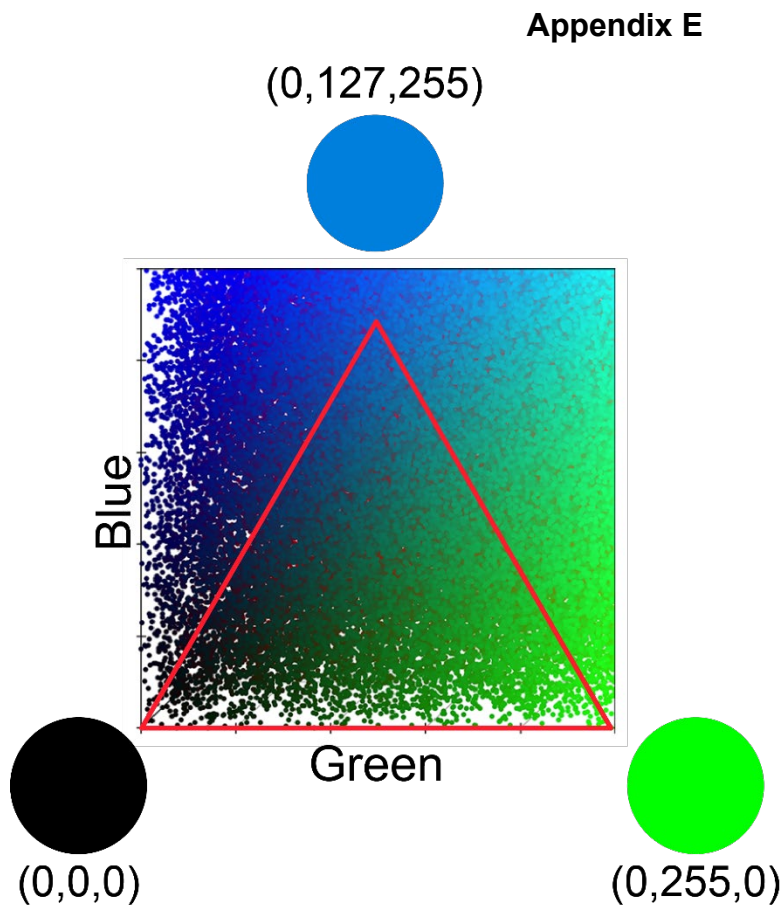


Figure E1. Euclidean distances in the RGB colourspace are not representative of perceptual differences. Displayed is only the Green (x) and Blue (y) axes of the RGB colourspace (Red in this figure would be the z axis) adapted from Weller and Westneat 2019. The red triangle is equilateral meaning that each of the three vertices are equally distance from each other. Most human viewers would identify the green and blue colours as being far more perceptually similar than either two colours are from black. However, their distances in RGB colourspace are identical, meaning the distance between black-and-green and black-and-blue are the same as that between blue-and-green.

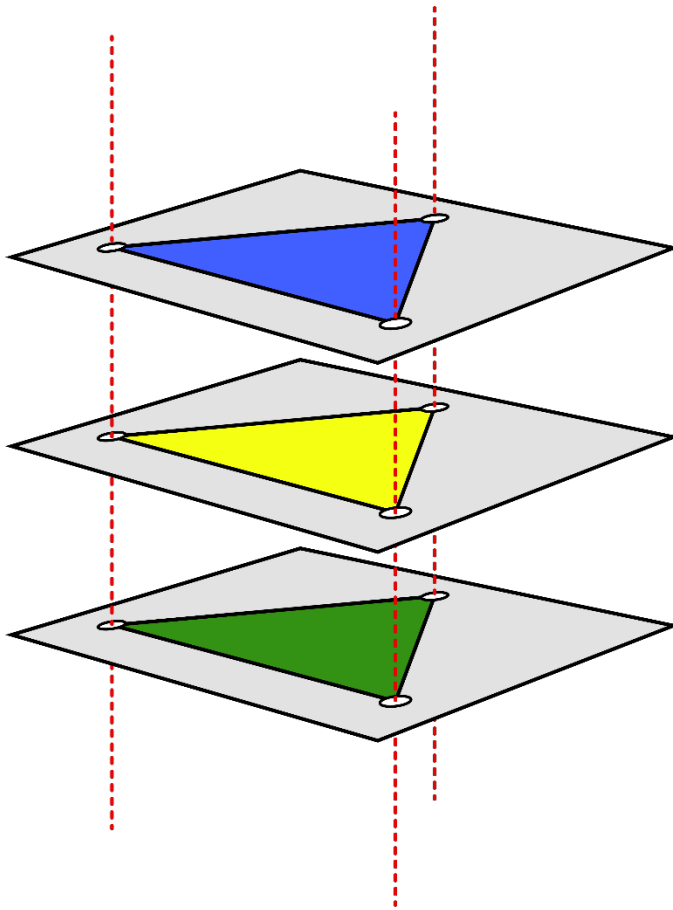


Figure E2. *Aligning landmarks in patternize. This is a representation of images after they have been aligned. Note how the landmarks in each image can be connected to the same landmarks in the other images with a perfectly straight, vertical line. This utility allows for the comparison between images in which the subjects vary in size and orientation.*